Optimization of the VITROCELL® Exposure System for *In Vitro* Toxicity Testing of Diesel Emissions at the Air-Liquid Interface

Rebecca Greenan, B.Sc. (Hons)

A thesis submitted to
the Faculty of Graduate and Postdoctoral Studies
in partial fulfillment of the requirements for the degree of
Master of Science in Biology
with Specialization in Chemical and Environmental Toxicology

Department of Biology
University of Ottawa
Ottawa, Canada

ABSTRACT

Relative to traditional methods, air-liquid interface (ALI) exposures constitute a superior *in vitro* model for assessing the toxicological activity of complex aerosols. By removing the medium barrier, aerosols can be delivered to the cells at their apical surface. This project investigated the utility of the commercially available VITROCELL® exposure system for comparative toxicological assessment of complex aerosols (freshly-generated diluted diesel exhaust and simulated urban smog). The system setup was modified to improve control of aerosol properties (temperature and humidity) and cellular responses (dynamic range). Following optimization, cytotoxicity (WST-1 and LDH assays) and expression of selected genes involved in proinflammatory signalling and oxidative stress responses (via quantitative RT-PCR) were quantified following 1 hour aerosol exposures. The results showed only limited, variable responses following exposures to high concentrations of diesel exhaust. Lack of consistent and robust responses are likely due to poor deposition of particulate matter from the test aerosols.

RÉSUMÉ

Par rapport aux méthodes classiques, l'exposition à l'interface air-liquide (IAL) est un modèle in vitro supérieur permettant d'évaluer l'activité toxicologique d'aérosols complexes. En retirant la barrière du milieu, les aérosols complexes dont on souhaite évaluer les risques qu'ils posent pour l'environnement ou en milieu de travail (p. ex., émission de moteur diesel, air en milieu urbain, etc.), peuvent être acheminés aux cellules, sur leur surface apicale. VITROCELL^{MD} est une chambre d'exposition vendue dans le commerce, conçue pour étudier l'exposition de cellules de mammifère en culture situées à une IAL. Le présent projet vise à examiner l'utilité de la chambre pour mener des évaluations toxicologiques comparatives d'aérosols complexes, c'est-à-dire, une émission de moteur diesel fraîchement produite, un smog urbain simulé. Après examen des paramètres d'exposition, la configuration de la chambre a été modifiée pour améliorer le paramétrage des propriétés des aérosols (p. ex., température, humidité) et les réponses cellulaires (c.-à-d., la gamme dynamique). Après l'optimisation, la cytotoxicité (c.-à-d., les essais de WST-1 et de LDH) et l'expression de certains gènes jouant un rôle dans la signalisation pro-inflammatoire et les réponses au stress oxydatif ont été quantifiées (par PCR-RT quantitatif) à la suite d'expositions de courte durée (1 h) à des aérosols. Les résultats ne révèlent que des réponses limitées et variables après l'exposition à des concentrations élevées d'émissions diesel. Le manque d'uniformité et de robustesse des réponses est probablement attribuable à un faible dépôt de la matière particulaire des aérosols mis à l'essai.

ACKNOWLEDGEMENTS

With my sincerest gratitude, I would like to thank my supervisor, Dr. Paul White, for giving me the opportunity to complete a Masters degree at the University of Ottawa, and for his constant support and insight throughout this project. Also, my committee members, Dr. Jules Blais and Dr. Deniz Karman; thank you for your guidance.

For all their assistance, I would like to thank the members of the Mechanistic Studies Division, Environmental Health Science and Research Bureau, Health Canada. Special thanks to John Gingerich, Lynda Soper, Kathy Nguyen, Rebecca Maertens, and Michèle Régimbald-Krnel for their continuous advice and support in and outside the lab. To my fellow graduate students, especially Julie Cox, Sarah Labib, and Alexandra Long, thanks for being there and thanks, always, for your help.

I would like to thank Debbie Rosenblatt, Tak Chan, and members of the Emissions Research and Measurement Section, Air Quality Research Division, Environment Canada for their collaboration and contributions to the light-duty diesel engine study. Thank you for the opportunity, and for all your hard work and advice.

To Dr. Mathias Könczöl, formerly of the Freiburg University Medical Center, thank you for sharing your expertise.

To everyone involved in our collaborative work at the National Health and Environmental Effects Research Laboratory, United States Environmental Protection Agency, I can't thank you enough. Thank you for your support, your guidance, and your invaluable input and assistance with experimental methods. Dr. David DeMarini, Dr. Ian Gilmour and Dr. Mark Higuchi, thank you for the opportunity. Dr. Jose Zavala, you were absolutely instrumental to our success. Nancy Hanley, Todd Krantz, and Charly King, we couldn't have done it without you. Special thanks to Dr. Brian Chorley and Gail Nelson for assistance with the quantitative RT-PCR assay, and to Judy Richards for assistance with the LDH assay.

To my family and friends, thanks for helping me get through this. James, always and forever, thank you.

Funding was provided by the Program of Energy Research and Development, Natural Resources Canada, and the government of Canada's CARA (Clean Air Regulatory Agenda) research fund. Collaborative work at the U.S. EPA was supported by intramural funding.

TABLE OF CONTENTS

TABLE OF TABLES

TABLE OF FIGURES

TABLE OF APPENDICES

LIST OF ABBREVIATIONS

A549	Human alveolar adenocarcinoma cell line
ACS	American Cancer Society
A-DEP	Automobile-derived diesel exhaust particulate
AHR	Aryl hydrocarbon receptor
ALI	Air-liquid interface
AP-1	Activator protein 1
APEI	Air Pollutant Emissions Inventory
ATCC	American Type Culture Collection
B20	20% biodiesel, 80% diesel fuel blend
B100	100% biodiesel fuel
B[a]P	Benzo[a]pyrene
BEAS-2B	Human bronchial epithelial cell line
BEBM	Bronchial epithelium basal medium
BPE	Bovine pituitary extract
BHT	Butylated hydroxytoluene
CACs	Criteria air contaminants
CeO_2	Cerium oxide
CEPA 1999	Canadian Environmental Protection Act, 1999
CI	Compression-ignition
CO	Carbon monoxide
CO_2	Carbon dioxide
CPC	Condensation particle counter
CV	Coefficient of variation
CVS	Constant volume sampling
DOC	Diesel oxidation catalyst
DPF	Diesel particulate filter
DPM	Diesel particulate matter
EGR	Exhaust gas recirculation
EHC	Environmental Health Centre
ELF	Epithelial lining fluid
ERMS	Emissions Research and Measurement Section
F-12K	Kaighn's modification of Ham's F-12 medium
FBS	Fetal bovine serum
$FeSO_4$	Iron (II) sulfate
H_2O_2	Hydrogen peroxide
HC	Hydrocarbon
hEGF	Human epidermal growth factor
HEPA	High-efficiency particulate absorption
HEPES	4-(2-hydroxyethyl)-1-piperazineethanesulfonic acid
HLDT	Heavy light-duty trucks
IARC	International Agency for Research on Cancer
LDH	Lactate dehydrogenase
LDV	Light-duty vehicles
LLDT	Light light-duty trucks
LNT	Lean NO_x trap
MAPK	Mitogen-activated protein kinase

MDA	Malondialdehyde
MDPV	Medium-duty passenger vehicles
MRC	Mobile reaction chamber
NHEERL	National Health and Environmental Effects Research Laboratory
NO_x	Nitrogen oxides
NPRI	National Pollutant Release Inventory
NR	Neutral red
NTDE	New technology diesel exhaust
PAHs	Polyaromatic hydrocarbons
PBS	Phosphate buffered saline
PCR	Polymerase chain reaction
PET	Polyethylene terephthalate
PM	Particulate matter
$PM_{0.1}$	Particles less than 100 nm aerodynamic diameter. Also called 'ultrafine' particulate matter.
$PM_{2.5}$	Particles less than 2.5 μm aerodynamic diameter. Also called 'fine' particulate matter.
PM_{10}	Particles less than 10 μm aerodynamic diameter. Also called 'inhalable' particulate matter.
PPM	Part per million
PTFE	Polytetrafluoroethylene
RFU	Relative fluorescence units
RH	Relative humidity
ROS	Reactive oxygen species
RPMI 1640	Roswell Park Memorial Institute 1640 medium
RTP	Research Triangle Park
SCRT	Selective catalytic reduction technology
SDS	Sodium dodecyl sulfate
SMPS	Scanning mobility particle sizer
SO_x	Sulphur oxides
SRM 2975	Standard reference material 2975
TBARS	Thiobarbituric acid reactive substances
TEOM	Tapered element oscillating microbalance
THC	Total hydrocarbons
TPM	Total particulate matter
ULSD	Ultra-low sulfur diesel
US EPA	United States Environmental Protection Agency
VOCs	Volatile organic compounds
WST-1	Water soluble tetrazolium salt-1

1.0 INTRODUCTION

1.1 Background

Diesel engine exhaust has been extensively studied as an occupational and environmental health hazard. However, the complexity of the emissions makes definitive toxicological characterization challenging.

Diesel engines have traditionally been favoured in commercial and industrial applications for their fuel efficiency, longevity, and reliability. Compared to gasoline, lower carbon dioxide (CO_2) emissions are favourable for the prevention of anthropogenic climate change. Carbon monoxide (CO) emissions are minimal, making them far superior for work in enclosed spaces such as the mining industry. Diesel fuel is also more stable, producing fewer flammable vapours. However, diesel engines have traditionally emitted more elemental carbon.

Typical industries using diesel engines are freight (e.g., overland trucking, rail, and marine applications), transportation (e.g., school buses, municipal bus and rail systems, and intercity bus and rail), and equipment for industrial, agricultural, mining, and construction industries. In the United Sates, over 90% of freight is transported by diesel vehicles (USDOE 2010). Diesel engine sales comprise roughly 3% of the passenger vehicle market in North America and 50% in Europe; the North American passenger vehicle market is forecasted to continue to increase (Fosten 2012). In Canada, diesel fuel consumption accounted for 3.1% of light-duty vehicles, 72.2% of medium-duty, and 97.5% of heavy-duty vehicles in 2009 (Office of Energy Efficiency 2009).

Diesel engines utilize a compression-ignition (CI) cycle to produce energy. Fuel is sprayed into the combustion chamber by a high-pressure injection system to mix with compressed intake air (IARC 2013). Vaporization of the fuel occurs as the droplets disperse. The autoiginition temperature is dependent on fuel chemistry. Compression pressures vary from 400 – 700 psi depending on the engine and usually substantially exceed the minimum ignition temperature (Bennett 2014). During combustion, a small region ignites first and then the flame propagates throughout the combustion chamber. Flammation of the fuel rapidly increases the pressure in the combustion chamber, resulting in the down stroke of the piston and transfer of energy to the crankshaft (Elliott 1958). This method of

combustion has certain implications for the resultant exhaust emissions. Complete fuel combustion is dependent on temperature and the availability of oxygen. Because the fuel is not pre-mixed with air, the fuel-air ratio of the local environment is highly variable. Fuel experiencing an unfavourable ratio may partially oxidize but not ignite; regions with excess air undergo oxidation with nitrogen in the air, resulting in the formation of nitrogen oxides (NO_x). Temperature also varies across the combustion chamber and falls rapidly as flammation ceases in the local area, resulting in unburned and partially oxidized hydrocarbons. Fuel that is not fully vaporized at the time of flammation undergoes thermal decomposition (Elliott 1958). Burned lubricating oil also contributes to engine emissions; moreover, engine design, maintenance, and operating conditions have a significant impact on emissions due to variations in temperature and combustion timing (IARC 2013).

Although the ultimate product of complete combustion is CO_2, the intermediate steps of the chemical reaction are numerous. Impurities in the fuel and lubricating oil contribute to non-hydrocarbon emissions, e.g., sulfuric and hydrochloric acid, sulfur and nitrogen oxides, metals, and minerals. In the presence of sufficient oxygen, unburnt fuel, which is composed of straight-chain and branched hydrocarbons and aromatics, tends to break down into smaller organic molecules. Larger hydrocarbon molecules produce more complex intermediates, e.g., higher aldehydes and other air toxics such as 1,3-butadiene. Organic radical intermediates also react with each other to form larger organic molecules such as polyaromatic hydrocarbons (PAHs) (Russell 2013).

The resultant diesel emissions are composed of, quite literally, thousands of chemical compounds in the gas and particulate phases. **Table 1.1** lists some compounds of interest in diesel exhaust, by phase, as published in the 2013 IARC (International Agency for Research on Cancer) Monograph that evaluated the carcinogenic risks to humans of diesel and gasoline engine exhausts (IARC 2013). Based on the available evidence, IARC declared diesel exhaust to be a known human carcinogen (group 1); there was sufficient evidence for an increased risk of lung cancer and limited evidence for an increased risk of bladder cancer. Gasoline exhaust was classified as a possible human carcinogen (group 2b), primarily due to a smaller, less definitive body of evidence. Several components known to be in engine exhausts had been previously evaluated by IARC with respect to

their carcinogenicity as independent agents. Of these, arsenic, beryllium, cadmium, chromium, 1,3-butadiene, benzene, formaldehyde, dioxins, and benzo[*a*]pyrene (B[a]P) were classified as known human carcinogens (group 1). Others were classified as probable (group 2a) or possible (group 2b) human carcinogens. Thorough review of the chemical composition of diesel exhaust is beyond the scope of this thesis. Additional, more detailed information is available in the literature (Claxton 2015, Totlandsdal et al. 2014, Zhang and Balasubramanian 2014).

Diesel particulate matter (DPM) is emitted in a trimodal size distribution. The *nuclei mode* consists of volatile hydrocarbon and sulfur particles with an aerodynamic diameter between 30nm and 3nm. This mode makes up 0.1 - 10% of particle mass, and 90% or more of the particle number. The *accumulation mode* particles have an aerodynamic diameter between 30 - 500 nm and are composed of carbon agglomerates and nuclei mode particles with adsorbed condensed hydrocarbon and sulfur vapors. This mode makes up 80 - 90% of particle mass and 10% of particle number. The *coarse mode* includes particles larger than 1 μm and makes up 5 - 20% of particle mass (Kittelson 1998, Kittelson et al. 2002).

For health effects research, particulate matter studies generally focus on size distributions that have been prioritised with respect to respirability and pulmonary deposition patterns (Cyrys et al. 2014, Gualtieri et al. 2014, Harkema et al. 2009, Weichenthal et al. 2014). Total particulate matter (TPM) refers to all particulate matter in a given exposure; however, inhalable particulate matter refers to the size fraction with an aerodynamic diameter smaller than 10 μm (PM_{10}). Operational categories such as *fine* refer to particles with an aerodynamic diameter less than 2.5 μm ($PM_{2.5}$), and *ultrafine* refers to particles with an aerodynamic diameter less than 100 nm ($PM_{0.1}$). $PM_{2.5}$ penetrates into the deep lung, whereas larger particles are generally trapped in the nose and upper airways where they can be removed by mucociliary clearance (Darquenne 2012, Yu and Yoon 1991). $PM_{0.1}$ are capable of translocating into the systemic circulation (Oberdorster et al. 2009). The vast majority of fresh diesel particles are within the ultrafine fraction. Assessments of PM emissions and exposure have traditionally been based on particle mass; however, it is now becoming clear that particle number and surface area may be more important metrics (Ramachandran et al. 2005).

The primary components of interest for investigations of engine exhaust toxicity are PM, CO, and NO_x. Although each of these has been shown to be individually toxic, they have been employed as surrogate markers for whole engine exhausts for operational reasons (i.e., they can be routinely and reliably measured). NO_x are also of interest due to their contribution to ozone formation. **Table 1.2** lists some ranges for environmental and occupational levels for DPM ($\mu g/m^3$), as adapted from the 2002 EPA health assessment document for diesel engine exhaust (USEPA 2002a). Notably, values for low occupational exposure are comparable to high environmental levels.

Table 1.1: Some compounds and classes of compounds in vehicle engine exhaust.

Gas phase	Particulate phase
Acrolein	Heterocyclics and derivatives
Ammonia	Hydrocarbons (C_{14} - C_{35}) and derivatives*
Benzene	Inorganic sulfates and nitrates
1,3-Butadiene	Metals (e.g. lead and platinum)
Formaldehyde	Polycyclic aromatic hydrocarbons and derivatives*
Formic acid	
Heterocyclics and derivatives*	
Hydrocarbons (C_1 - C_{18}) and derivatives*	
Hydrogen cyanide	
Hydrogen sulfide	
Methane	
Methanol	
Nitric acid	
Nitrous acid	
Oxides of nitrogen	
Polycyclic aromatic hydrocarbons and derivatives*	
Sulfur dioxide	
Toluene	

*Derivatives include acids, alcohols, aldehydes, anhydrides, esters, ketones, nitriles, quinones, sulfonates, halogenated and nitrated compounds, and multifunctional derivatives.

Reproduced with permission from IARC (2013). Originally compiled from National Research Council (1983), Lies et al. (1986), Schuetzle & Frazier (1986), Carey (1987), Johnson (1988), Zaebst et al. (1988).

Table 1.2: Ranges for environmental and occupational levels of diesel particulate matter (DPM).[a]

Exposure	Occupational DPM (µg/m^3)	Environmental DPM (µg/m^3)
Rural Environmental	-	0.6 (0.3 – 0.7)[b]
Urban Environmental	-	1.6 (0.8 – 2.0)[b]
Miners	10 – 1,280[c]	2 – 269[d]
Railroad workers	39 – 191[c]	8 – 40[d]
Firefighters	4 – 748[c]	1 – 157[d]
Airport crew and public transit workers	7 – 98[c]	2 – 21[d]
Dockworkers and mechanics	5 – 61[c]	1 – 13[d]
Long- and short-haul truckers	2 – 7[c]	0.4 – 2[d]

a. Adapted from USEPA (2002a).
b. US nationwide annual average values for 1996 with 25th percentile – 75th percentile in parentheses. Obtained using the HAPEM4 statistical model.
c. Summary of published experimental data. Sampling years: Miners, 1980s – 1990s; Railroad workers, 1980s; Firefighters, 1985 and later; airport crew, not available; Dockworkers, 1990; Truckers, 1990.
d. Levels based on *(10 m^3/shift/20 m^3/day) * (5 days/7 days) * (48 weeks/52 weeks) * (45 years career/70 year lifetime)*.

1.2 Regulatory Framework for Emission Control

Emissions reduction strategies have been implemented to protect human health and prevent anthropogenic climate change. In Canada, emissions standards have become progressively stringent since first regulated in 1971. Currently, legislative authority is held by Environment Canada under the Canadian Environmental Protection Act 1999 (CEPA 1999). Generally, emissions regulations have been harmonized with the United States Environmental Protection Agency (US EPA) federal standards. The *On-Road Vehicle and Engine Emission Regulations*, which is currently in force (Government of Canada 2003), was designed to align with the US Tier 2 emissions standards, with a phase-in period between 2004 and 2010. These regulations enforce maximum levels of criteria air contaminants (CACs), i.e., volatile organic compounds (VOCs), CO, NOx, PM, and sulphur oxides (SO_x). They also regulate certain "toxic substances" as per Schedule 1 of CEPA 1999, including benzene, 1,3-butadiene, acetaldehyde, acrolein and PM_{10}. Formaldehyde is also regulated with the expectation of eventual inclusion in Schedule 1. Vehicles must comply with the regulations for their "full useful life", e.g., 10 years/192 000 km for light-duty vehicles (LDV) and light light-duty trucks (LLDT). Manufacturers must also meet fleet average NO_x standards for each model year. Allowed NO_x emissions were progressively decreased from each model year between 2004 and 2009; from 0.25 g/mile to 0.07 g/mile for LDV and LLDT, and 0.53 g/mile to 0.07 g/mile for heavy light-duty trucks (HLDT) and medium-duty passenger vehicles (MDPV). On average, this regulation represents a 90% reduction in smog-forming emissions relative to previous levels.

Off-road diesel engines, e.g., those used in construction, mining, farming, and forestry, are regulated by the *Off-Road Compression-Ignition Engine Emission Regulations* (Government of Canada 2005). These regulations apply to 2006 and later model years. An amendment to this regulation applies to 2012 and later model years (Government of Canada 2011). Engines used exclusively in underground mines are exempt from this regulation, and are regulated by provincial standards for ventilation requirements.

Greenhouse gases, i.e. carbon dioxide, methane, and nitrous oxide, are regulated by the *Passenger Automobile and Light Truck Greenhouse Gas Emission Regulations*

(Government of Canada 2010a) and the *Heavy-duty Vehicle and Engine Greenhouse Gas Emission Regulations* (Government of Canada 2013). The *Renewable Fuels Regulations* require an average 2% renewable fuel content in diesel fuel, based on volume, from July 2011 (Government of Canada 2010b). The *Sulphur in Diesel Fuel Regulations* mandated a 15 ppm maximum allowable limit for sulphur in on-road diesel fuel since June 2006 (Government of Canada 2002).

Emissions inventories, i.e., the National Pollutant Release Inventory (NPRI) and the related Air Pollutant Emissions Inventory (APEI), indicate that concentrations of criteria air contaminants have generally been decreasing across Canada since 1985. **Table 1.3** and **1.4** show emission trends data for select CACs from the APEI. **Table 1.3** shows total emissions per year for all mobile sources, i.e., including air transportation, on- and off-road gasoline and diesel vehicles, motorcycles, rail transportation, and tire wear and brake lining. **Table 1.4** shows per year emissions for on-road diesel vehicles only, i.e., summed emissions from heavy-duty diesel vehicles, light-duty diesel trucks, and light-duty diesel vehicles.

Table 1.3: Total mobile source emissions per year, from the Air Pollutant Emissions Inventory[a]. Values in thousands of tonnes unless otherwise indicated.

Year	TPM	PM_{10}	$PM_{2.5}$	SO_x	NOx	VOCs	CO	B[a]P (kg)
1985	96.9	96.2	87.0	173	1600	1090	12500	.
1986	99.1	98.4	89.3	166	1620	1090	12700	.
1987	102	101	92.4	168	1630	1080	12500	.
1988	104	103	93.8	184	1640	1070	12600	.
1989	104	104	94.4	191	1630	1050	12400	.
1990	103	103	93.6	182	1560	985	11700	1070
1991	100	99.4	90.9	163	1500	963	11500	996
1992	98.8	98.2	89.9	166	1490	955	11500	962
1993	98.8	98.2	89.9	174	1470	916	11100	944
1994	100	99.5	91.1	168	1510	902	10800	956
1995	97.1	96.6	88.3	151	1490	860	10300	897
1996	92.0	91.5	83.8	139	1410	811	9750	809
1997	91.4	90.9	83.2	144	1430	779	9450	788
1998	88.7	88.2	80.4	126	1430	748	8850	770
1999	84.9	84.4	76.9	124	1400	746	8840	717
2000	82.7	82.2	74.7	122	1380	745	8870	700
2001	80.9	80.4	73.4	123	1370	719	8510	681
2002	78.4	77.9	71.1	115	1350	682	8280	642
2003	76.3	75.9	69.0	112	1310	659	7800	603
2004	76.5	76.0	67.9	109	1290	626	7380	564
2005	75.2	74.7	67.7	110	1260	592	7100	541
2006	73.7	73.2	66.1	108	1230	572	6960	523
2007	72.5	72.0	64.9	102	1210	554	6850	502
2008	69.8	69.3	62.3	93.3	1170	530	6750	480
2009	68.8	68.2	61.1	95.4	1130	510	6610	462
2010	68.8	68.3	61.1	94.7	1140	491	6520	446
2011	65.8	65.3	58.2	94.9	1060	470	6320	424
2012	63.0	62.4	55.5	96.8	994	440	6023	370

a. Available at the Air Pollutant Emissions Data Online Search, hosted by Environment Canada (http://www.ec.gc.ca/inrp-npri/donnees-data/ap/index.cfm?lang=En) [accessed September 2014].

Table 1.4: Emissions per year for on-road diesel vehicles[a], from the Air Pollutant Emissions Inventory[b]. Values in thousands of tonnes unless otherwise indicated.

Year	TPM	PM_{10}	$PM_{2.5}$	SO_x	NO_x	VOCs	CO	B[a]P (kg)
1985	17.7	17.6	16.3	19.1	236	24.5	89.8	.
1986	18.0	18.0	16.7	18.4	242	24.8	92.9	.
1987	18.9	18.9	17.5	19.6	254	25.4	98.5	.
1988	19.4	19.4	17.9	19.8	260	25.2	100.5	.
1989	19.6	19.5	18.1	20.1	265	24.2	97.7	.
1990	19.2	19.2	17.8	22.1	259	22.3	91.9	263
1991	17.7	17.7	16.4	20.5	240	19.9	84.2	243
1992	16.8	16.7	15.5	21.1	232	18.3	79.7	232
1993	17.5	17.5	16.2	23.9	254	18.9	84.6	243
1994	18.9	18.9	17.5	23.5	308	20.0	94.7	259
1995	16.8	16.8	15.6	14.7	318	18.6	89.5	233
1996	13.8	13.8	12.8	12.4	285	15.9	76.1	193
1997	13.2	13.2	12.2	13.3	299	15.5	74.6	186
1998	12.9	12.9	11.9	5.09	342	16.3	79.5	181
1999	10.9	10.9	10.1	5.44	327	14.3	69.2	156
2000	10.2	10.2	9.40	5.50	318	14.3	67.7	148
2001	9.91	9.9	9.15	6.02	323	14.5	68.4	144
2002	9.11	9.1	8.41	5.78	309	13.9	65.3	133
2003	8.51	8.5	7.86	5.76	291	12.9	62.6	125
2004	8.37	8.4	7.73	6.18	291	13.0	63.7	123
2005	8.08	8.1	7.47	6.55	282	12.8	63.7	118
2006	7.37	7.4	6.80	3.66	266	12.3	62.0	108
2007	6.50	6.5	5.98	0.592	247	11.8	58.7	95.0
2008	5.76	5.8	5.31	0.606	229	11.2	54.1	84.6
2009	5.13	5.1	4.73	0.618	213	10.8	49.1	75.7
2010	4.57	4.6	4.21	0.630	194	10.3	44.3	67.4
2011	3.99	4.0	3.67	0.639	171	9.78	39.0	58.2
2012	3.42	3.4	3.15	0.704	150	9.19	33.3	51.1

a. Summed emission totals from heavy-duty diesel vehicles, light-duty diesel trucks, and light-duty diesel vehicles.

b. Available at the Air Pollutant Emissions Data Online Search, hosted by Environment Canada (http://www.ec.gc.ca/inrp-npri/donnees-data/ap/index.cfm?lang=En) [accessed September 2014].

1.3 Technologies for Emission Control

The ability to implement stricter emissions control regulations is dependent on the availability of control technologies. At the same time, technological developments are driven by the need to maintain profit while meeting regulations. The current regulations are considered to be a major catalyst to the development of emission control technologies developed and deployed by 2007, such that post-2007 models can be considered *new-technology diesel exhaust* (NTDE). NTDE emissions have significantly reduced levels of PM, CO, total hydrocarbons (THC), non-methane hydrocarbons, formaldehyde, ethylene, benzene, acetaldehyde, and total PAHs (Hesterberg et al. 2009, Hesterberg et al. 2011).

Novel technologies and products to reduce emissions include electronic engine controls, ultra-low sulfur diesel (ULSD) fuel, oxidation catalysts (DOCs), wall-flow diesel particulate filters (DPFs), and some combination of exhaust gas recirculation (EGR) technology, selective catalytic reduction (SCR) technology, lean NO_x catalysts, and lean NO_x traps (LNTs) (MECA 2010). DOCs and DPFs are used for the control of DPM, whereas EGR and SCR are used for NO_x control. DOCs act by oxidizing unburnt components in the fuel; DPFs filter the engine exhaust. EGRs recirculate exhaust gases. The recirculated gas has a higher heat capacity and lower oxygen content than fresh intake air and this lowers the combustion temperature in the engine thus inhibiting NO_x formation. Lean NO_x catalysts reduce NO_x to N_2, but they currently have seen only limited use since they generally do not permit adherence to new NO_x regulations. LNTs trap NO_x as NO_2 and then catalytically convert NO_2 to N_2 while operating at fuel rich conditions. SCRs reduce NO_x, PM, and HC emissions, with NO_x reduced to N_2 via catalytic reaction with gaseous ammonia.

The majority of emission control technologies work by catalyzing a chemical reaction to remove the emission component of interest (e.g., DPM, NO_x). As such, there is a concern that unintended effects on other DE components may contribute to unexpected toxicological effect. Studies on the chemical composition of NTDE indicate reductions in elemental carbon, organic carbon, PAHs, nitro-PAHs, dioxins/furans, and metals (Hesterberg et al. 2011). However, very few toxicological studies have examined NTDE, and even recent studies examined traditional and transitional (i.e., pre-2007) engines.

Nevertheless, some recent studies do indicate a reduction in toxicity for NTDE (Health Effects Institute 2012, McDonald et al. 2004). However, the complexity of diesel emissions, and the variation in emissions due to engine design, maintenance, fuel, and operating conditions, complicate thorough toxicological characterizations and generalizations. Additionally, additives related to aftertreatments may have some toxicological effect. For example, there is evidence that cerium compounds used in DOCs produce cerium oxide (CeO_2) nanoparticles that can augment the toxicity of DPM (Ma et al. 2014, Snow et al. 2014).

1.3.1 Alternative Fuels

Current regulations in Canada require a 2% renewable fuel content, by volume, in diesel fuel. Biodiesel is of interest as a renewable alternative to petroleum-derived diesel. Biodiesel is composed of fatty acid esters, usually methyl esters, produced by reacting vegetable oils or animal fats with methanol. In Canada, canola is the main feedstock used for biodiesel production; in the U.S., soybean oil is more common. Biodiesels are usually in blends with petroleum diesel, denoted by BX, where X is the percent by volume of biodiesel in the blend (e.g., B2, B5, B10 or B20). In general, increasing the biodiesel content results in decreased emissions of PM, CO, and HC, and increased emissions of NO_x (USEPA 2002b).

1.4 Health Effects of Diesel Exhaust Emissions

The toxic potency of diesel exhaust is generally low. However, its widespread use indicates that even limited toxicological effect can have a significant impact on population health. Strong epidemiological evidence for the health effects of diesel exhaust is somewhat limited due to methodological confounders such as concurrent exposures and limited documentation of actual exposure. Effects observed have generally been mild, and the aforementioned confounders contribute to marginal statistical significance. However, the large number of studies conducted supports the strength of the evidence, and the observed empirical relationships between exposure and disease are supported by experimental evidence from controlled human and animal exposures (Watson and Green 1995, USEPA 2002a, Hesterberg et al. 2009, IARC 2013).

Acute exposures cause transient neurophysiological symptoms (i.e., headache, lightheadedness, nausea, vomiting, and numbness) and contact irritation, i.e., eye, throat, and bronchial irritation (USEPA 2002a). These are likely caused by gas-phase constituents, e.g. NO_x and formaldehyde. Impacts on lung function are generally not significant, but may be exacerbated by co-exposures, e.g., cigarette smoke (USEPA 2002a). Controlled human exposures indicate proinflammatory effects in the lung, and suggest thrombogenic and ischemic cardiovascular effects at elevated exposures (Hesterberg et al. 2009). In animal studies, responses to acute exposure included accumulation of DPM in the lungs, aggregation of alveolar macrophages, non-specific inflammation, type II alveolar cell proliferation, and thickening of the alveolar walls (Watson and Green 1995). DPM also acts as an adjuvant for allergens and may modulate susceptibility to infection (Pandya et al. 2002).

Epidemiological evidence of chronic exposures provides support for increased prevalence of cough, phlegm, and chronic bronchitis. Impairment of pulmonary function was also observed in some studies at occupational exposure levels (USEPA 2002a). Effects were generally mild and may be attributable to confounders. In animals, chronic exposure resulted in extensive inflammation and pulmonary fibrosis pursuant to the effects observed in acute exposures (Watson and Green 1995). As noted, there is sufficient epidemiological evidence to indicate that diesel exhaust exposure significantly increases the likelihood of lung cancer in humans (IARC 2013).

As an environmental pollutant, diesel exhaust significantly contributes to ambient air pollution (Hasheminassab et al. 2014, Zhang et al. 2014), and extensive evidence supports the association between increased air pollution levels and cardiopulmonary morbidity and mortality. Famously, the Harvard Six Cities study showed increased cardiopulmonary and lung cancer mortality. The association was stronger for levels of $PM_{2.5}$, PM_{10}, and sulfate particles, in comparison with TPM, aerosol acidity, sulfur dioxide, or NO_x (Dockery et al. 1993). The American Cancer Society (ACS) study showed a 4%, 6%, and 8% increased risk for all-cause, lung cancer, and cardiopulmonary mortality, respectively, with each 10 $\mu g/m^3$ increase in $PM_{2.5}$ (Pope et al. 2002).

1.4.1 Mechanisms of Toxicity

Particles deposited in the airways must be removed by biological clearance mechanisms. Organic compounds adsorbed to particles are released in accordance with their partition coefficients. Poorly-soluble elemental particles are engulfed by alveolar macrophages for subsequent physical clearance (Watson and Green 1995). Therefore, pulmonary exposure to DPM organics is dependent on the ratio of the half-life for dissolution to the half-life for particle clearance; soluble organics can diffuse through membranes and bind to receptors in the cell, e.g., the aromatic hydrocarbon receptor (AHR) (Takenaka et al. 1995). The mucociliary escalator transports macrophages from the tracheobronchial region of the lung to the esophagus via the beating of cilia. Co-exposures to toxics that inhibit the beating of cilia, e.g., cigarette smoke, may inhibit clearance (Wolff 1986). Macrophages may also translocate through the alveolar interstitium for clearance by the lymphatic system (Yu and Yoon 1991). Nanoscale particles may be phagocytised by endothelial cells and translocate through the interstitium independently of macrophages (Thorley et al. 2014). In rats, high particle concentrations induce macrophages to form cellular aggregates, whereupon they are not cleared from the lung. Termed *particle overload*, this induces inflammation, lung remodeling, and carcinogenesis that may not be mechanistically relevant to humans (Valberg et al. 2006). Particle overload begins at about 1 mg particles/g lung tissue and clearance is completely blocked at about 10 mg particles/g lung tissue (Morrow 1988).

Diesel exhaust toxicity has been attributed to oxidative stress and inflammatory responses (Ristovski et al. 2012). Deposited particles induce the release of cytokines and chemotactic factors from immune cells and structural airway cells; additional immune cells, e.g. neutrophils, monocytes, and dendritic cells, are recruited in response. DPM stimulates the production of IgE, IL-4, IL-5, IL-8 and RANTES, and promotes T_H2 responses (Pandya et al. 2002). Oxidative stress is stimulated both directly and indirectly by particulate matter. Redox active compounds, e.g., quinones and embedded transition metals generate reactive oxygen species (ROS) directly; ROS (e.g., superoxide O_2^- and hydroxyl radical OH^-), are also generated indirectly by interactions with cells (Sagai et al. 1993). ROS reacts with cellular components to cause damage, e.g., oxidation of membrane lipids and cellular DNA, and may promote apoptosis (Hiura et al. 1999). Oxidative stress activates redox-sensitive transcription factors cascades, e.g., mitogen-activated protein kinase (MAPK),

activator protein 1 (AP-1) and NF-κB (Hashimoto et al. 2000, Ristovski et al. 2012). These cascades induce the expression of proinflammatory cytokines (IL-4, IL-6, IL-8, TNF-α), chemokines, and adhesion receptors. Therefore, oxidative stress induces inflammation, which in turn generates more oxidative stress. DPM may also reduce antioxidative capacity by inhibiting the scavenging activity of related enzymes (Kumagai et al. 1995, Mori et al. 1996).

Diesel engine exhaust, particulates, and particulate extracts induced DNA damage, including oxidative lesions and bulky adducts, gene mutations, DNA strand breaks, chromosome breaks, sister chromatid exchanges, aneuploidy, and morphological cell transformations in *in vivo* and *in vitro* studies (IARC 2013). A review of studies examining microarray profiles of gene expression changes following exposure to complex mixtures indicated that diesel exhaust, DPM, or DPM extracts altered the expression of genes for generalized stress responses, oxidative stress responses, inflammation, DNA repair, xenobiotic metabolism, cell cycle, proliferation, apoptosis, transport, adhesion, and RNA processing (Sen et al. 2007).

In vivo, the pulmonary epithelial lining fluid (ELF) may protect against PM-driven oxidative stress and DNA damage. The ELF contains surfactant proteins, lipids, and antioxidants. *In vitro* exposures indicate that direct-acting components, i.e., transition metals and the carbonaceous core, induce greater damage in a system lacking ELF, and are attenuated by ELF. DPM organic extracts generally do not increase ROS production, but do increase the levels of DNA strand breaks at high concentrations (Chuang et al. 2013). The lack of effect observed for some DPM organic extracts examined *in vitro* is potentially due to limited capacity for metabolic transformation. For example, PAHs are biotransformed by phase I metabolic enzymes into chemically reactive intermediates (IARC 2013), with further metabolism of metabolites by phase II enzymes contributing to the formation of excretable conjugates. Compared to other combustion emissions, polycyclic aromatic compounds in diesel emissions contain a high proportion of nitro-compounds, including nitro-PAHs and nitro-PAH lactones (IARC 2013). Nitro-PAHs are direct acting mutagens, but can undergo both oxidative and reductive metabolism (Mutlu et

al. 2013). 3-nitrobenzanthrone is an unusually potent mutagen found in diesel exhaust (Lewtas 2007).

The mutagenic activity of DPM may be highly dependent on the origin of the sample. Several standard reference materials have been employed for toxicological studies of DPM. For example, standard reference material 2975 (SRM 2975) (Claxton et al. 1992) and automobile-derived diesel exhaust particulates (A-DEP) (Sagai et al. 1993) have been widely used. SRM 2975 was derived from forklift truck emissions and has been used primarily for mutagenicity studies; A-DEP has been used primarily for studies of pulmonary toxicity. Comparison of these two standards indicated that they have highly disparate chemical composition and biological activity due to the conditions used for their generation and collection (Singh et al. 2004). A SRM known as C-DEP was recently generated and comprehensively characterized (Arey 2004). The mutagenicity and chemical/physical profile of C-DEP is different from the aforementioned standards (Mutlu et al. 2013). The mass distribution is similar to A-DEP; the mutagenicity is largely attributable to PAHs, nitroarenes, aromatic amines, and nitro-PAHs. Compared to A-DEP and SRM 2975, C-DEP exhibited intermediate PAH mutagenicity and lower nitroarene-associated mutagenicity.

Aerosolized and gas-phase components, e.g., acid aerosols, volatile organic compounds, and gases, are also respiratory irritants, and the gaseous phase has been shown to be mutagenic in bacteria (IARC 2013). In healthy subjects, short-term NO_2 exposure impairs lung host defense at concentrations below 1 ppm, and induces airway inflammation and nonspecific hyper-responsiveness below 2 ppm (U.S. EPA 2008). NO_2 acts synergistically with SO_2 to increase airway responsiveness in asthmatics (Jorres and Magnussen 1990).

DPM has also been shown to increase allergic sensitivity (Pandya et al. 2002). When co-exposed with an allergen, DPM induces increased IgG production and recruitment of eosinophils. Exposure to DPM prior to exposure to a novel antigen increased allergic sensitization (Diaz-Sanchez et al. 1999).

Extrapulmonary effects are beyond the scope of this report, but have been covered extensively elsewhere (Lewtas 2007).

1.5 Toxicity Testing Methods

Traditional methods for toxicity testing of complex aerosols, such as vehicular emissions, include *in vivo* animal inhalation testing, primarily in rodents, with some studies conducted in dogs, primates, and other animals (Phalen et al. 2008). Controlled human exposures have been used to examine acute responses (Ghio et al. 2012, Utell and Frampton 2000). Sample collection, preparation, and delivery methods employed in animal and human studies vary significantly across studies, thereby complicating generalisations. Animal inhalation studies of freshly generated exhaust have been termed the gold standard; however, these are costly, time consuming, and pose significant challenges regarding facility requirements (Cooney and Hickey 2008, Wong 2007). In addition, nebulization of collected and suitably diluted exhaust for inhalation studies may affect the composition of the mixture due to losses of some components and chemical transformation of others. Tracheal instillation of exhaust components poses similar concerns regarding chemical speciation and alterations of the normal pattern of pulmonary deposition. Rodent studies are also limited by differences between human and rodent nasopharyngeal structure, and moreover, that high rodent doses contribute to the aforementioned phenomenon known as particle overload, which is thought to have limited relevance to humans (Morrow 1988, Valberg et al. 2006).

In vitro testing methods include exposures of cultured mammalian and bacterial cells. The Ames test in *Salmonella typhimurium* has been extensively used to assess the mutagenic activity of DPM extracts or fractions of organic DPM extracts (Ames et al. 1973, Mutlu et al. 2013). Tests in mammalian cells have focused on the mechanisms and effects previously noted in animal studies, i.e., mutagenicity and cell transformation, inflammation, oxidative stress, and general cytotoxicity (IARC 2013). *In vitro* assays also suffer from problems related to maintaining the chemical profile of exhaust during collection and preparation for exposure. Additionally, most studies in cultured mammalian cells are dissimilar to pulmonary exposures in that the sample must interact with the liquid media that supports the cells (Bakand and Hayes 2010). Air-liquid interface (ALI) exposures of cultured animal cells have been pursued as more representative of *in vivo* pulmonary exposure conditions.

In vivo characterization of diesel emission toxicity across variations in engine class, engine design, operating conditions, maintenance state, emission aftertreatment, and fuel composition, is quite simply not possible. It would be cost-, time- and ethically-prohibitive to use animals for detailed emission studies. *In vitro* methods, using a standardized protocol and a battery of assays, must be designed and employed to permit screening for relative toxicity changes across the aforementioned conditions (Krewski et al. 2010). Exposures to whole exhaust, including gaseous emissions, are preferred to maintain potential synergistic effects. To prevent confounders due to sample preparation, the exhaust should be freshly generated. ALI exposures are thus ideal, at least in principal, to permit *in vitro* analyses while preventing aforementioned difficulties (e.g., interactions with culture medium and exposures to whole exhaust).

1.6 The VITROCELL® Exposure System

The VITROCELL® is a commercially available ALI exposure system from VITROCELL Systems GmbH, Germany. Originally developed as the CULTEX system, (Aufderheide and Mohr 1999, Aufderheide and Mohr 2000), the VITROCELL® diverged as an independent company in approximately 2008. Although ALI exposure systems have been designed by other researchers (Brahmajothi et al. 2010, Cooney and Hickey 2011, Hawley and Volckens 2013, Herzog et al. 2013, Lenz et al. 2009), and presented in the scientific literature, the VITROCELL® is one of the few commercially available systems. Use of a commercially available system has the distinct advantage of easier comparisons across laboratories and widespread availability of experimental techniques.

A schematic of the VITROCELL® exposure module is shown in **Figure 1.1**. The module is designed to support *in vitro* cultures during ALI aerosol exposures. Cultures are prepared on commercially-available semiporous membranes and during exposure cells are basally nourished while the aerosol is passed over the apical surface. The aerosol enters the exposure area via a trumpet-shaped inlet designed for even dispersal and the aerosol is pulled through the module by a vacuum pump at the system outlet. The area around the exposure wells is heated by a circulating water bath. Each triplicate exposure well/position draws from an overhead manifold, and receives an independent dose of aerosol. Usually, a second module is exposed in parallel to clean air as a negative control. The number of

wells in the module and some specifics of fabrication are dependent on the model purchased. Although not used in this study, an alternate model can be purchased specifically for bacterial exposures.

Table 1.5 provides a summary of published works that employed the VITROCELL® or its predecessor CULTEX system. Details of cell line, exposure aerosol, and endpoints examined for cellular response are listed. The system has primarily been used to examine tobacco smoke; however, other aerosols have been investigated including nanoparticles, atmospheric gases, combustion-derived aerosols, and volatile organics. A small number of studies used the system to examine diesel exhaust (Aufderheide et al. 2003a, Knebel et al. 2002, Seagrave et al. 2007). However, only a few possible engine exposure scenarios have been examined and exposure methods are dissimilar between studies. There is significant potential for a more robust comparison of multiple exposure scenarios following the development of reliable routine exposure protocols.

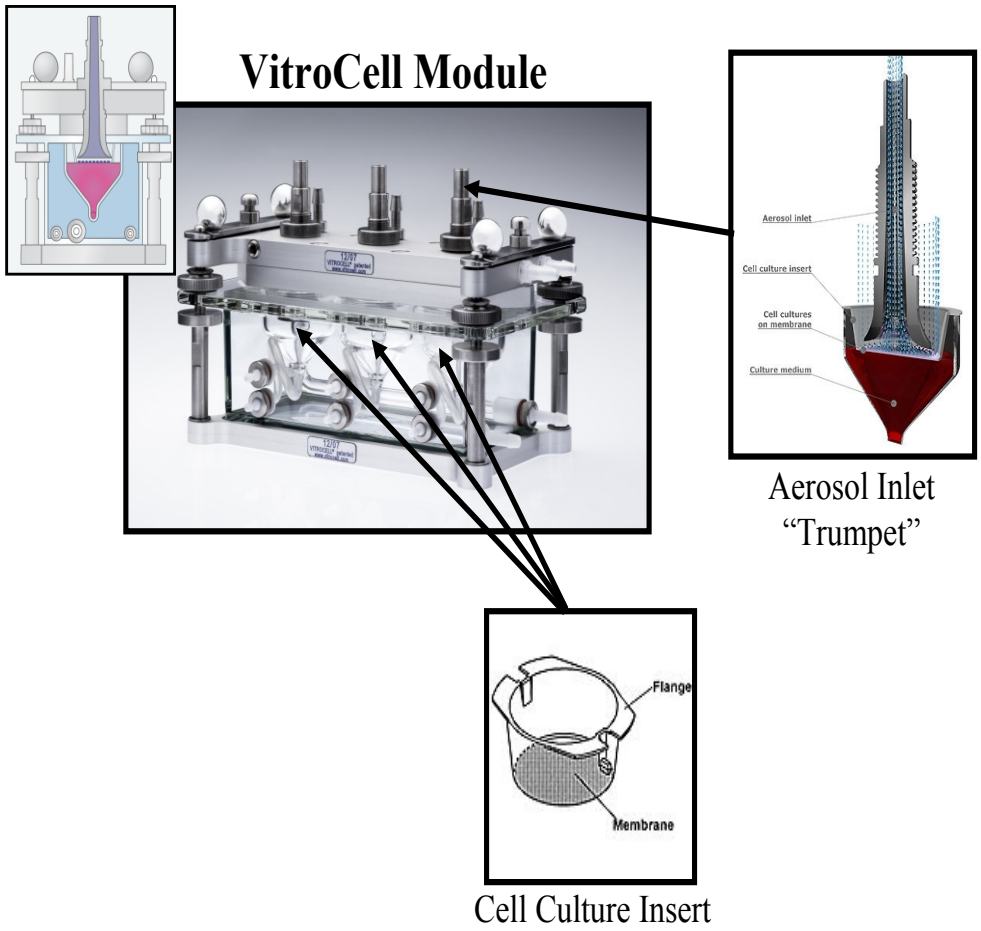

Figure 1.1: Schematic of a VITROCELL® exposure module showing the overhead manifold for triplicate exposures, a cross-sectional schematic (upper left), the position of the inserts, and a cross-section of an aerosol inlet trumpet (upper right).[a]

a. Adapted from www.vitrocell.com.

Table 1.5: Peer reviewed publications that utilised the VITROCELL® or predecessor exposure system to assess the toxicological properties of aerosols.

Reference	Cell line	Exposure Aerosol	Endpoints Examined
(Aufderheide and Mohr 2000)[a]	HFBE-21	Titanium dioxide nanoparticles, diesel soot	Viability (WST-1, cell count)
(Aufderheide et al. 2001)[a]	HFBE-21	Sidestream cigarette smoke	Viability (WST-1, cell count), intracellular glutathione content
(Ritter et al. 2001)[a]	Lk004, HFBE-21	Nitrogen dioxide, ozone	Viability (WST-1, cell count), ATP/ADP ratio, intracellular glutathione content
(Knebel et al. 2002)[a]	HFBE-21	Diesel exhaust	Viability (WST-1, cell count)
(Wolz et al. 2002)[a]	HFBE-21	Sidestream cigarette smoke	Viability (WST-1), comet assay
(Aufderheide et al. 2003a)[a]	HFBE-21	Sidestream cigarette smoke, diesel exhaust, nitrogen dioxide, ozone	Viability (WST-1, cell number), ATP/ADP ratio, intracellular glutathione content, ratio of oxidized and reduced glutathione
(Ritter et al. 2003)[a]	HFBE-21	Mainstream cigarette smoke	Viability (WST-1, cell countr), intracellular glutathione content, ATP/ADP ratio
(Aufderheide et al. 2003b)[a]	A549, HFBE-21	Mainstream cigarette smoke	Viability (WST-1, cell count), ATP/ADP ratio, intracellular glutathione content, ratio of oxidized and reduced glutathione
(Ritter et al. 2004)[a]	A549	Mainstream cigarette smoke	Intracellular glutathione content
(Aufderheide and Mohr 2004)[a]	*Salmonella typhimurium* (strain TA98)	Mainstream cigarette smoke	Bacterial mutagenicity
(Pariselli et al. 2006)[a]	A549, HaCaT	Toluene, benzene	Viability (WST-1), cytotoxicity (LDH leakage), IL-8 release, intracellular glutathione, ROS production
(Seagrave et al. 2007)[a]	EpiAirway human primary lung epithelium	Diesel exhaust	Tissue integrity (TEER), macromolecular permeability, viability (WST-1), cytotoxicity (LDH leakage), secretion of mucus-like substances, ATPase, glutathione, HO-1, cytokines
(Olivera et al. 2007)[a]	Calu-3	Mainstream cigarette smoke	Viability (WST-1), macromolecular permeability
(Aufderheide and Gressmann 2007)[a]	*Salmonella typhimurium* (strains TA98, TA100)	Whole cigarette smoke and gas vapour phase	Bacterial mutagenicity

(Mulhopt et al. 2007)[a]	Co-culture (BEAS-2B, THP-1)	Resuspended municipal waste incinerator fly ash	Viability (alamar blue), cytotoxicity (LDH leakage), IL-8 release
(Diabate et al. 2008)[a]	Co-culture (BEAS-2B, THP-1)	Resuspended municipal waste incinerator fly ash	Viability, IL-8 release, intracellular glutathione, HO-1 expression
(Anderson et al. 2010)	A549	Dicarbonyls (4-oxopentanal, glutaraldehyde, methyl glyoxal, glyoxal, diacetyl)	Viability, cytokine expression and secretion
(Koehler et al. 2010)	Primary nasal epithelium	Nitrogen dioxide	Viability (trypan blue), comet assay, micronucleus
(Persoz et al. 2010)	A549	Formaldehyde	Morphology, viability (XTT), cytokine release
(Gminski et al. 2010)	A549	Volatile organic compounds emitted from pine wood and oriented strand boards	Viability (counting), comet assay
(Switalla et al. 2010)	Murine precision-cut lung slices	Nitrogen dioxide, ozone	Viability (WST-1), immunostaining, cytokine release, protein determination
(Koehler et al. 2011)	Primary nasal epithelial mucosa	Nitrogen dioxide	Viability (trypan blue), comet assay, micronucleus
(Persoz et al. 2011)	A549	Formaldehyde, *Aspergillus fumigatus*	Cytotoxicity (LDH leakage), cytokine expression and secretion
(Tang et al. 2012)	A549	Laser printer emissions	Viability (WST-1), micronucleus
(Xie et al. 2012)	Mouse nontumorigenic alveolar type II epithelial cell line (C10)	Zinc oxide nanoparticles	Proliferation (MTS), cell death (propidium iodide and Hoechst staining), cytotoxicity (LDH leakage), ROS generation (DCF)
(Li et al. 2012)	CHO	Mainstream cigarette smoke, gas vapor phase, whole smoke	Cytotoxicity (neutral red uptake)
(Persoz et al. 2012)	A549, BEAS-2B	Formaldehyde	Cytotoxicity (LDH leakage), cytokine release
(Kim et al. 2013)	A549	Copper nanoparticles	Viability (alamar blue), generation of intracellular ROS
(Frohlich et al. 2013)	A549	Polysterene nanoparticles and carbon nanotubes	Immunocytochemistry, TEER, cytotoxicity (MTS),

(Anderson et al. 2013)	A549, MucilAir™ epithelial tissue from Epithelix	Limonene, limonene/ozone	Viability (XTT), cytokine release
(Elihn et al. 2013)	A549	Copper nanoparticles	Viability (trypan blue)
(Mathis et al. 2013)	EpiAirway human bronchial epithelial cells	Mainstream cigarette smoke	MMP-1 release, microarray, microRNA profiles
(Weber et al. 2013)	A549, BEAS-2B	Whole cigarette smoke	Viability (cell count), comet assay
(Klein et al. 2013)	3D co-culture (A549, THP-1, HMC-1, and EA.hy 926)	SiO_2-rhodamine nanoparticles	Viability, morphology, immunostaining
(Thorne et al. 2013)	BALB/c 3T3 clone A31, *Salmonella typhimurium* (strain YG1042)	Whole cigarette smoke	Neutral red uptake, bacterial mutagenicity
(Lenz et al. 2014)	A549	Aerosolized bortezomib	Efficacy of new exposure system design (ALICE-CLOUD). Morphology, cell number, IL-8 promoter activity, proteosome activity, viability (WST-1), cytotoxicity (LDH)
(Kilford et al. 2014)	*Salmonella typhimurium* (multiple strains)	Mainstream cigarette smoke	Bacterial mutagenicity
(Breheny et al. 2014)	*Salmonella typhimurium* (strain YG1042)	Whole cigarette smoke, ethylene oxide	Bacterial mutagenicity
(Thorne et al. 2014)	BALB/c 3T3 clone A31	Mainstream cigarette smoke and gas vapour phase	Cytotoxicity (neutral red uptake), particle deposition
(Bardet et al. 2014)	human Airway Epithelial Cells of Nasal origin (hAECN) from Epithelix	Formaldehyde	Morphology, viability (XTT), cytotoxicity (LDH leakage), cytokine production
(Schlage et al. 2014)	EpiOral™ buccal and EpiGingival™ 3D organotypic tissue cultures	Mainstream cigarette smoke	Cytotoxicity (LDH leakage), tissue integrity (TEER), histology/immunohistochemistry, inflammatory markers, CYP1A1/CYP1B1 activity, microarray
(Panas et al. 2014)	A549	Silica nanoparticles	Cytotoxicity (LDH leakage), cytokine release (IL-6, IL-8), western blot (COX-2, p38)
(Talikka et al. 2014)	MucilAir human fibroblasts (HF) bronchial, MucilAir HF nasal tissue	Whole cigarette smoke	Cytotoxicity (LDH leakage), tissue integrity (TEER), histology (immunostaining), inflammatory marker secretion, microarray

[a]Studies that employed the CULTEX system.

1.7 Objectives and Hypothesis

Given the number of variables affecting the chemical composition of diesel emissions, the need for a time- and cost-effective method for toxicity screening of complex aerosols, and the benefits of ALI exposures relative to traditional methods, it is evidently necessary to develop and deploy suitable methods for routine comparative toxicological profiling of diesel emissions. The VITROCELL® exposure system was chosen as a suitable, commercially-available platform. In order to ensure the effectiveness of the system for routine use, there needs first to be a systematic examination of the individual factors that could improve and standardize the use of the VITROCELL® for revealing the mechanisms of toxicity associated with diesel emissions. Therefore, the objectives of this thesis are (i) to develop optimized toxicity assessment protocols for use with the VITROCELL® exposure system and (ii) to verify the utility of the system for toxicological assessment of diluted diesel emissions.

To allow for detection of relative changes in toxicity related to changes in the composition of the exposure aerosol, the system should appropriately support the cells during exposure, i.e., no significant effect of clean air exposure should be observed. Additionally, diesel emissions should induce effects at concentrations comparable to previously published literature and exposure responses should be repeatable between exposures. Endpoints selected for examination were chosen based on the known mechanisms of action for diesel emissions (section 1.4.1), e.g., inflammation and oxidative stress. Markers of cell viability and cytotoxicity were utilized to select dose ranges for aerosol exposure, and to evaluate the effectiveness of the system in supporting the cells during exposure.

Research Hypothesis:

The commercially-available VITROCELL® system for *in vitro* air-liquid interface exposure of cultured animal cells can be deployed for reliable toxicological characterization of complex aerosols such as diluted diesel exhaust. For the purposes of this thesis, the assessment system will be deemed reliable if the coefficients of variation for responses to control air and test aerosols are less than 25%, and the test system can detect the toxicity of test aerosols that have been well characterised (e.g., ozone, NO_2, diesel

emissions). For the purposes of the thesis, *detection* is defined as a statistically significant difference from simultaneous controls at $p<0.05$.

2.0 MATERIALS AND METHODS

2.1 The VITROCELL® Exposure System

The VITROCELL® exposure system (i.e., model VITROCELL® 6 CF) was purchased from VITROCELL® Systems GmbH (Waldkirch, Germany). Details regarding the system are available at www.vitrocell.com. This exact model is no longer in production, although the current VITROCELL 6/3 CF Stainless is similar.

The supplied system is comprised of two identical glass modules for cell exposures, two manifolds for aerosol delivery, a circulating water bath to maintain a heated environment around the cell exposure areas, six precision flow valves for independent vacuum control, a vacuum pump, and a metal cart that supports the entire system. **Figure 2.1** shows the system set up at Health Canada. Water is heated to 37ºC by the water bath, and pumped through polytetrafluoroethylene (PTFE) tubing connected to the base and lid of each module. The outlet returns the water to the bath for recirculation. Quick-disconnect connectors allow easy disassembly.

The exposure module is designed for simultaneous exposure of three independent replicates (i.e., 3 positions for cells cultured on membrane inserts). The module wells accept commercially available 24mm semiporous membrane tissue culture inserts (e.g., Greiner Bio-One Thincert™ or Corning Transwell®) used with conventional 6-well culture plates. **Figure 2.2** shows the module base that accepts culture inserts. The ports in the back of the module allow for circulation of basal media during exposure via the medium pump included with the system. Medium exposure is generally required only for longer exposure times, and was not used for this project. Medium ports on each module were "capped" with PTFE tubing, and uncapped as required for maintenance. The lid of the module has three stainless steel trumpet-shaped aerosol inlets to deliver the aerosol to the wells. The positions of the inlet trumpets above the exposure wells are shown in **Figure 2.3**. The height of the trumpet is adjustable, allowing the distance between the trumpet and the surface of the culture insert to vary between 0 and 3 mm. Clasps on either side of the module lid allow it to be securely fastened to the base.

Aerosol is delivered to the system via tubing connected to a manifold. For most exposures, Tygon® tubing was employed to deliver the aerosol. In some instances, carbon

impregnated conductive tubing was used for delivery of diluted diesel exhaust. The aerosol is drawn through the modules by vacuum and each well outlet is connected to an independent flow controller. Posterior to the valves, these flows combine into a single airstream that is connected to a vacuum pump. **Figure 2.4** shows a close-up of the aerosol delivery system. The white block contains the precision valves and the flow rate is determined by measuring the vacuum draw at the open connectors using a handheld mass flow meter (0 - 20 sccm, Air/N_2) (Cole-Parmer, Montreal, QC), and opening or closing the valves as required using a hex key until the desired flow rate is obtained. After confirming flow rates, the vacuum connectors are joined to the module outlet connectors to permit draw of the aerosol through the module. Aerosols are always delivered to the modules in parallel, with one module (left) receiving clean air as a negative control, and the second module (right) receiving the aerosol of interest. **Figures 2.5 and 2.6** show the glass manifolds for delivery of the aerosol to the negative control and exposure module, respectively.

Prior to exposure, the wells are filled with nutrient medium such that it contacts the basal surface of the insert membrane. The apical surface of the membrane is exposed for direct contact to the test aerosol, i.e., ALI exposure. Medium is replaced between each exposure. The system is cleaned following each exposure by washing the exposure wells with 70% ethanol and wiping surfaces down with 70% ethanol. At the start of the exposure day, the wells are rinsed with exposure medium to remove any residual ethanol.

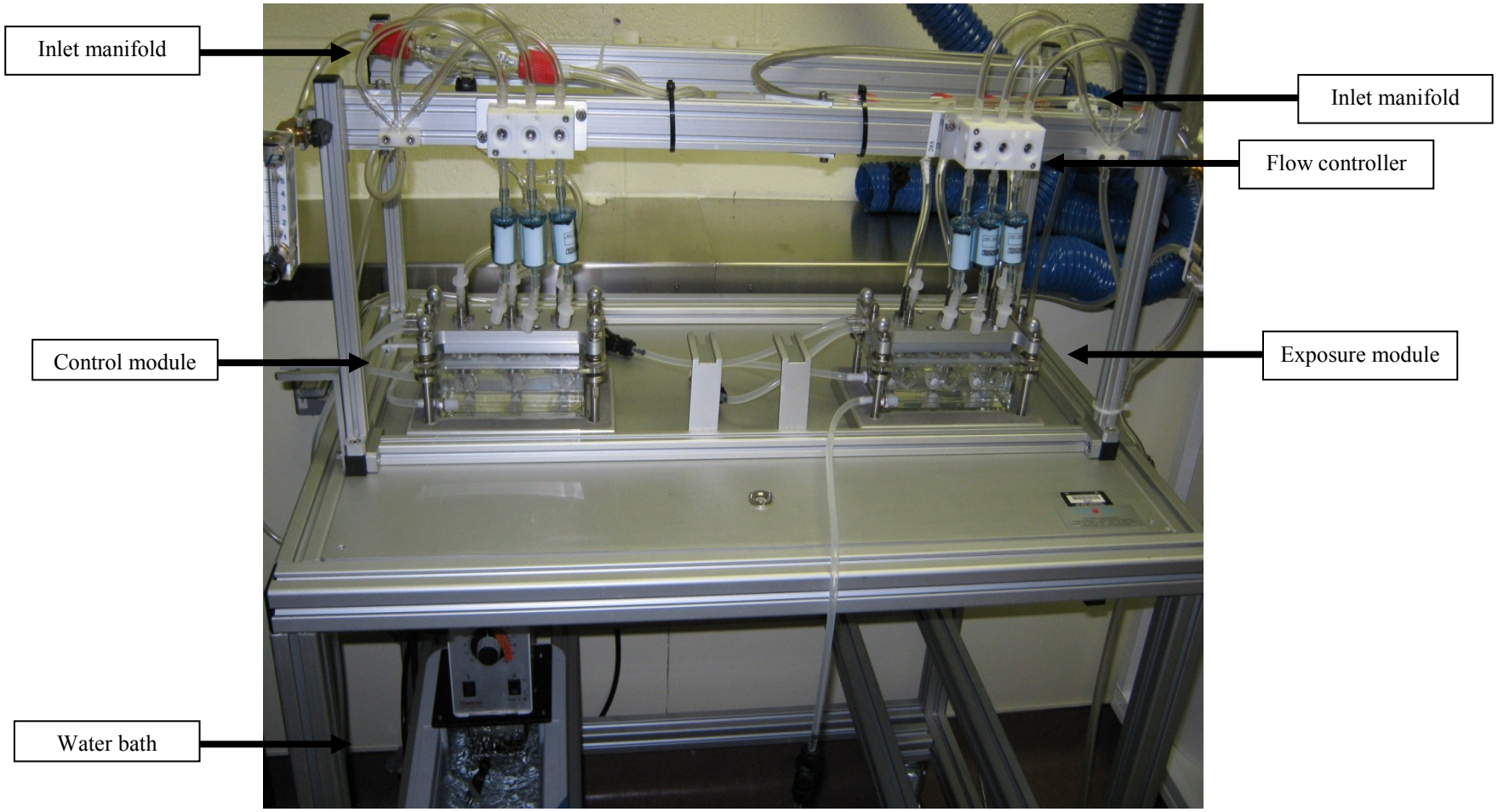

Figure 2.1: Front view of the cart-mounted VITROCELL® system. The aerosol exposure module with above inlet manifold is shown at the right. The matching control (i.e., clean air) module is shown at the left. The water bath for temperature control is below. The vacuum pump is not shown.

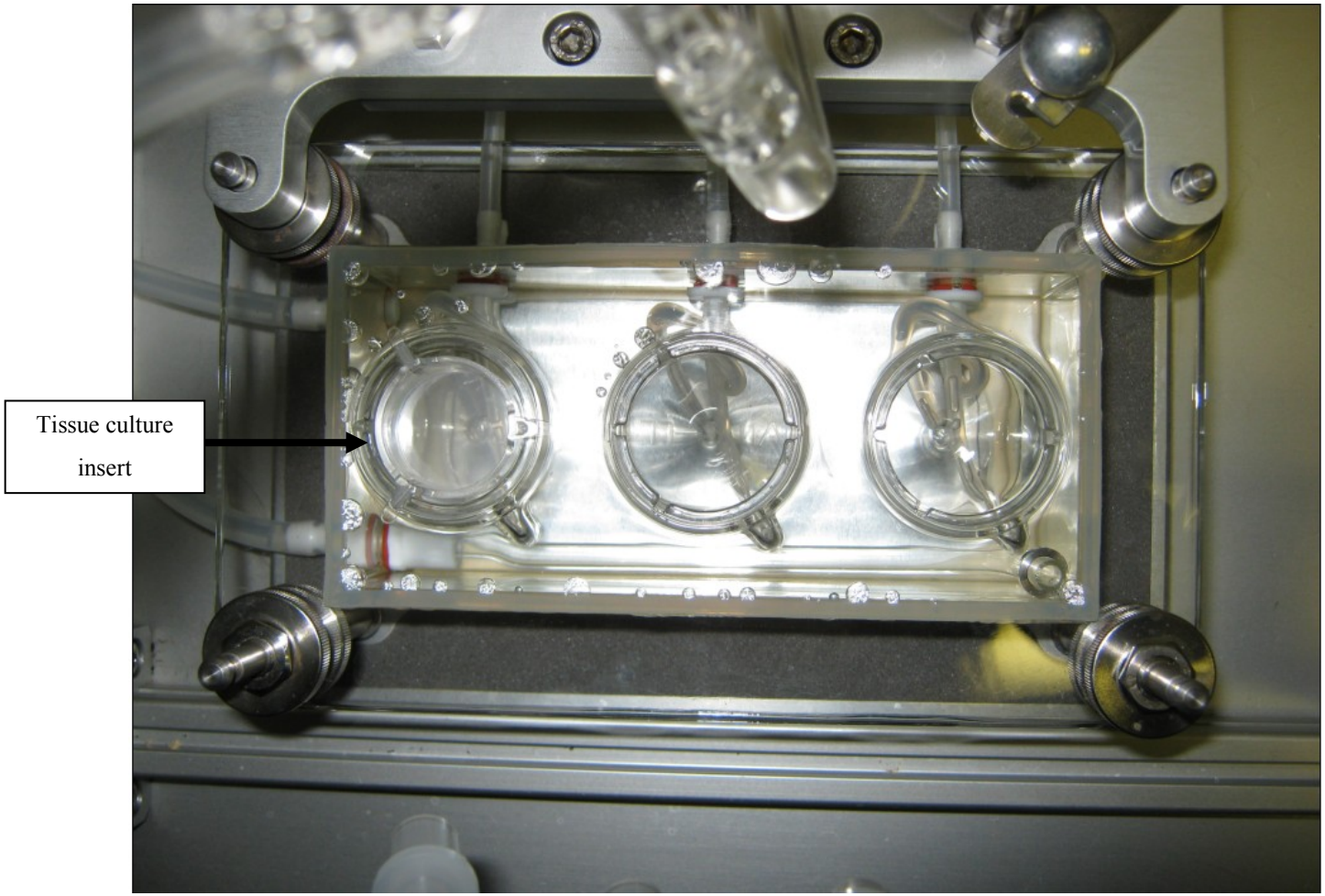

Figure 2.2: Top view of the base of a VITROCELL® module. Each well receives a tissue culture inserts. An insert (i.e., Greiner Bio-One 6-well Thincert™) is shown in the leftmost well.

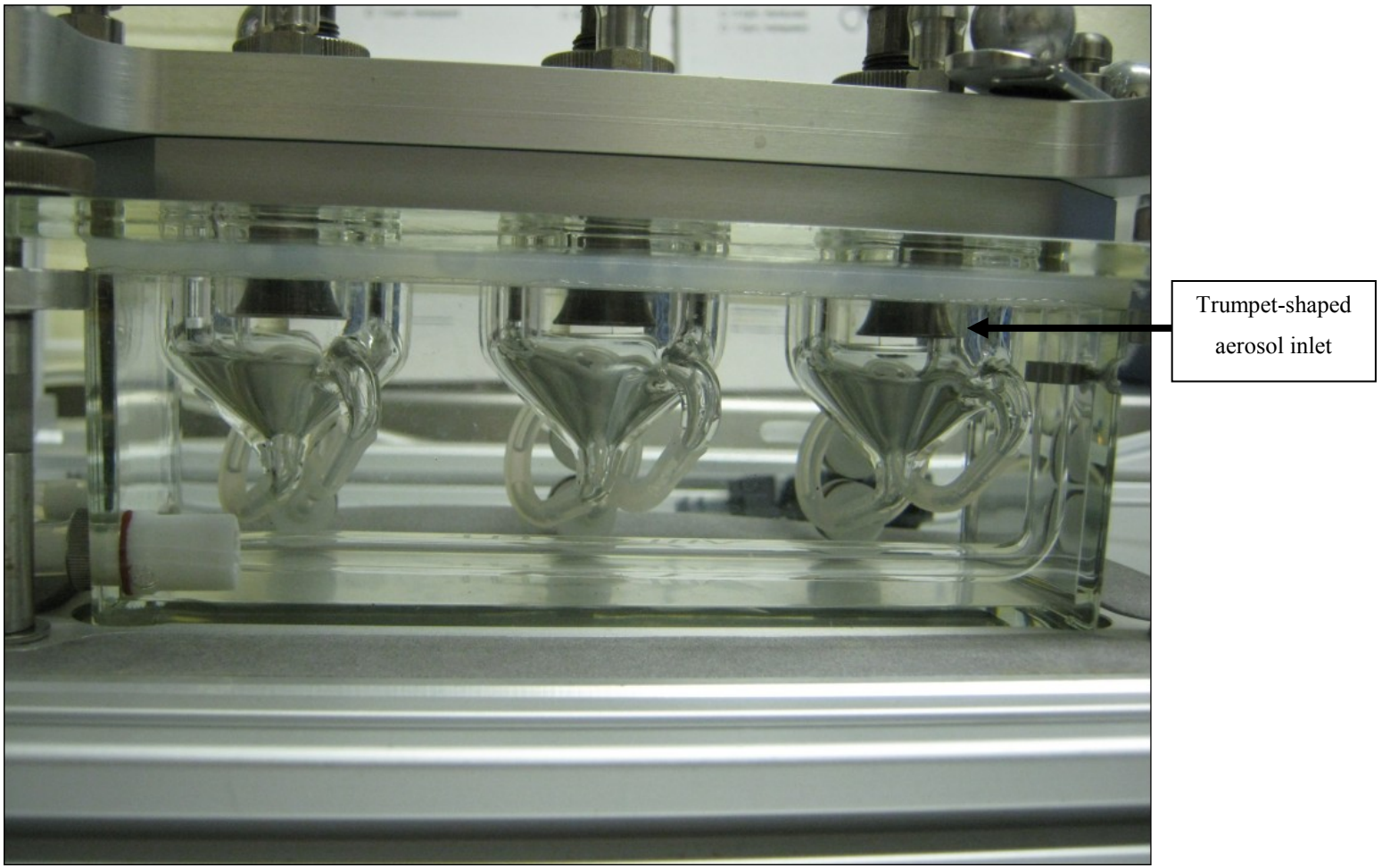

Figure 2.3: Side view of a VITROCELL® module. Trumpet-shaped aerosol inlets are visible above the cell exposure areas (tissue culture inserts not present).

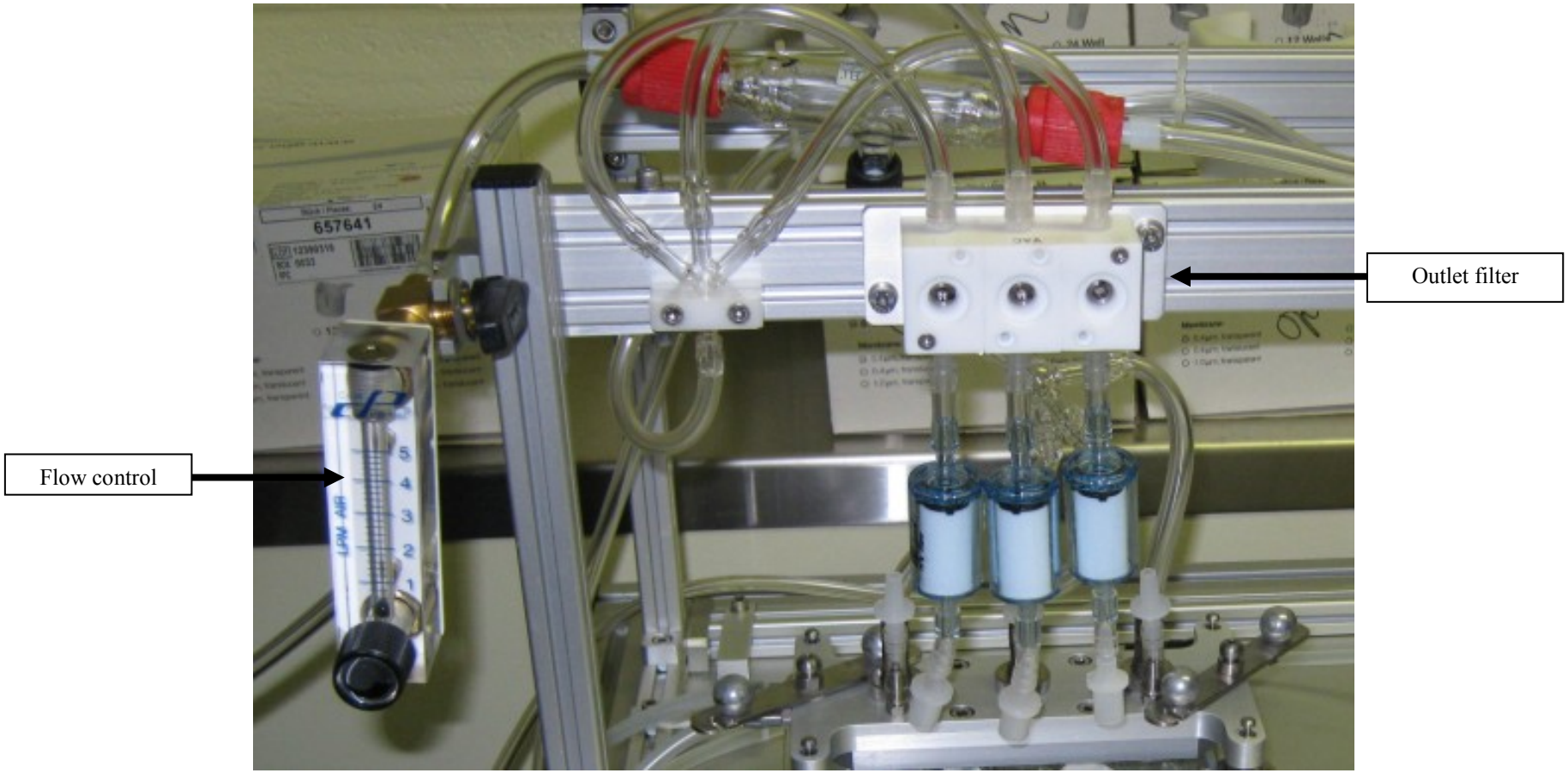

Figure 2.4: View of the aerosol delivery system. Flow control and outlet filters were added to the system to improve performance.

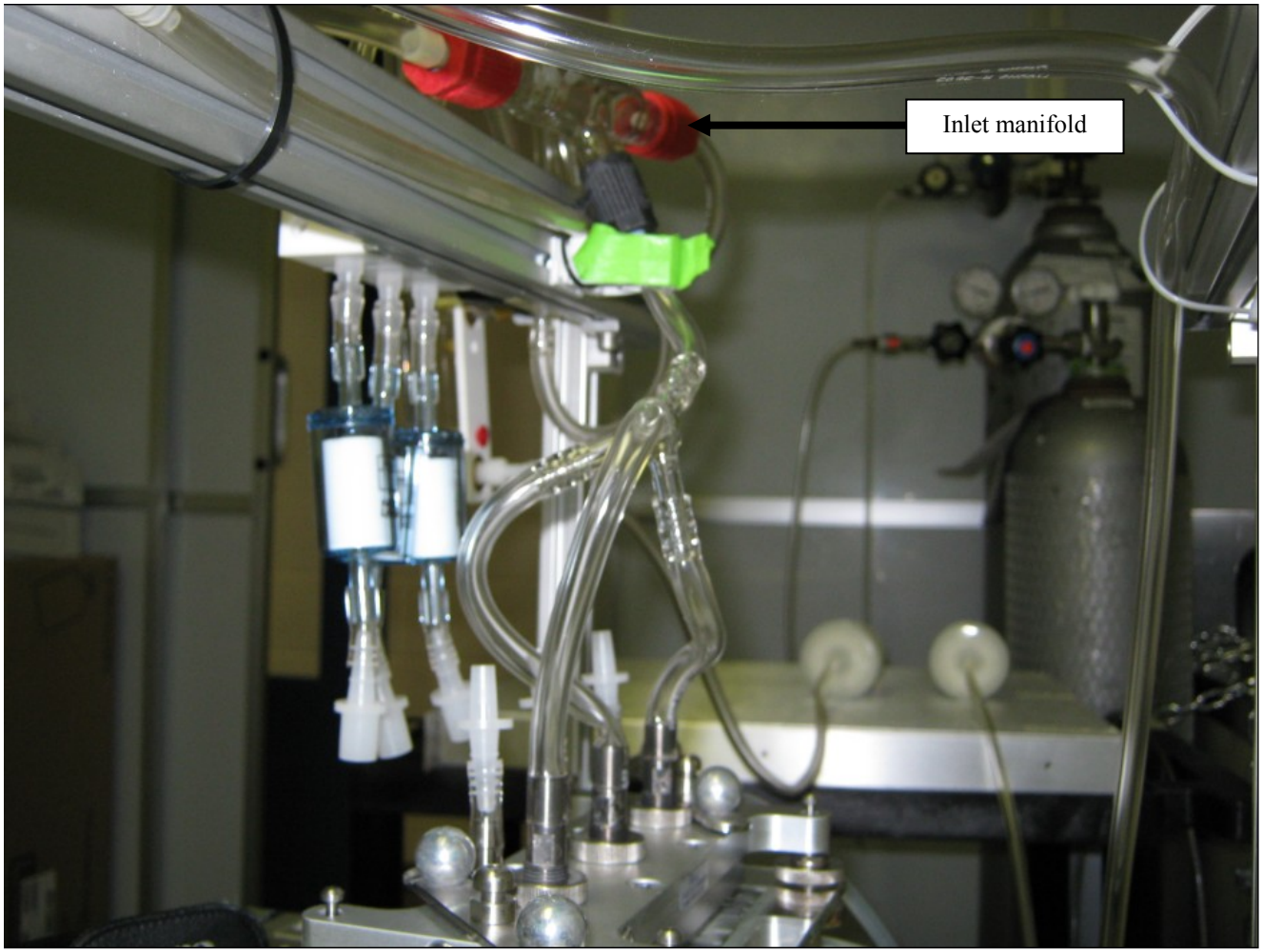

Figure 2.5: View of glass manifold for delivery of aerosol to the negative control module.

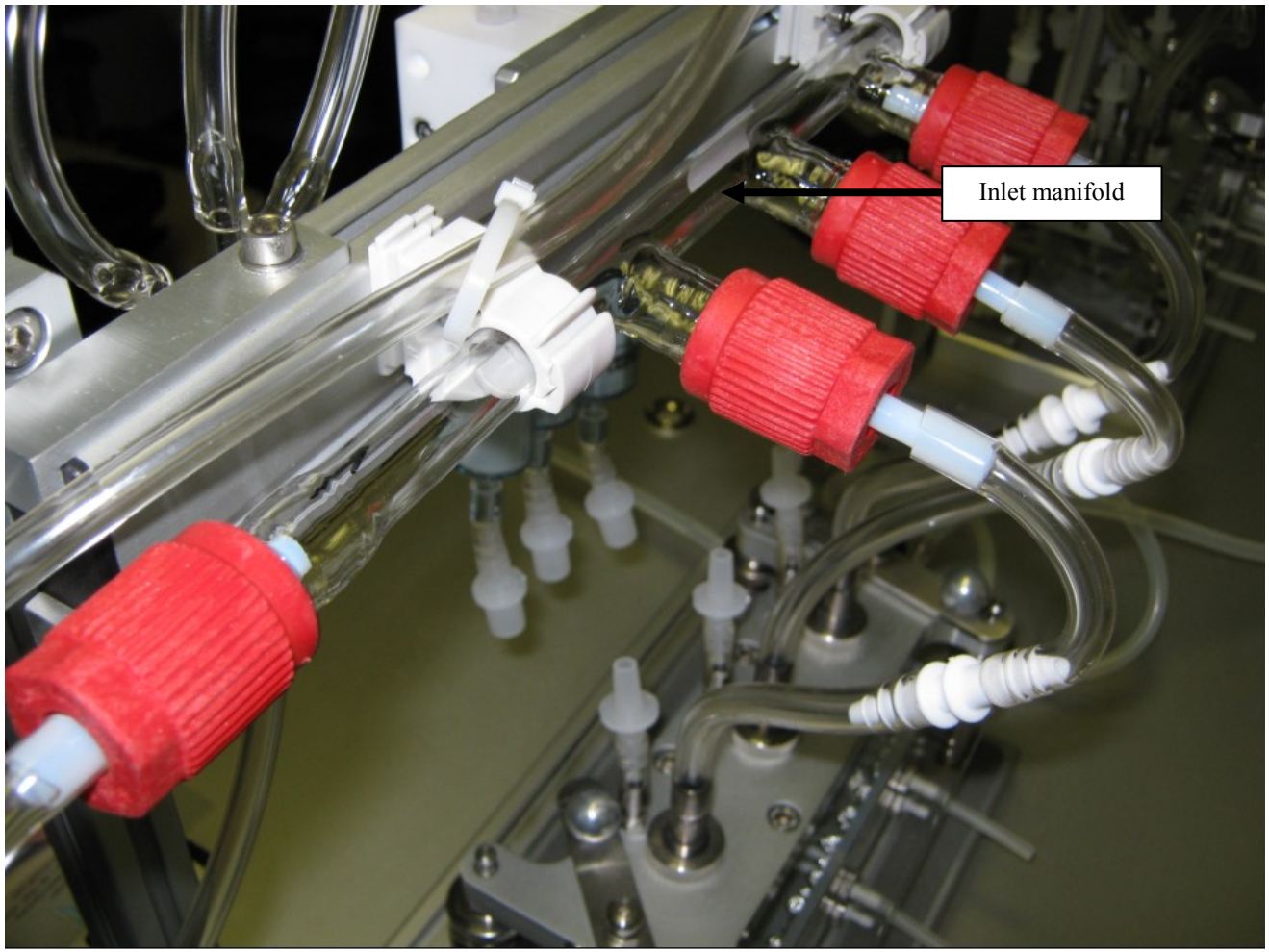

Figure 2.6: View of the glass manifold for delivery of test aerosol to the exposure module.

2.2 Modifications of the VITROCELL® System

To improve the performance of the VITROCELL® system, several notable modifications were introduced over the course of the project. Valved flowmeters (0.4 – 5 lpm, Cole-Parmer) (as seen in **Figure 2.4**) were added to allow flow control to the manifold when utilizing compressed gases as the test aerosol (e.g., NO_2). Microfibre filters (VWR International, Mississauga, ON, Canada) were added between the module outlets and the vacuum flow valves to prevent particle deposition in the valves.

Based on preliminary results, i.e. results of *Phase 1*of the project, it was determined that the intrinsic humidity generation of the basal media was insufficient to maintain the cells during the aerosol exposure. For example, the humidity of the diluted diesel exhaust corresponded to the humidity of the dilution air and was 22.4% - 27.7% relative humidity (RH) at room temperature (21.3°C - 21.8°C), depending on the day (Chan 2010a). The humidity of the compressed gases, i.e. synthetic air and dilute NO_2, were only 0.5% - 2% RH at room temperature. In contrast, humidity in the alveolar and bronchial regions of the lung is maintained at 100% RH at 37ºC (Williams et al. 1996).

A bubble humidifier (Fideris TesSol, Washington, USA) was employed during the initial attempts to provide supplementary humidity to the delivered aerosols, i.e. *Phase 2* experiments. However, the system was not amenable to the concurrent humidification of two disparate aerosol streams, and retention of humidity between the humidifier and the exposure modules proved to be extremely difficult.

Subsequent system modifications designed to permit an ambient environmental temperature around the VITROCELL® system of 37ºC and to humidify the aerosol streams in-line immediately before delivery to the modules, were designed and implemented in collaboration with scientific and engineering staff at the U.S. EPA (NHEERL, Research Triangle Park, NC). A Plexiglas box (**Figure 2.7**) was built to enclose the top of the VITROCELL® cart; doors in the front of the box allow access to the VITROCELL®. Heating pads and insulation (**Figure 2.8**) were placed underneath the VITROCELL® modules to prevent heat loss to the metal cart. A heater and circulating fan were placed at the rear of the box (not shown). The heater was replaced with a higher wattage heater following initial experiments (i.e., clean air exposures). Environmental

temperature was confirmed by temperature monitors inserted in the Plexiglas box, and by a handheld infrared thermometer. A sheet metal base was added to the bottom of the VITROCELL® cart to permit equipment storage, and a lid was added to the circulating water bath. **Figure 2.9** shows the completed set-up for temperature control, excluding the additional supplementary heater. The VITROCELL® vacuum pump is also visible.

An in-line humidification system is based on previous work by Dr. José Zavala-Mendez (Zavala 2014). The initial design employed modifications of commercially available diffusion dryers (TSI, Shoreview, MN, USA); the internal tube of the dryer was wrapped with microporous nylon film and craft felt. The felt was wetted by hand before starting the exposures, and dried by passing air overnight following exposures. Aerosol passed through the dryer was humidified in proportion to the flow rate. Two humidifiers were placed in the VITROCELL® chamber, one immediately before delivery to the manifold of each module. The temperature maintenance afforded by the chamber prevented condensation of the humidity. A water trap was added to the outlet line to prevent condensation from reaching the vacuum pump. **Figure 2.10** shows the initial in-line humidifiers in the VITROCELL® chamber. The design was refined and custom manufactured stainless steel versions were employed. A disassembled humidifier is shown in **Figure 2.11**. The interior tube, which has laser drilled openings to replace the mesh of the diffusion dryer, was wrapped with microporous nylon film and craft felt, as shown in **Figure 2.12**. Digital hygrometers in plastic vessels were used to measure temperature and humidity at the manifold outlets during each exposure. The complete system is shown in **Figure 2.13**. The supplementary heater (increased wattage) and circulating fan are also visible in this figure.

Figure 2.7: Plexiglas box built to maintain temperature.

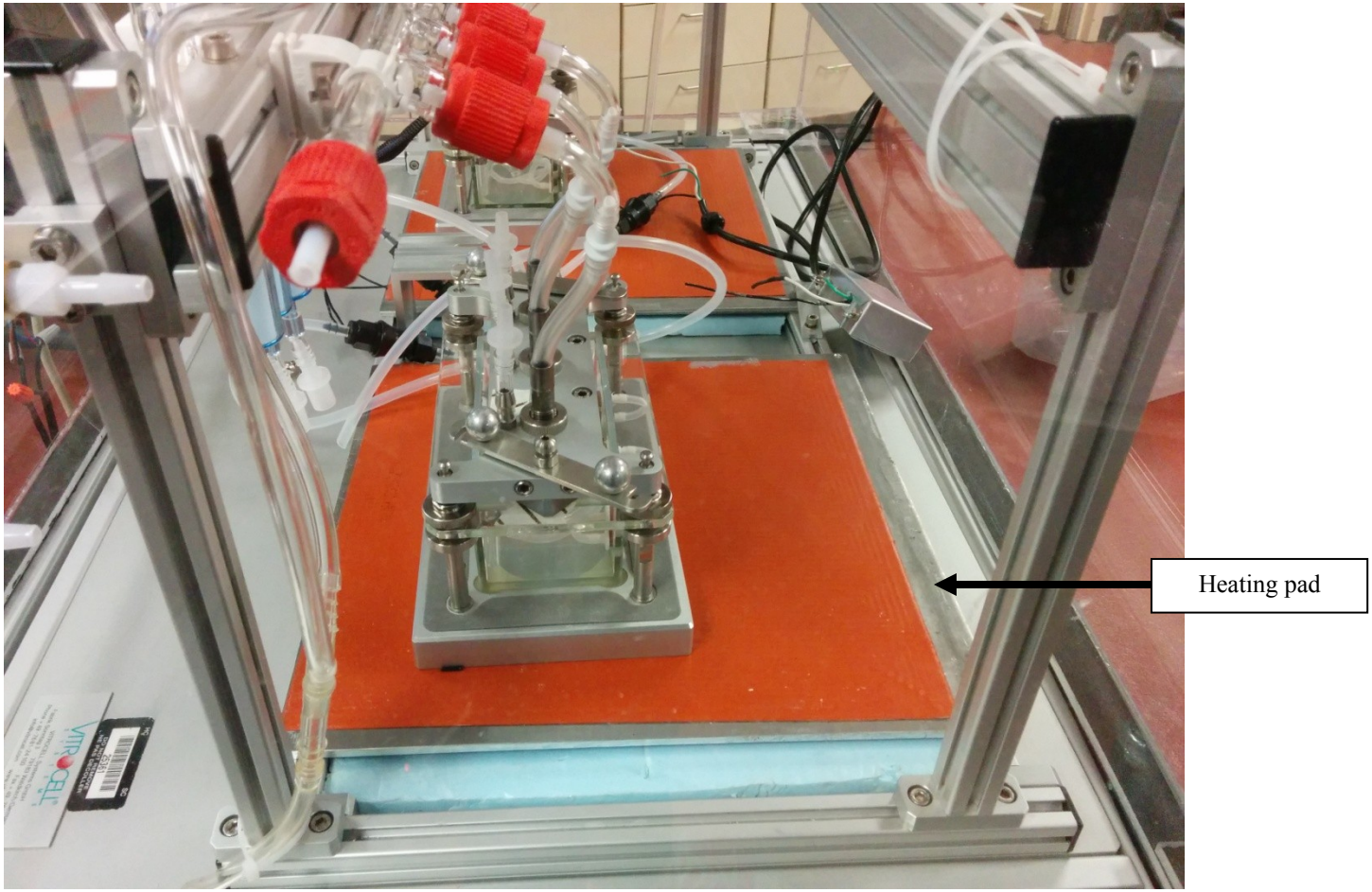

Figure 2.8: Heating pads and insulation below modules to permit temperature maintenance.

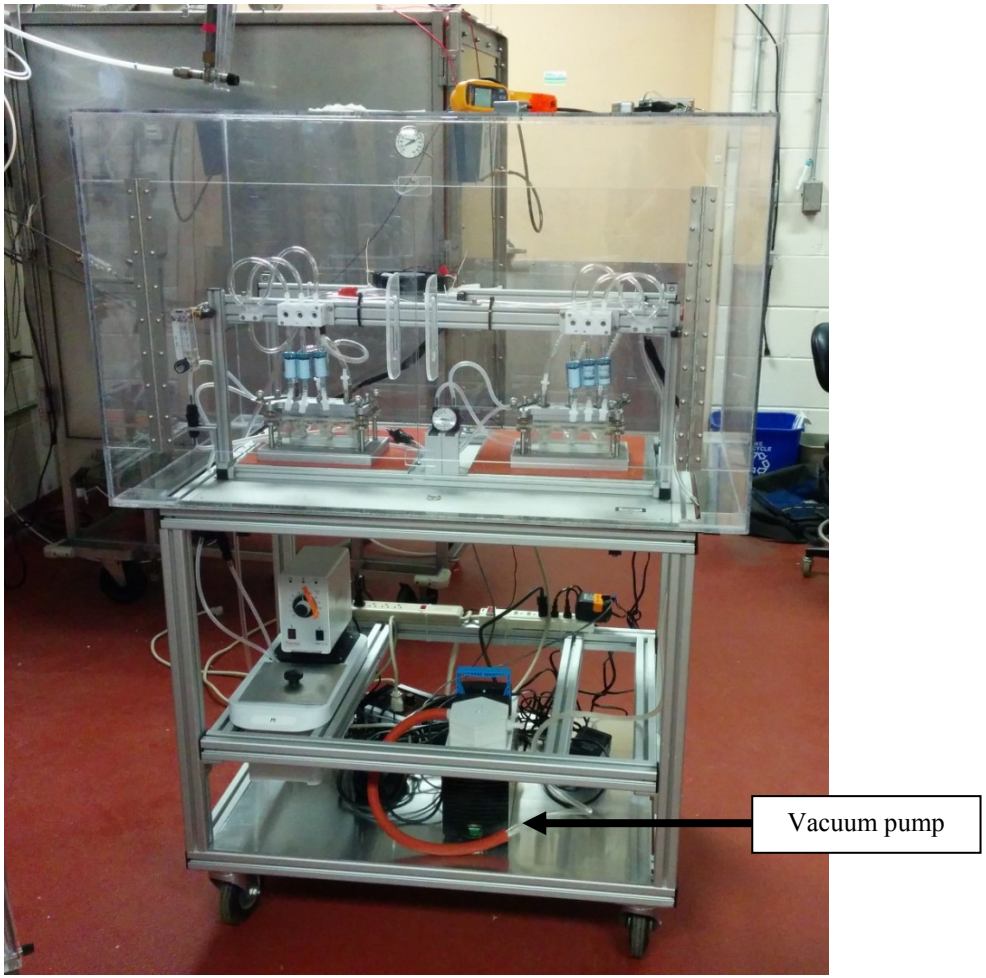

Figure 2.9: Modified VITROCELL® setup in the U.S. EPA facility. Installation shows modifications for environmental temperature control, excluding the supplementary heater that was added later. The vacuum pump is shown at the bottom of the cart.

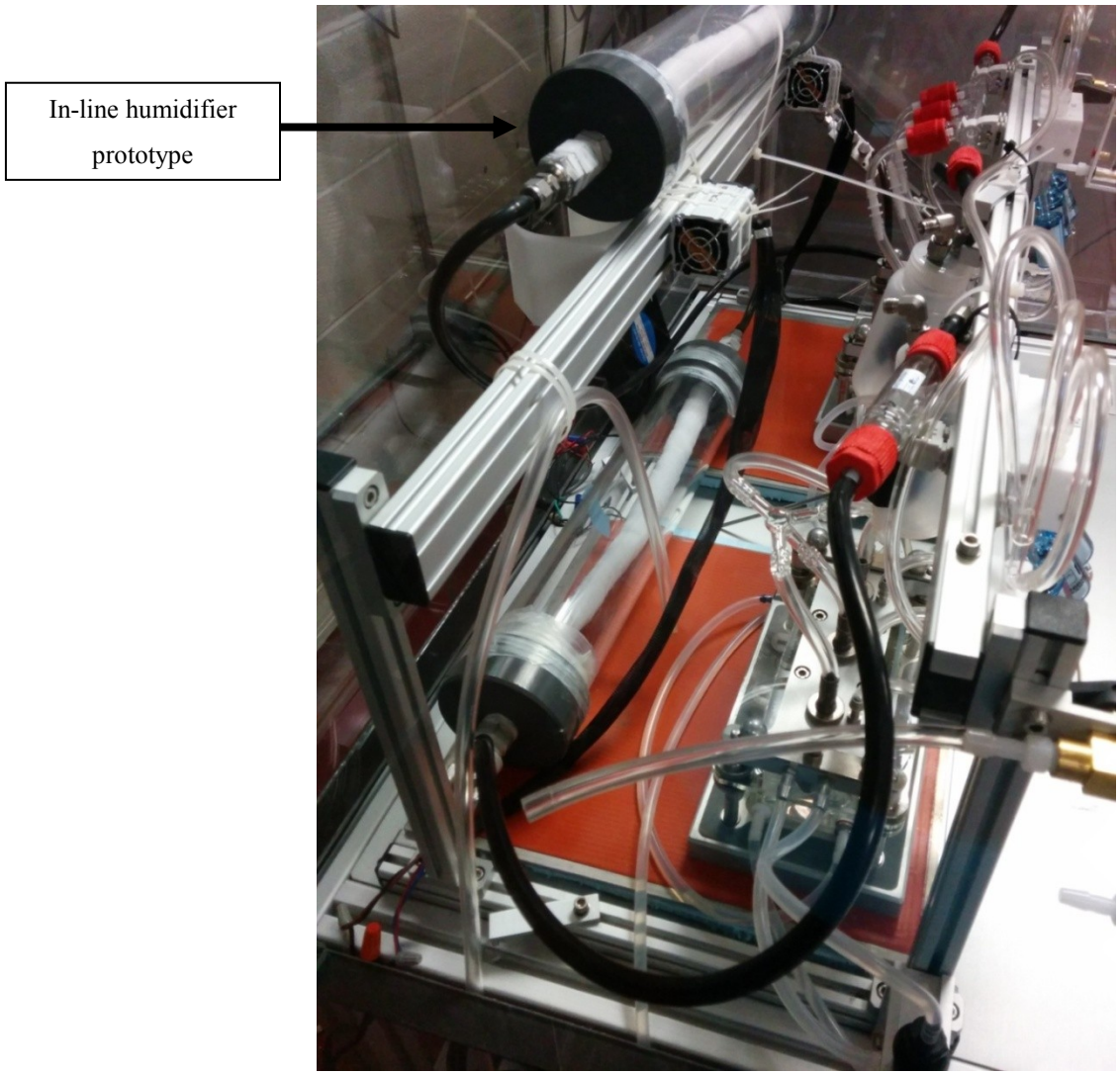

Figure 2.10: Initial design for humidification system.

Figure 2.11: Fabricated parts for humidification system.

Figure 2.12: Assembly of fabricated humidifiers.

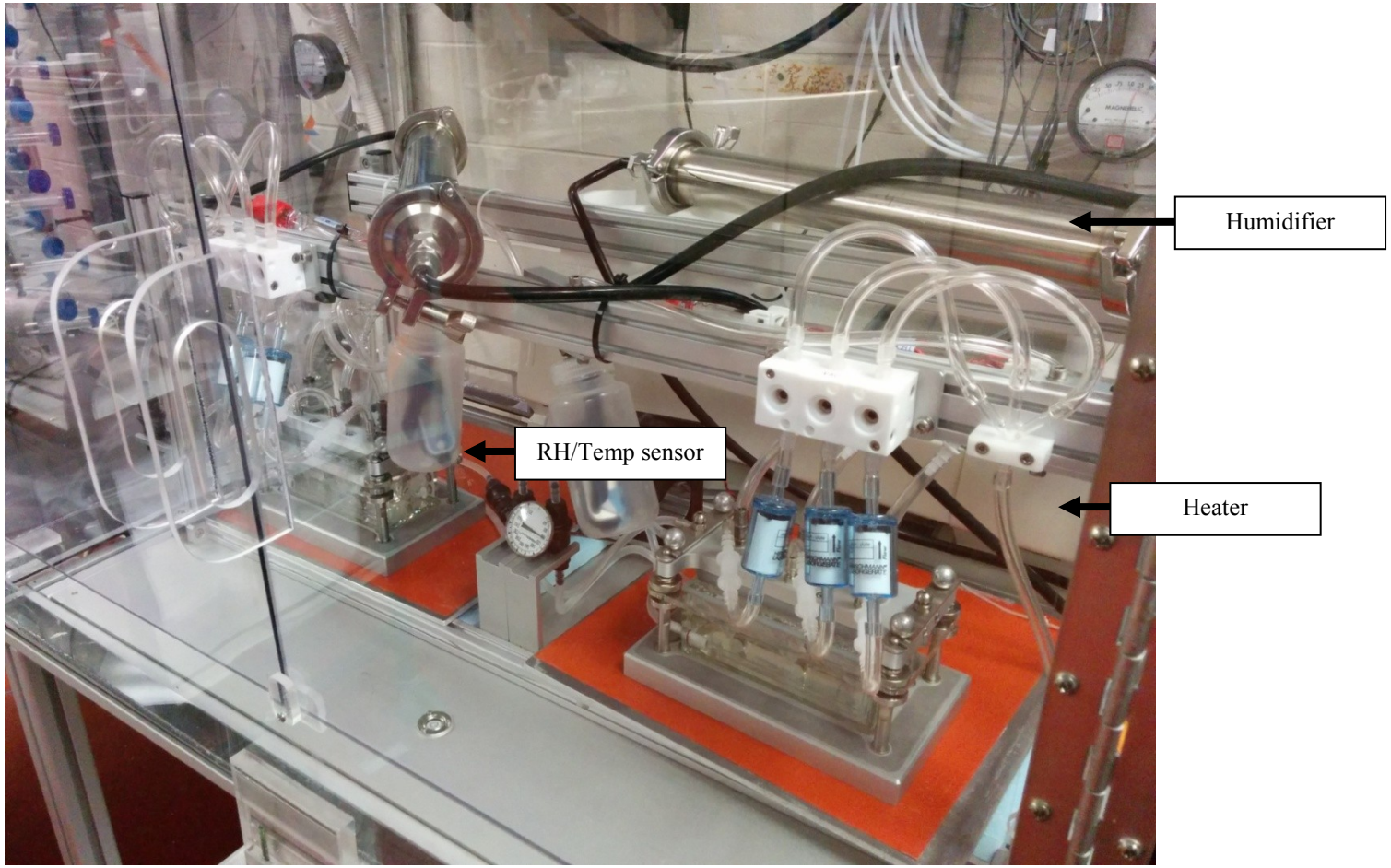

Figure 2.13: Complete, modified VITROCELL® system with temperature control and humidification apparatus.

2.3 Generation of Exposure Aerosols

Aerosol generation protocols varied with the type/identity of the aerosol and the facility apparatus, e.g., exposures to nitrogen dioxide were conducted at the Environmental Health Centre (EHC, Health Canada, Ottawa) and exposures to diesel emissions were conducted at Environment Canada (River Road facility) and the U.S. EPA's Highbay facility (NHEERL, Research Triangle Park, NC). Exposures to simulated urban atmospheres (smog) were conducted at U.S. EPA's Highbay facility.

Grade 0.1 compressed synthetic air (Linde Canada Limited, Mississauga, ON, Canada; Linde North America Inc., Murray Hill, NJ, USA) was used as a negative control for all experiments.

2.3.1 Nitrogen Dioxide Exposures (Health Canada, Ottawa)

All aerosol exposures conducted at Health Canada used compressed gases purchased from Linde Canada Limited (Mississauga, ON, Canada). Nitrogen dioxide mixtures were purchased by special order at concentrations of 5 ppm, 10 ppm, and 20 ppm balanced with grade 0.1 synthetic air.

2.3.2 Light-duty Diesel Exhaust Exposures (Environment Canada, Ottawa)

A 4-cylinder, turbo charged, direct injection, light-duty diesel engine (1998 - 2003 ALH engine from a 2001 Volkswagen beetle) with 1.9 liter displacement mounted on an engine dynamometer was used for all experiments. An OEM (original equipment manufacturer) diesel oxidation catalyst (suitable for fuels with < 300 ppm sulfur) was installed, and emissions were generated under a steady-state condition (2000 rpm engine speed, 19 kW power, 72 ft-lb dynamometer load) derived from the US06 drive cycle. The engine was fueled with ULSD (< 15 ppm sulfur), canola and tallow biodiesel, and diesel-biodiesel blends (B20). Whole diesel emissions were diluted with high-efficiency particulate absorption (HEPA)-filtered room air in a constant volume sampling (CVS) dilution tunnel and delivered to the VITROCELL® by a Venturi mini-diluter. Total dilution was 40:1. **Figure 2.14** shows the VITROCELL® set up in front of the CVS.

Emissions were characterized as previously published (Rosenblatt et al. 2008). Emissions of CO, CO_2, NO_x, NO, NO_2, and THC were measured for each experiment in the CVS

upstream of the VITROCELL®, and adjusted to reflect the dilution delivered to the VITROCELL®. Particle number concentration was measured for each experiment using a condensation particle counter (CPC) and an ultrafine CPC (models 3022A and 3025A, TSI, Shoreview, MN, USA). For preliminary characterization of aerosol delivery to the VITROCELL® particle number and size concentration were measured upstream and downstream of the VITROCELL® module. Polydisperse aerosol particles were size-selected by a nano-scanning mobility particle sizer (SMPS), followed by measurement of particle number concentration by a TSI 3776 CPC. For PM characterization, a combined flow of 300 ml/min was sent through the VITROCELL® module to meet the flow requirements of the SMPS.

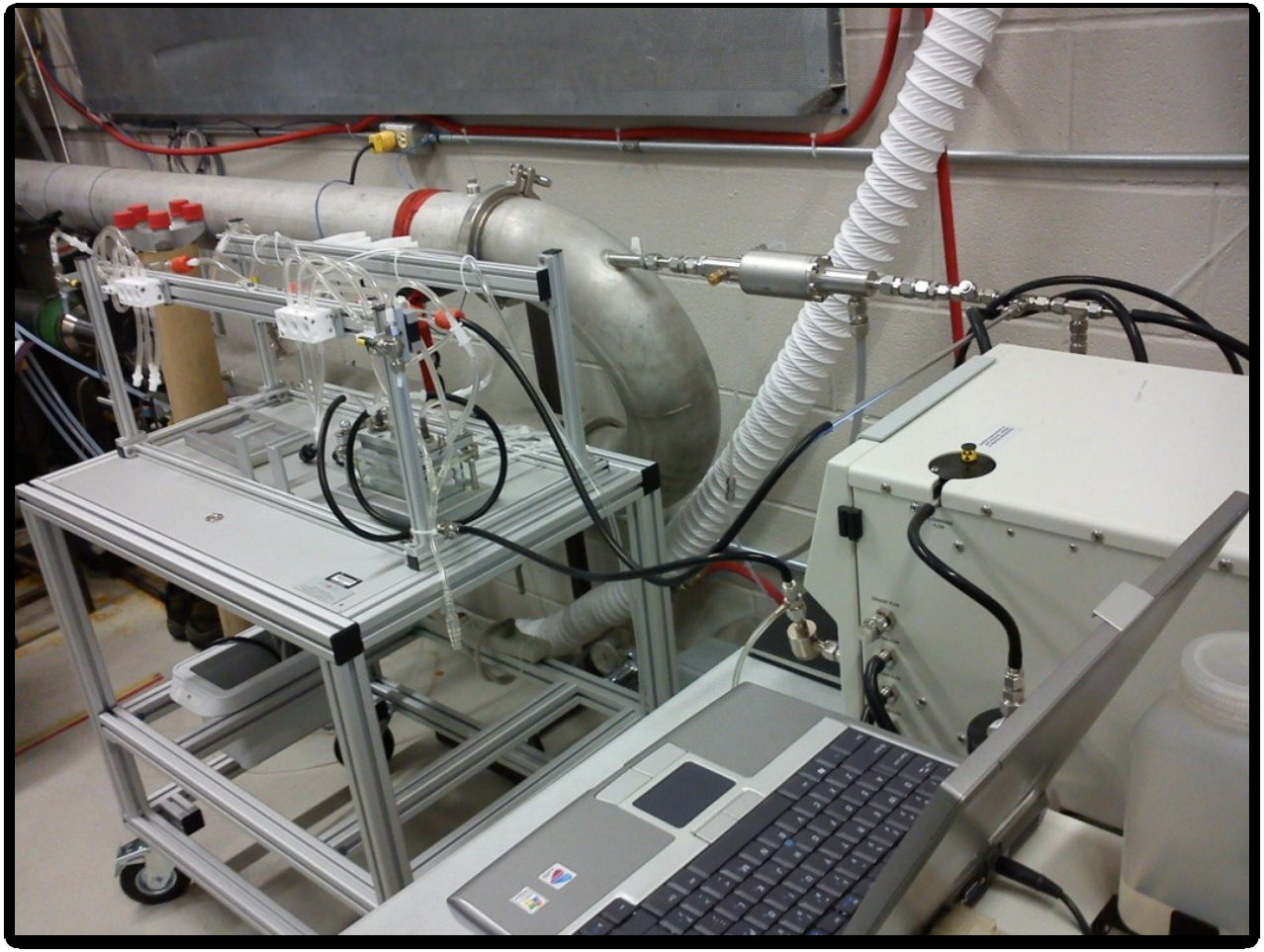

Figure 2.14: VITROCELL® set-up in front of the dilution tunnel at Environment Canada's River Road facility. The Venturi mini-diluter is shown drawing diluted exhaust from the CVS (curved large diameter pipe). The foreground shows PM-monitoring apparatus.

2.3.3 Diesel Generator Exhaust Exposures (NHEERL Highbay facility, US EPA, Research Triangle Park, NC)

Emissions were generated as described previously (Kodavanti et al. 2013, Gordon et al. 2012). A 4.8 kW single-cylinder direct injection diesel generator (Yanmar L70 V) with 0.32 L displacement was operated at a constant 3 kW load. ULSD fuel (< 15 ppm) was used for all experiments. A single eductor operating near the engine exhaust port drew in approximately 2 L/min of diesel exhaust to mix with HEPA-filtered dilution air. Diluted whole exhaust was directed to a Hazelton-1000 (984 L) exposure chamber, used as a sampling chamber. Emissions were aspirated from the chamber using an eductor (Fox Valve, model 611210-015, Dover, NJ, USA) at a 2.5:1 or 5:1 dilution for delivery to the VITROCELL®. Compressed synthetic air (Linde North America Inc.) was used for all dilution air. Carbon-impregnated conductive tubing was used for delivery from the sampling manifold to the VITROCELL® system. **Figure 2.15** shows the VITROCELL® set up next to the sampling chamber.

Dilution ratios from the engine to the sampling chamber were changed for each exposure day to reach the target particle concentration. The target concentration was progressively increased based on the limited cell response observed. I.e., the ratio for dilution from the engine to the sampling chamber ranged from 2.9:1 to 5.2:1, the ratio for dilution from sampling chamber to VITROCELL® ranged from 2.5:1 to 5:1, and total dilution (engine to VITROCELL®) ranged from 7.1:1 to 25:1.

Emissions of particle mass concentration (tapered element oscillating microbalance (TEOM), Thermo Scientific., series 1405, Fitchburg, WI, USA), CO (Thermo Scientific, model 48i-TLE, Fitchburg, WI, USA), and NO_x (Thermo Scientific, model 42i, Fitchburg, WI, USA) were measured for each experiment.

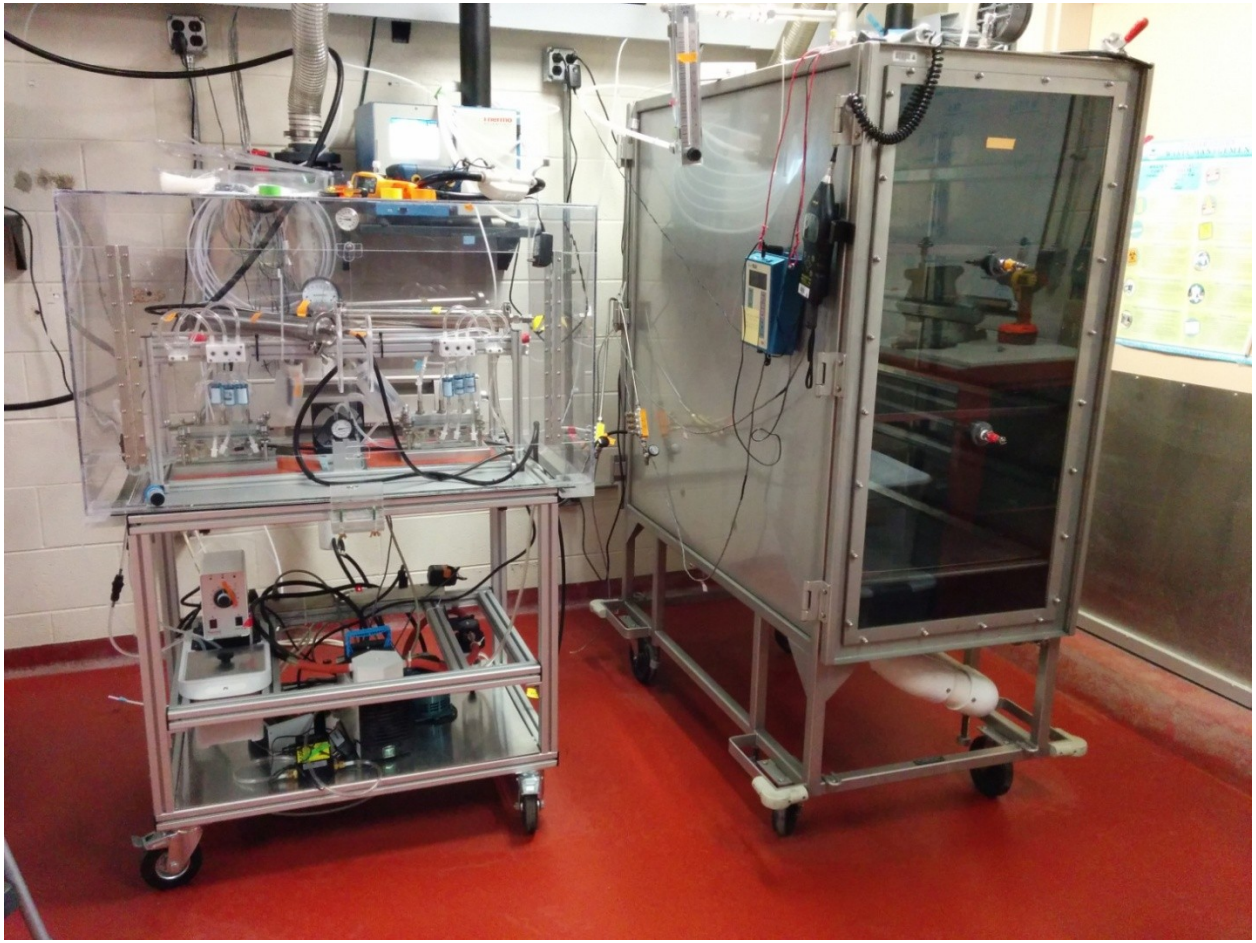

Figure 2.15: The modified VITROCELL® system adjacent to the diluted diesel sampling chamber (U.S. EPA NHEERL Highbay facility in Research Triangle Park, NC).

2.3.4 Simulated Urban Atmosphere Exposures (NHEERL Highbay facility, US EPA, Research Triangle Park, NC)

A state of the art mobile photochemical reaction chamber (MRC) was used to generate simulated urban atmospheres (i.e., smog) for an ongoing murine study. The custom-built 14 m^3 chamber was contained in a 24' trailer. The chamber contains 120 fluorescent tubes evenly mixed with black lights and UV sources (300 – 400 nm). 10 mg/liter ammonium sulfate, 6 ppmC alpha pinene, and 24 ppmC gasoline, were injected into the chamber for continuous generation of smog until the completion of the two-week exposure. PpmC represents the concentration of carbon atoms in the gas. The MRC contents were drawn via an aspirator at a ~2:1 dilution ration and pushed into the nose-only animal exposure. The VITROCELL® was connected by Tygon® tubing to one of the nose-only chamber ports of the negative control and smog exposure chamber, respectively. Murine exposures were conducted in the morning, with VITROCELL® exposures conducted in the afternoon when the animal, nose-only exposure chambers were not in use. **Figure 2.16** shows the VITROCELL® set up in front of the nose-only exposure chambers.

Particle mass concentration was determined via TEOM (Thermo Scientific., series 1405, Fitchburg, WI, USA). NO_x (Thermo Scientific, model 42i, Fitchburg, WI, USA), and O_3 (API, model 400, San Diego, CA) were also measured for each experiment.

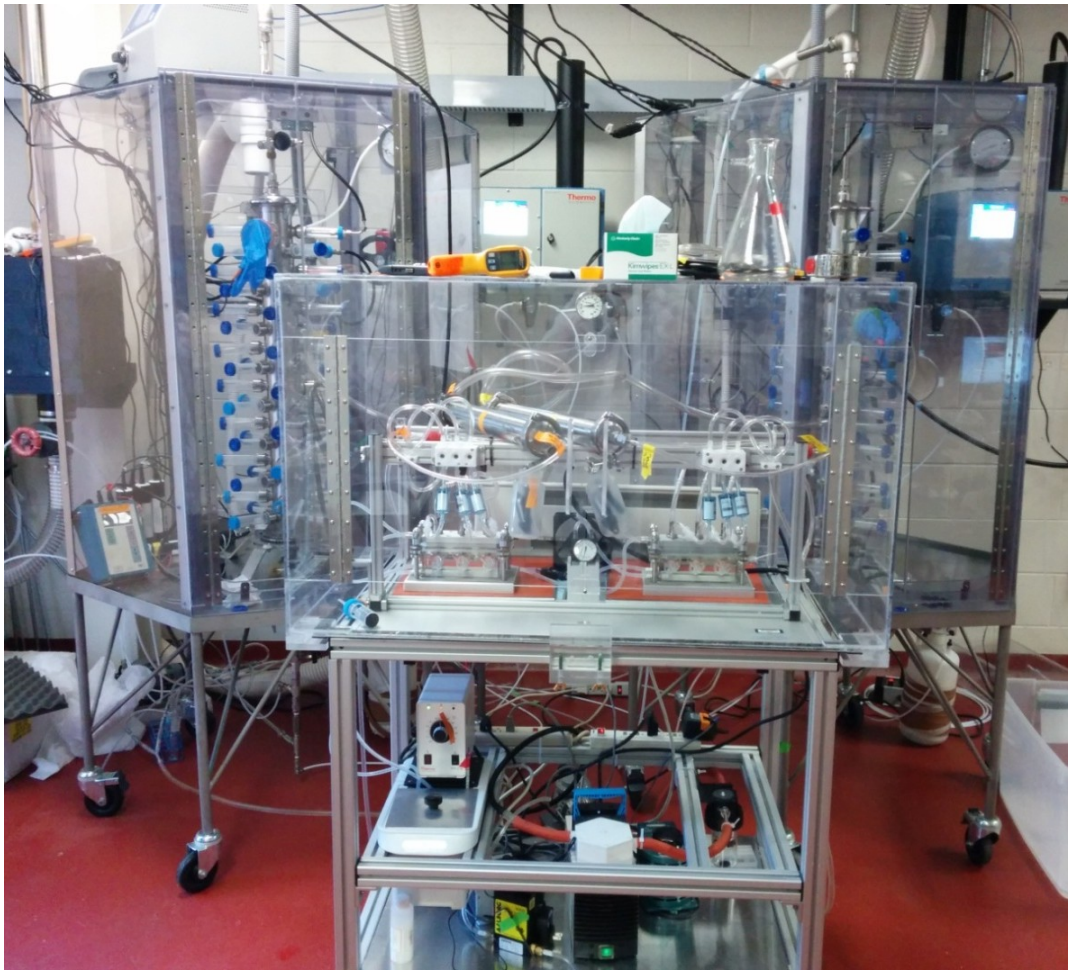

Figure 2.16: VITROCELL® system showing the sampling chamber for simulated smog exposures (back left). The chamber contains nose-only animal exposure instrumentation, which was not in use during VITROCELL® exposures (Highbay facility, Research Triangle Park, NC).

2.4 Cell Culture

Cells were grown using conventional methods for routine passaging. For air-liquid interface exposures, cells were seeded on commercially available semiporous membranes. Adenocarcinomic human alveolar epithelial cells (A549) (Giard et al. 1973) were used for exposures at Health Canada and Environment Canada facilities. For exposures at the U.S. EPA's NHEERL facility, virus-transformed normal human bronchial cells (BEAS-2B) (Lechner and LaVeck 1985, Reddel et al. 1988) were used. The change in cell line was justified based on the decision to re-evaluate exposure protocols (e.g. insert brand selection, collagen coating) concurrently with physical optimizations of the VITROCELL® system. Wherein the A549 cell line is adenocarcinomic and the BEAS-2B cell is a virally transformed cell line, it was expected that the BEAS-2B line would be more reflective of the expected physiologic response. Additional differences in cellular response are also expected as A549 is an alveolar epithelial cell line whereas BEAS-2B is a bronchial epithelial cell line.

2.4.1 Human Alveolar Adenocarcinoma (A549) Cells

A549 cells were purchased from the American Type Culture Collection (ATCC, Manassas, VA,) and used within 20 passages of receipt. Frozen aliquots were stored in liquid nitrogen. Cells were cultivated in Kaighn's Modification of Ham's F-12 Medium (F-12K, ATCC) or RPMI 1640 (Life Technologies Inc., Burlington, ON) depending on the experiment. For both media formulations, media was supplemented with 10% fetal bovine serum (FBS, ATCC) and 100 U/ml penicillin-streptomycin (Life Technologies) in a standard humidified tissue culture incubator maintained at 37 °C and 5% CO_2. For propagation, cells were cultured on standard 100 mm tissue culture dishes (Corning Life Sciences, Tewksbury, MA).

For ALI-exposure experiments, cells were collected by trypsinization (0.25% trypsin, Life Technologies) and seeded on commercially available tissue culture-treated inserts (ThinCert^{TM} inserts 657640 or 657641, Greiner Bio-One, Monroe, NC, USA). These polyethylene terephthalate (PET) inserts have a 4.52 cm^2 culture surface area and hanging geometry compatible with 6-well plates. Pore size is 0.4 μm. The 657640 inserts have 1 x

10^8 cm^{-2} pore density and translucent optical properties. The 657641 inserts have 2 x 10^6 cm^{-2} pore density and transparent optical properties.

Pre-exposure culture conditions, including seeding density, handling, and growth time varied in order to optimize the conditions for aerosol analyses.

2.4.2 Virus-transformed Normal Human Bronchial Cells (BEAS-2B)

BEAS-2B cells (ATCC) were used within 20 passages of receipt, and frozen aliquots were stored in liquid nitrogen. Cells were cultivated in Bronchial Epithelium Basal Medium (BEBM) as recommended by ATCC. 500ml BEBM (Lonza/Clonetics Corp, Walkersville, MD) was supplemented using BEGM SingleQuot supplementation kits (Lonza/Clonetics Corp.) containing 2 ml bovine pituitary extract (BPE), 0.5 ml hydrocortisone, 0.5 ml human epidermal growth factor (hEGF), 0.5 ml epinephrine, 0.5 ml transferrin, 0.5 ml insulin, 0.5 ml retinoic acid, and 0.5 ml triiodothryonine. 5 ml of 10,000 U/ml penicillin-streptomycin (Life Technologies, Grand Island, NY), was used instead of the gentamycin-amphotericin B mix included with the BEGM kit. For propagation, cells were cultured in T75 flasks (Corning Life Sciences, Tewksbury, MA, USA).

For ALI-exposure experiments, cells were collected by trypsinization and seeded on commercially available tissue culture-treated inserts (Transwell®, Corning Life Sciences). These inserts are PET, with 4.67 cm^2 growth area compatible with 6-well plates, 0.4 µm pore size and 4 x 10^6 cm^{-2} pore density, and transparent optical properties. Inserts were coated with PureCol® type I bovine collagen solution (Advanced BioMatrix, San Diego, CA) at least 18 hours before cells were seeded. Coated inserts prepared more than 18 hours in advance were stored in sterile packaging at 4°C. 400,000 cells were seeded per insert and incubated 24 hours before exposure. Cells were grown submerged, i.e., with both apical and basal media, until 30 minutes before exposure when the apical media was removed and inserts transferred to plates with fresh basal medium.

2.5 Cell Exposures Using the VITROCELL® Exposure System

For ALI exposure experiments, cells were grown to confluence on semiporous inserts as described. Three replicate inserts were prepared for each exposure condition. Test aerosol (i.e., NO_2, diesel emissions, or smog) and clean air exposures were conducted

simultaneously. A third set of replicates for each exposure was kept in the cell culture incubator (i.e., handling control). The clean air control constituted a negative control for the effects of the test aerosols; the incubator control constituted a control for the effects of handling and air-liquid interface exposure.

Prior to exposure, the apical media was removed from each insert. Cells were washed twice with phosphate-buffered saline (PBS, Life Technologies) and subsequently transferred to the prepared VITROCELL® system (i.e., fresh basal medium). All VITROCELL® exposures used the media formulation employed to culture the cells, with HEPES (4-(2-hydroxyethyl)-1-piperazineethanesulfonic acid, Life Technologies) as required. Unless otherwise noted, all exposure media was supplemented with FBS.

Unless otherwise noted, all VITROCELL® exposures were 1 hour in duration. Vacuum flow rates were checked immediately before initiating each exposure, and basal medium was changed before each exposure. The vacuum flow rate varied, with 8.3 ml/min for each well employed at Environment Canada and 5 ml/min employed for experiments conducted at the Highbay facility.

For exposures conducted at Health Canada and Environment Canada, exposure inserts under ALI conditions in 6-well plates were transported from the nearby cell culture lab to the VITROCELL® (i.e., about 1 minute delay at Health Canada, about 5 minutes at Environment Canada). Transport at Environment Canada employed a Styrofoam box. The 6-well carrier plates were returned to the culture lab incubator for the duration of the exposure, and then transported back to the VITROCELL® location at the end of the exposure for transportation of the exposed cells back to the culture lab.

For exposure of BEAS-2B cells at the NHEERL Highbay facility, cells were transferred from the main laboratory to a humidified incubator (37°C, no CO_2 supplementation) at the exposure location and allowed to re-equilibrate for approximately 20 minutes. Following the exposure, inserts were returned to the main lab for post-exposure incubation and manipulation. Transportation between the main lab and the Highbay area took approximately 10 minutes. ALI inserts in 6-well plates with fresh BEGM basal medium supplemented with 20 mM HEPES were transported in a Styrofoam box. Three replicates

of unexposed inserts were also prepared, transported to the Highbay facility, and maintained at the Highbay incubator for the duration of the exposure. These were designated 'Field' controls (i.e., manipulation controls). Initially, both Incubator (main lab) and Field controls were analysed; later comparative analyses used only Field controls. Basal medium for all Highbay VITROCELL® exposures was supplemented with 20 mM HEPES. Inserts were transferred to new 6-well plates with fresh basal media without HEPES for post-exposure incubation. Incubator controls were not supplemented with HEPES. Post-exposure incubation times varied across exposure aerosol (i.e., diesel, smog) and endpoint.

2.6 Endpoints

Following each aerosol/gas exposure, cells were examined for induction of a variety of toxicological responses. The endpoints examined varied across the exposure type and phase of the project. Post-exposure incubation times ranged from 0 to 24 hours. In general, for aerosol exposures, preliminary exposures utilized a post-exposure incubation of 0 hours to detect overt cytotoxicity following exposure. Cells were analyzed after 24 hours post-exposure incubation to detect responses induced by the exposure aerosol. As at 24 hours cells have had time to repair and replicate, this was later shortened to 6 hours post-exposure to detect short-term changes in gene expression.

Multiple assays for cell viability or cytotoxicity were used to provide a broader understanding of the response. For example, an increase in cytotoxicity measured by LDH is indicative of cell death, whereas a decrease in cell viability as measured by WST-1 may indicate decreases in cellular metabolism without cell death, e.g. senescence.

2.6.1 WST-1 Assay for Cell Viability

The Cell Proliferation Reagent WST-1 kit (Roche Applied Science, Laval, QC) was used to measure cell viability. The tetrazolium salt 4-[3-(4-iodophenyl)-2-(4-nitrophenyl)-2H-5-tetrazolio]-1,3-benzene disulfonate (WST-1) is an alternative to the traditional MTT assay (Ishiyama et al. 1993, Berridge and Tan 1998). Reduction of WST-1 results in a water-soluble formazan dye that is detectable by spectrophotometry. WST-1 is reduced extracellularly by trans-plasma membrane electron transport via an intermediate electron acceptor, e.g. 1-methoxy phenazine methosulfate (PMS) (Berridge et al. 2005). NADH is

proposed to be the primary cellular reductant, and is generated primarily by the mitochondrial citric acid cycle. In contrast to the MTT assay, cells are not lysed before analysis; therefore, the assay can be conducted concurrently or sequentially with other endpoints. In addition, WST-1 is more stable than other commonly used tetrazolium salts such as XTT and MTS.

For early experiments conducted at Environment Canada, exposed cells were collected from insert membranes by trypsinization and pipetted in triplicate into a clear 96-well plate for analysis. WST-1 reagent was added according to manufacturer's instructions, i.e., 10 µl per well to achieve to a 10:1 final dilution. Plates were incubated for 2 hours at 37ºC before measuring spectrophotometric absorbance at 435 nm, with reference at 620 nm.

The protocol was later modified to reduce cellular manipulations. Following exposure, any remaining apical or basal media was removed and 2% WST-1 reagent in culture media added directly to the apical surface of the insert. Inserts were then incubated for 30 minutes at 37ºC and the apical medium then pipetted in 150 µl triplicates into a clear 96-well plate. Culture medium containing 2% WST-1 reagent (i.e., without cells) was used as a control. Absorbance was measured at 435 nm with reference at 620 nm. Data were expressed as viability relative to the negative control (i.e., % control).

2.6.2 Neutral Red Uptake Assay for Cell Viability

The neutral red (NR) assay for viability and cytotoxicity is based on the ability of cells to take up and bind the supravital dye neutral red (Borenfreund and Puerner 1985, Repetto et al. 2008). The dye is weakly cationic and crosses cellular membranes by non-ionic passive diffusion. In viable cells, lysosomes maintain a lower pH than the rest of the cell and inside the lysosome the dye becomes charged and binds to anionic and phosphate groups of the lysosomal matrix by electrostatic and hydrophobic bonds. Non-viable cells do not maintain a lysosomal proton gradient and pH, and do not retain the dye.

The assay was modified for use with membranes insert according to protocols utilized by Mathias Könczöl (Konczol 2012). Briefly, following the exposures, cells were incubated with the NR stain to allow dye uptake. The NR stain was then removed, the cells washed with PBS, and the intracellular stain then released using a destaining solution (50%

ethanol, 49% dH_2O, 1% glacial acetic acid, by volume). The amount of released NR stain was quantified by spectrophotometry.

The NR stock solution (4 mg/mL neutral red, Sigma-Aldrich, Oakville, ON) was prepared in 15ml centrifuge tubes and stored in the dark at 4ºC for up to 4 weeks. The NR-staining solution was prepared 24 hours before use. Briefly, 250 µl NR stock solution was added to 20 ml culture medium, vortexed for 60 seconds, and incubated at 37ºC in a cell culture incubator with a slightly loosened cap to equilibrate pH. Immediately before conducting the assay, the solution was filtered through a 0.2 µm Acrodisc® syringe filter (Pall Corporation, Ville St. Laurent, QC, Canada). The NR-destaining solution was prepared in 100 ml quantities and stored at 4ºC until use.

Following the aerosol exposure, basal medium was removed and 800 µl of NR-staining solution added to the apical surface. Cells were incubated for 2 hours at 37ºC, NR-staining solution removed, and membranes washed twice with PBS. 600 µl NR destaining solution was then added to the apical membrane, and the plate shaken on an orbital shaker for 5 minutes. 150 µl aliquots of the sample were pipetted in triplicate into a clear 96-well plate and absorbance measured at 540 nm, with reference at 645 nm. Data were expressed as viability relative to the negative control (i.e., % control).

The neutral red assay was regularly combined with the WST-1 assay. Following removal of the incubated WST-1 reagent, inserts were washed with PBS and the neutral red stain added as described.

2.6.3 Lactate dehydrogenase (LDH) leakage assay for cytotoxicity

Lactate dehydrogenase is produced ubiquitously by mammalian cells and released following cytotoxic damage. It is commonly measured in *in vitro* supernatants as a marker of cytotoxicity (Korzeniewski and Callewaert 1983).

For all exposures, cells on an unexposed insert (i.e., additional Incubator Control) were lysed in 1x lysis buffer (Pierce LDH Cytotoxicity Assay kit, Thermo Fisher Scientific, Middletown, VA) one hour prior to sample collection and used as a positive control. Following post-exposure incubation, the basal media was mixed using a pipette and 50 µl triplicate aliquots were collected for analysis. A medium blank and lysis buffer blank were

included in each experiment. Aliquots were stored at 4°C in capped vials for up to 7 days until analysis. LDH leakage was measured by Judy Richards (NHEERL, US EPA) and raw data was provided for analysis. In brief, an LDH cytotoxicity kit (Thermo Fisher Scientific) was modified for use on a Konelab Arena 30 (Espoo, Finland). Data were expressed as percent cytotoxicity relative to the negative control. Values were normalized to the maximal cytotoxicity of the positive control, i.e., (Sample value - Mean negative control value)/(Positive control value - Mean negative control value) * 100% for each sample.

2.6.4 Caspase III/VII Assay for Apoptosis

Cysteine-aspartic proteases (caspases) are involved in programmed cell death, i.e., apoptosis. Caspase-3 and -7 are effector caspases. Apoptotic stimuli activate initiator caspases, which in turn activate effector caspases by cleaving an inhibitory domain from the procaspase (Boatright and Salvesen 2003, Lamkanfi and Kanneganti 2010). Effector caspases cleave specific substrates to dismantle the cell. Caspases are not activated in necrosis (Krysko et al. 2008).

The Promega Caspase-Glo® 3/7 assay contains a homogenous reagent for caspase activity, luciferase activity, and cell lysis. The caspase substrate contains an Asp-Glu-Val-Asp (DEVD) amino acid sequence that is specifically cleaved by caspase-3 and -7 during apoptosis. This cleavage product is a substrate for a proprietary thermostable luciferase (Ultra-Glo^{TM} Recombinant Luciferase) that is quantitatively detectable in cell lysate using a luminometer.

This assay was adapted for use with membrane inserts. Briefly, in a darkened room equal parts assay reagent and FBS-free media were added to the apical surface of the insert, mixed gently on an orbital shaker, and incubated for 1 hour at 37ºC. 150 µl aliquots of the sample were pipetted in triplicate into a white 96-well plate and luminescence was measured. Data were expressed as percent of the negative control. To determine the effectiveness of the assay, cells were exposed under non-ALI exposure conditions to a positive control, staurosporine in DMSO (Sigma-Aldrich).

2.6.5 Thiobarbituric Acid Reactive Substances (TBARS) Assay for Lipid Peroxidation

Lipid peroxidation occurs as a product of oxidative stress. Thiobarbituric acid reacts with the end-product of lipid peroxidation, i.e., malondialdehyde (MDA), to yield a fluorescent product (Fraga et al. 1988). The protocol for this assay was adapted from work by Mathias Könczöl (Konczol 2012).

Sufficient TBA-reagent (40 mg thiobarbituric acid, Toronto Research Chemicals, Toronto, ON), 500 µl 10% sodium dodecyl sulfate (SDS), Sigma-Aldrich, 500 µl glacial acetic acid, per 10 ml dH_2O) was prepared in a centrifuge tube immediately prior to conducting the assay, vortexed for 30 seconds, and sonicated for 5 minutes. Exposed cells were collected from plates or inserts by trypsinization, placed in 1.5 ml microcentrifuge tubes, centrifuged for 5 minutes at 1,000 g (1,200 rpm), and the supernatant discarded. 500 µl PBS was added to the tubes, samples were vortexed for 10 seconds, centrifuged for 5 minutes at 1200 rpm, and the supernatant discarded. 215 µl PBS was the added and the samples vortexed for 30 seconds. If necessary, samples were frozen at -80ºC at this step for later analysis. 15 µl of sample was removed for protein analysis and 800 µl TBA-reagent added to the remaining 200 µl sample; TBA samples were incubated for 60 minutes at 95ºC. Samples were then incubated for 5 minutes on ice, centrifuged for 10 minutes at 13,100 g (14,000 rpm), and pipetted in 200 µl triplicates into a black 96-well plate. Fluorescence was measured at 530 nm excitation, and 550 nm emission. The addition of butylated hydroxytoluene (BHT, Sigma-Aldrich) was used to prevent artifactual oxidation during sample handling.

Malonaldehyde bis-(dimethyl acetal) (Sigma-Aldrich) in 200 µl PBS was used to create a standard curve between 0.04 µM and 1.25 µM MDA equivalents, and the assay was conducted as above from the point of the addition of the TBA-reagent. The standard curve slope, expressed as relative fluorescence units (RFU) per µM MDA equivalents was used to determine the MDA concentration for the each analyzed sample.

Protein analysis was conducted via the Bradford assay (Bradford 1976) using the Bio-Rad Quick Start™ Bradford Protein Assay (Bio-Rad, Mississauga, ON) as per the manufacturer's directions. Briefly, the sample was pipetted in 5 µl triplicates into a clear 96-well plate, and aliquots of bovine serum albumin standard (0.125 mg/ml - 2 mg/ml)

were pipetted in 5 µl triplicates into the same plate. 150 µl of Bradford dye reagent provided was added to each well and the plate incubated for 15 minutes at room temperature on a plate shaker. Absorbance was measured at 595 nm. The standard curve slope of absorbance units per mg/ml protein content was used to determine the protein concentration of each sample.

Final TBARS data were expressed as MDA concentration per unit protein, i.e., nmol MDA equivalents/mg protein. To determine the effectiveness of this assay, cells were exposed under non-ALI exposure conditions to hydrogen peroxide (Sigma-Aldrich) and iron (II) sulfate heptahydrate (Sigma-Aldrich).

2.6.6 Gene Expression of Inflammatory Cytokines and Markers of Oxidative Stress

Following analysis for WST-1 and LDH, cells were lysed and the lysate frozen for subsequent gene expression analysis via quantitative real-time PCR (Q-RT-PCR). Briefly, 1 ml of RNeasy lysis buffer (Qiagen, Valencia, CA) was added to each insert, scraped with a pipette tip, and the solution pipetted into a microcentrifuge tube. Samples were frozen at -80°C until analysis. RNA isolation, cDNA synthesis, and Q-RT-PCR were conducted by Brian Chorley and Gail Nelson (NHEERL, USEPA). Cycle threshold (C_t) values were provided for analysis. Briefly, RNA was isolated from cell lysates using Qiagen RNeasy columns with RNA quantity and quality assessed using a Nanodrop spectrophotometer. An A260/280 ratio $\geq$ 2.0 was used as the acceptable quality control value. cDNA was prepared by reverse transcription using SuperScript ViLO cDNA synthesis kits (Life Technologies), and real-time qPCR was performed using TaqMan probe assays (Applied Biosystems, Life Technologies) on a BioRad CFX384 thermocycler in 384-well plate format. Commercially available TaqMan primer probe sets were used to measure the expression of *HMOX1* (Assay ID Hs01110250_m1), *COX2* (Hs00153133_m1), *TNFA* (Hs01113624_g1), *IL8* (Hs00174103_m1), *IL6R* (Hs01075666_m1), and the reference gene *ACTB* (Hs01060665_g1). C_t values were determined by a regression fit calculation of the background-corrected amplification curves (BioRad CFX Manager software, version 3.0). Gene expression relative to vehicle treated controls was determined using the $\Delta\Delta C_t$ method (Livak and Schmittgen 2001).

2.7 Statistical Analysis

Data were analyzed by unpaired two-sample student's t-test or analysis of variance (ANOVA) for more than two treatment conditions. Post-hoc analysis utilized the Duncan's new multiple range test for comparison of multiple means, or the Dunnett's test for comparison of different treatments with their concurrent controls.

3.0 RESULTS

3.1 Particle Loss Measurement

Prior to conducting ALI exposures for toxicity assessment, pilot work examined particle losses within the VITROCELL® system. This work used the same light-duty diesel engine and operating conditions as the subsequent cell exposures and toxicity assessment; the work was conducted at Environment Canada's River Road facility. Particle number and size concentration were measured both up- and downstream of the VITROCELL® module. More specifically, particles were size-selected by a nano-SMPS, followed by measurement of particle number concentration using a CPC. A combined flow of 300 ml/min was sent through the VITROCELL® module to meet the flow requirements of the SMPS system. Two analyses, with five replicates each, examined the up- and downstream PM content of the aerosol stream (Chan 2010b). Specifically, particle size and concentration where measured prior delivery of aerosol to the VITROCELL®, and again in the exhaust exiting the VITROCELL®. The results, which are shown in **Figure 3.1**, show considerable reductions in particle number concentration downstream of the VITROCELL® module; however, very little change was observed for ultrafine particles below 6 nm.

Log-normal fitted parameters are summarized in **Table 3.1**. The total particle number concentration was determined by integrating the average size distributions, and the results show a 62% reduction in total particle number concentration downstream of the VITROCELL® cell-exposure module. Peak number concentration showed a marked decrease; peak particle size showed relatively little change. The standard deviation of the particle size distribution did not differ. The reduction in particle number concentration suggests substantial particle deposition along the walls of the tubing and the surfaces of the exposure chamber. The small shifts in peak diameter suggest agglomeration as the particles pass through the VITROCELL® module, or a slight size bias in particles trapped in the apparatus.

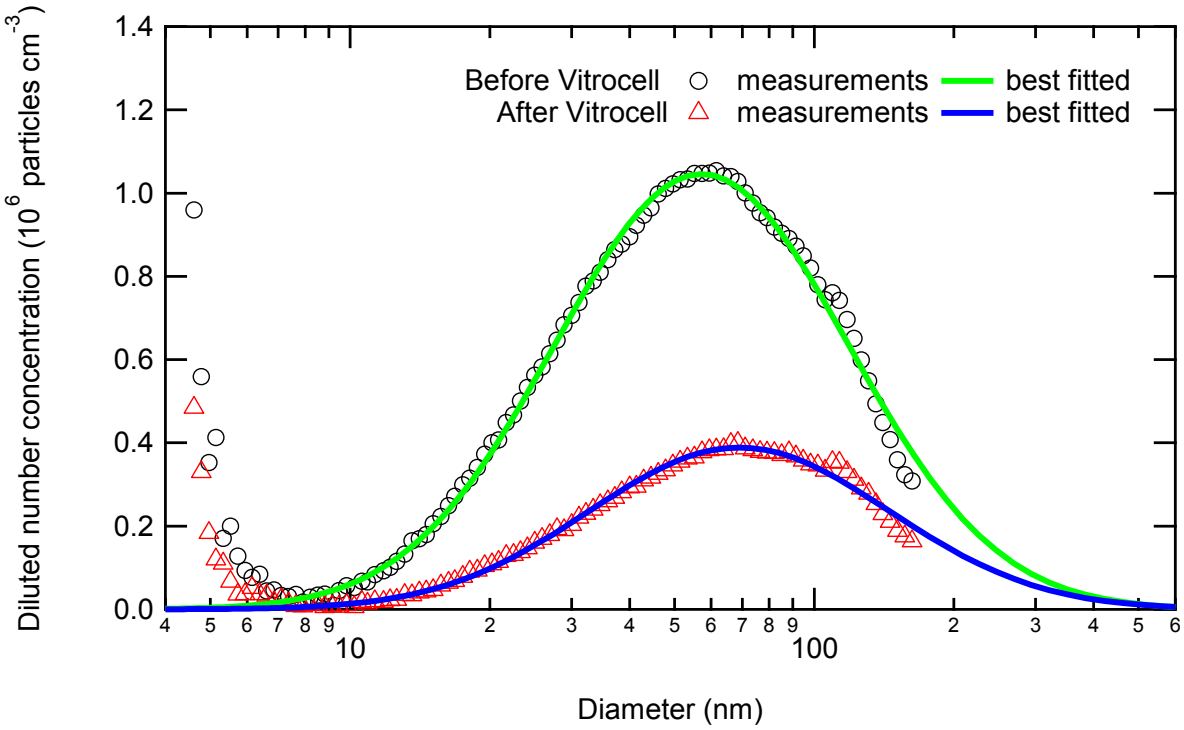

Figure 3.1: Comparison of the average particle number size distributions measured upstream and downstream of a VITROCELL® cell-exposure module.

Table 3.1: Comparisons of particle number concentration and size distribution up- and downstream of a VITROCELL® module.

	Before VITROCELL®	**After VITROCELL®**
Standard deviation (nm)	0.73	0.75
Peak diameter (nm)	57.2	69.0
Peak concentration (particles/cm^3)	1.92E+06	0.73E+06
Total concentration (particles/cm^3)	8.32E+06	3.16E+06

3.2 Comparative Toxicity Assessment of Diesel and Biodiesel Exhaust

Using cell culture and exposure protocols developed prior to the start of this project, the unmodified VITROCELL® system was deployed at Environment Canada's Emissions Research and Measurement facility for comparative toxicity testing of emissions representing a variety of fuel formulations, i.e., ULSD, canola- and tallow-derived biodiesel, B20 diesel-biodiesel blends. The work employed a single light-duty engine operated under steady-state conditions. A549 cells were exposed in triplicate, and cell viability was assessed using a single endpoint (i.e., WST-1) immediately following a 1 hour exposure.

The results of the emissions characterizations are shown in **Table 3.2**. To determine particle number concentration the aerosol was sampled from the diluted exhaust manifold to allow characterization without modifying the flow rates entering the VITROCELL®. Generally, particle number concentration decreased and NO_x concentration increased with increasing biodiesel concentration in the fuel blend. Carbon monoxide was higher in the ULSD and B20 tallow formulations, but no trend was identified.

A total of 35 independent exposures were conducted for assessment of cytotoxicity, i.e., nine ULSD, seven B20 canola, six B20 tallow, five B100 canola, and eight B100 tallow, with up to four replicate exposures conducted per day. A total of nine biological samples were assayed per exposure (i.e., three incubator controls, three clean air exposures, and three diesel exhaust exposures). In all cases, the diesel or biodiesel exhaust results were expressed relative to the mean negative control (i.e., clean synthetic air) for each individual exposure. To examine the effect of treatment (i.e., none, synthetic air, diesel exhaust), ULSD data were grouped by date (i.e., Sept. 28, Sept. 29, Sept. 30). A significant effect of treatment was found for all dates ($p < 0.05$). ULSD results from a typical exposure day (Sept. 29; $n = 4$ exposures, 36 samples in total) is shown in **Figure 3.2**. Duncan post-hoc analysis showed significant differences between all means ($p < 0.05$). The statistically significant decrease in cell viability following synthetic air exposure (i.e., incubator control versus clean air control) is cause for concern since it indicates a negative effect related to exposure conditions in VITROCELL®, rather than an effect of diesel exhaust. Moreover, the toxic response (i.e., increased cytotoxicity) to the clean air limits the dynamic range of

the assessment tool in terms of its ability to detect the toxicological activity of diluted diesel exhaust (i.e., relative to clean air). It was therefore deemed necessary to optimize the cell culture and exposure protocols to reduce the adverse effects of cell handling and air exposure in the VITROCELL®. In addition, an expanded array of toxicological endpoints would allow more in-depth characterization of the responses to exhaust exposures.

To determine the relative effects of emissions for the different fuel formulations, responses for all exposures were normalised to the matched mean clean air response, grouped by treatment, and compared across treatments. **Figure 3.3** shows the mean responses for each fuel formulation. ANOVA showed a significant treatment effect; however, Dunnett post-hoc analysis indicated that only B20 Canola was significantly different (i.e., lower) from ULSD ($p < 0.05$). As the only parameter that varied between exposures was the fuel blend used, the observed variations in response reflect changes in the composition of the exhaust. For example, as discussed regarding **Table 3.2**, particle concentrations generally decreased and NOx concentrations increased with increasing biodiesel concentration.

Table 3.2: Emissions characteristics across the fuel formulations examined (Volkswagen light-duty diesel engine).

Fuel	CO (ppm)	NO_x (ppm)	NO (ppm)	NO_2 (ppm)	THC (ppm)	Particle number concentration (#/cm^3)
ULSD	3.9 (± 1.3)	16.7 (± 1.0)	9.8 (± 0.6)	7.1 (± 0.6)	3.6 (± 0.4)	4.9E+06 (± 3E+05)
B20 Canola	3.0 (± 0.4)	18.4 (± 0.5)	10.6 (± 0.6)	8.0 (± 0.2)	3.2 (± 0.2)	5.0E+06 (± 2E+05)
B20 Tallow	3.6 (± 0.5)	18.6 (± 0.2)	10.7 (± 0.9)	7.9 (± 0.7)	3.0 (± 0.2)	4.9E+06 (± 2E+05)
B100 Canola	3.0 (± 0.3)	20.2 (± 0.9)	11.0 (± 0.6)	9.3 (± 0.3)	2.9 (± 0.3)	2.5E+06 (± 4E+05)
B100 Tallow	3.0 (± 0.4)	19.0 (± 1.1)	9.4 (± 0.7)	9.7 (± 1.2)	3.2 (± 0.2)	2.1E+06 (± 1.4E+06)

(± standard deviation)

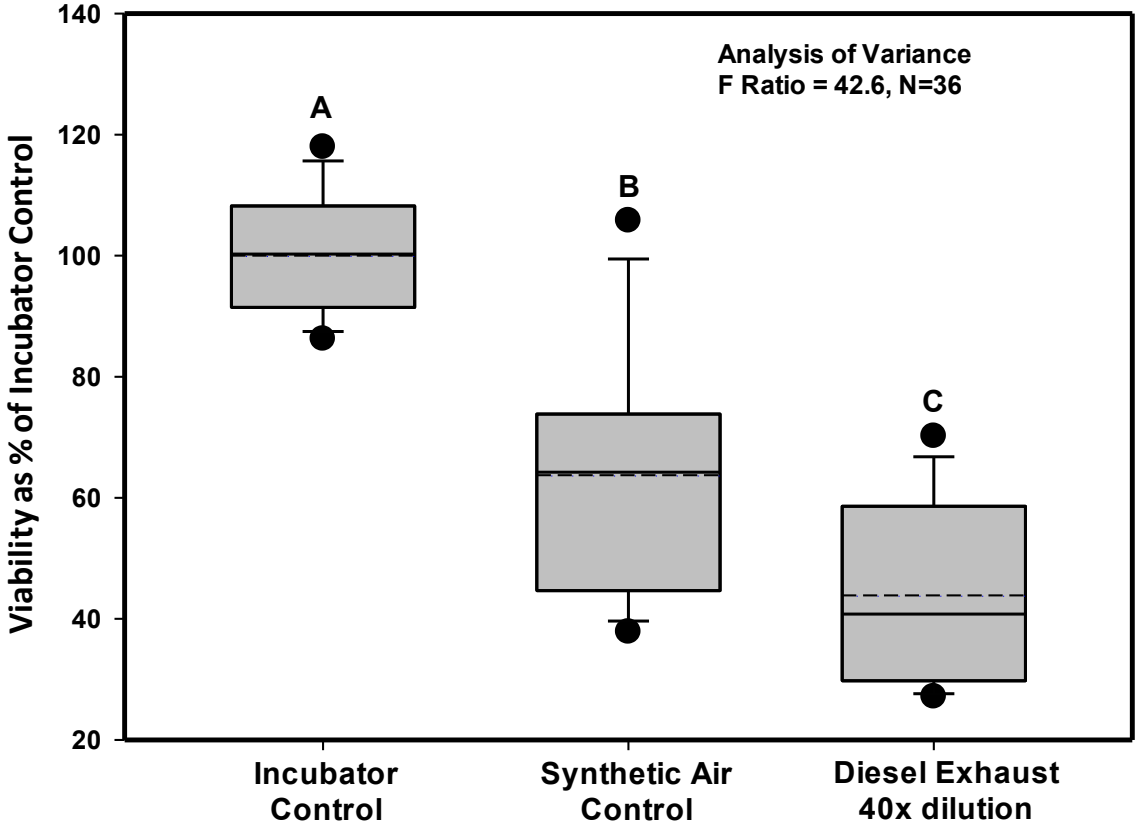

Figure 3.2: Comparison of mean cell viability, as determined using the WST-1 assay, for clean air and diluted ULSD exhaust. Values are expressed relative to the mean incubator control. Bars accompanied by different letters indicate that all means are significantly different at $p<0.05$ as determined by ANOVA with Duncan post-hoc analysis. Analysis of a single representative day; n = 4 exposures, 36 samples in total). The dotted line indicates the mean value; the solid line indicates the median. Box limits are the 25th and 75th percentiles, respectively, with whiskers showing the 10th and 90th percentiles.

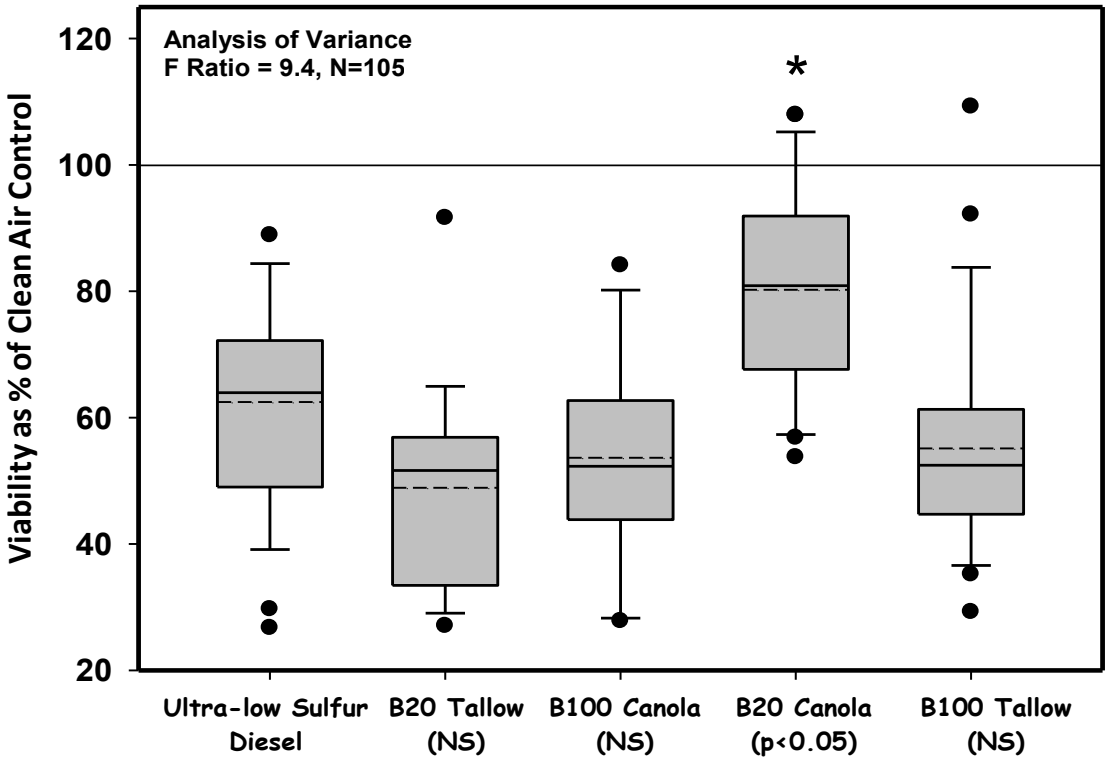

Figure 3.3: Comparisons of mean cell viability, as determined using the WST-1 assay, for diluted diesel exhaust generated using different fuels and fuel blends. All values are expressed relative to the clean air control. * indicates significantly different from ULSD at $p<0.05$ as determined by ANOVA with Dunnett post-hoc analysis. (n = 27 ULSD, 21 B20 canola, 18 B20 tallow, 15 B100 Canola, 24 B100 tallow).The dotted line indicates the mean value; the solid line indicates the median. Box limits are the 25th and 75th percentiles, respectively, with whiskers showing the 10th and 90th percentiles.

3.3 ULSD Exposures Utilizing Refined VITROCELL® Protocols

Exposure protocols were modified in collaboration with Mathias Könczöl, based on his previous work conducted at Freiburg University Medical Center (Konczol 2012, Tang et al. 2012). The culture surface for exposures was changed from translucent to transparent inserts (Greiner Bio-One Thincerts) to permit monitoring of cell growth and behaviour via optical microscopy. In addition, 25 mM HEPES buffer was added to the VITROCELL® exposure medium to improve pH stability in lieu of CO_2 supplementation. The aerosol flow rate through the VITROCELL® module was reduced from 8.3 ml/min to 5 ml/min to reduce mechanical stress on the cells, and the WST-1 assay protocol was modified to accommodate analysis directly on the insert membrane. Assays for Neutral Red, caspase III/VII activity, and TBARS were also incorporated into the toxicity assessment procedures.

All ULSD exhaust exposures conducted using revised protocols were carried out at Environment Canada's River Road facility. The engine specifications, operating conditions, and emissions characterization protocols were identical to the previous exposures. WST-1 and Neutral Red assays were conducted on the same cell samples; the TBARS assay was not used due to requirements for further protocol refinements. Mean emission characteristics for all exposures are shown in **Table 3.3.** Compared to previous ULSD exposures, CO, THC, and particle number concentrations were lower and NO_x was higher. A total of 11 independent exhaust exposures were examined using the modified WST-1 assay. Inserts were assayed independently as biological replicates for each exposure, and total inserts assayed (i.e., n = 32 incubator control, 31 clean air, 32 diesel exhaust) were grouped for analysis by ANOVA. The n number may be slightly lower than the maximum number (i.e., 3 * 11 = 33) in instances where some inserts could not be analysed, e.g. membrane breakage. A total of 9 exhaust exposures were examined using the Neutral Red assay (i.e., n = 27 incubator control, 25 clean air, 23 diesel exhaust), and a total of 7 exposures were examined for Caspase III/VII activity (i.e., n = 21 incubator control, 21 clean air, 21 diesel exhaust). WST-1 and caspase III/VII assays were conducted immediately following the exposure; the Neutral Red assay was conducted immediately following the WST-1 assay, i.e., 30 minutes post-exposure.

Data toxicity assessment results are displayed in **Figure 3.4** (WST-1), **Figure 3.5** (Neutral Red), and **Figure 3.6** (Caspase III/VII activity). Data were analysed by ANOVA with Duncan post-hoc comparisons of mean values. The results showed a significant treatment effect at $p < 0.05$ for each endpoint. For WST-1 and Neutral Red assays, cell viability was significantly reduced for each treatment group (i.e., clean air and diesel) relative to the incubator control. Caspase III/VII activity was also reduced for each treatment group relative to the incubator control. While this may indicate reduced apoptosis, it may also be due to alternative mechanisms such as increased necrosis. However, as the samples were assayed immediately following exposure, it is possible that insufficient time had elapsed following cellular stress for Caspase activation to occur. In contrast to these findings, Bayram et al. (2013) found increased apoptosis following exposure of A549 cells to 50 μg/ml diesel exhaust particulate.

Cell viability following clean air exposures, as indicated using the WST-1 and Neutral Red assay results, was only 70% and 60%, respectively, relative to the incubator control. Viability following ULSD exhaust exposures was 55% relative to incubator control and 79% relative to clean air control for WST-1 reduction, and 43% relative to incubator control and 77% relative to clean air control for Neutral Red uptake. These results, particularly the 30-40% reduction in cell viability for clean air exposures, indicated that further optimization of the exposure system is required to improve the ability to successfully detect responses attributable to combustion emissions. The observed responses to the clean air controls were likely related to the low humidity of the aerosol. The clean air employed for the analyses shown in **Figures 3.4**, **3.5** and **3.6** was a grade 0.1 compressed air with humidity between 0.5 - 2% RH at room temperature. Diesel exhaust was diluted in HEPA-filtered ambient air. The RH of the diluted diesel exhaust was comparable to ambient air humidity, i.e. 22.4% - 27.7% RH, when measured at room temperature.

Table 3.3: Characteristics of the light-duty Volkswagen diesel exhaust used for the VITROCELL® exposures that incorporated refined protocols and additional endpoints. All values are averages and N=27.

Fuel	CO (ppm)	NO_x (ppm)	NO (ppm)	NO_2 (ppm)	THC (ppm)	Particle number concentration (#/cm^3)
ULSD	2.4 (± 0.7)	19 (± 1.9)	11.3 (± 1.9)	8.1 (± 0.3)	2.1 (± 0.9)	4.1E+06 (± 3E+05)

(± standard deviation).

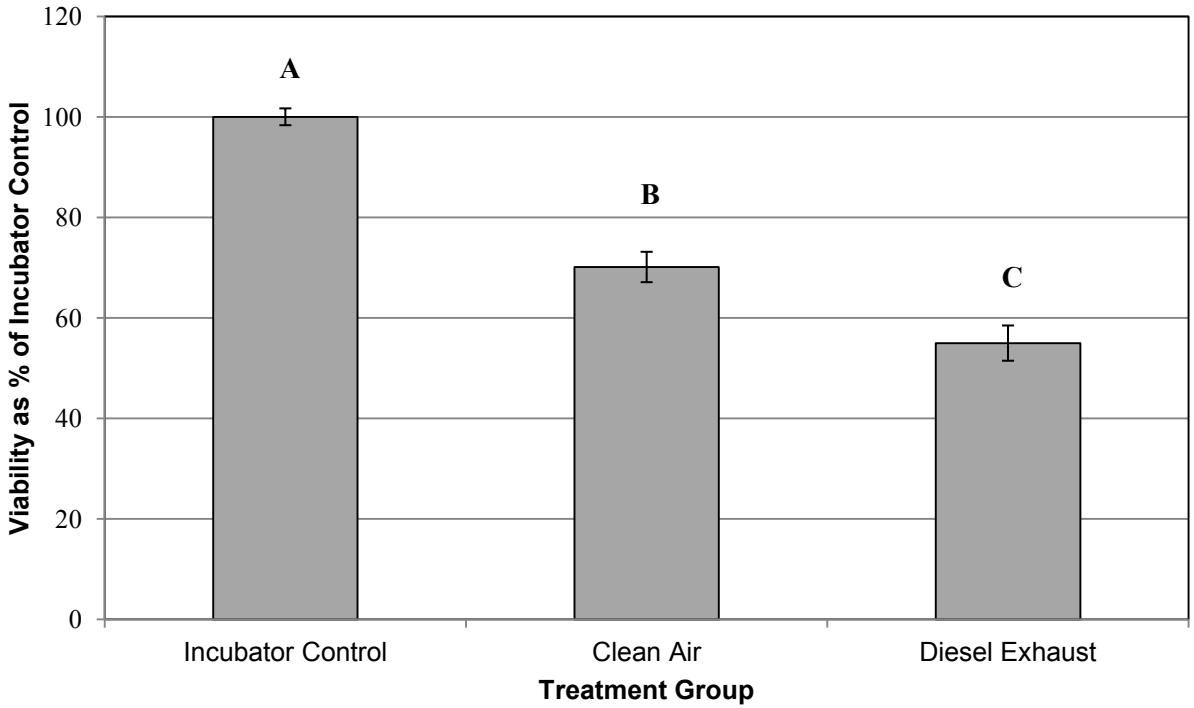

Figure 3.4: Effect of cell treatment on cell viability determined using the modified WST-1 assay. All values are expressed relative to the incubator control. Error bars show the standard error of the mean. Bars accompanied by different letters indicate that all means are significantly different at $p<0.05$ as determined by ANOVA with Duncan post-hoc analysis. (n = 32 Incubator Control, 31 Clean Air, 32 Diesel Exhaust).

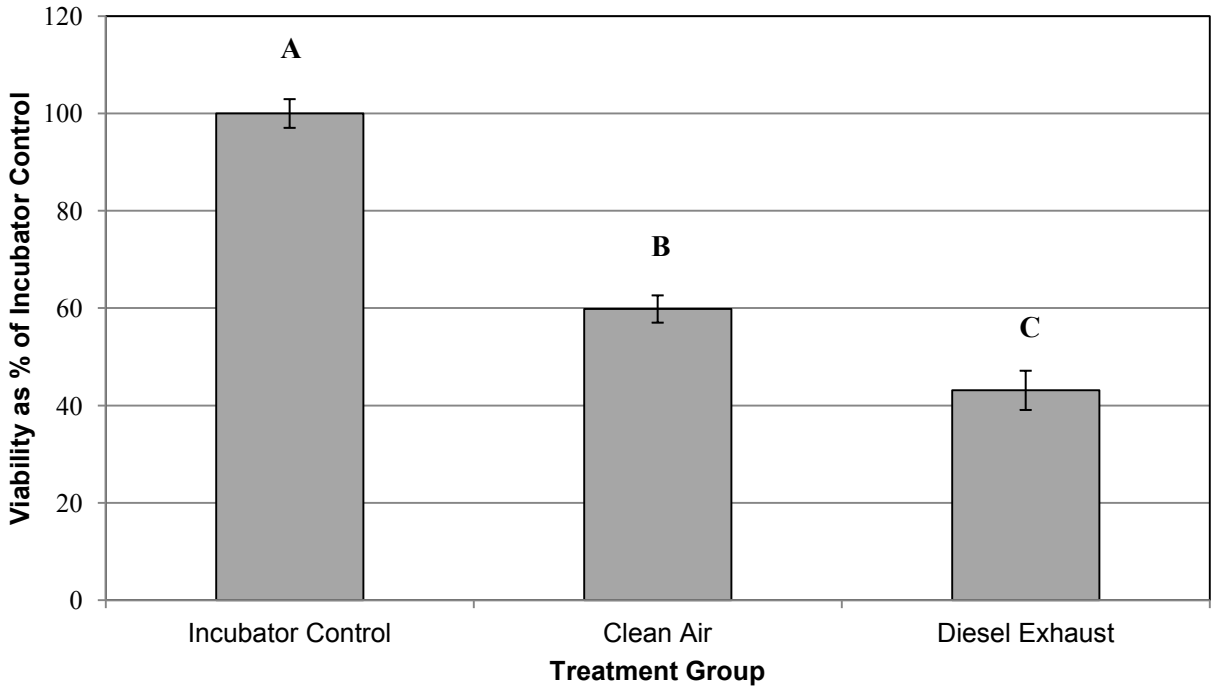

Figure 3.5: Effect of cell treatment on cell viability determined using the modified Neutral Red assay. All values are expressed relative to the incubator control. Error bars show the standard error of the mean. Bars accompanied by different letters indicate that all means are significantly different at $p<0.05$ as determined by ANOVA with Duncan post-hoc analysis. (n = 27 Incubator Control, 25 Clean Air, 23 Diesel Exhaust).

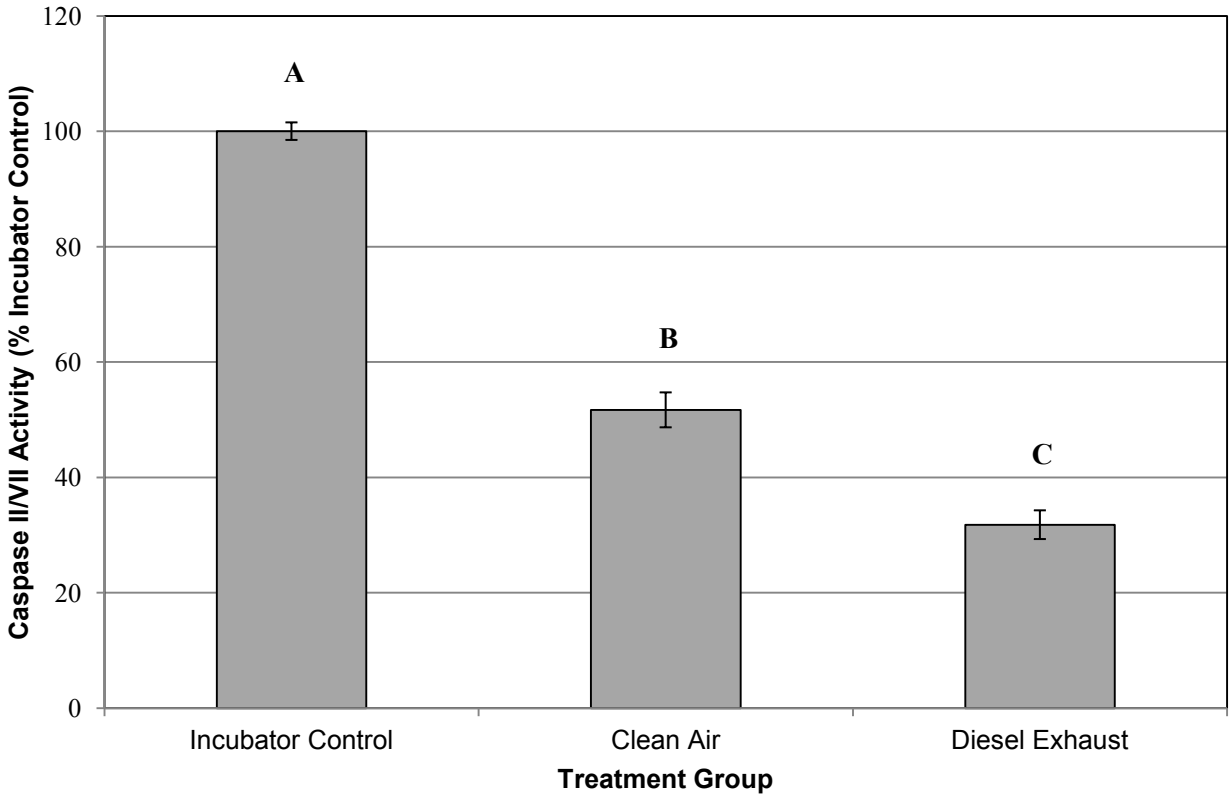

Figure 3.6: Effect of cell treatment on Caspase III/VII activity. All values are expressed relative to the incubator control. Error bars show the standard error of the mean. Bars accompanied by different letters indicate that all means are significantly different at $p<0.05$ as determined by ANOVA with Duncan post-hoc analysis. (n = 21 Incubator Control, 21 Clean Air, 21 Diesel Exhaust).

3.4 Aerosol Humidification via the Fideris TesSol Bubble Humidifier

A custom-built bubble humidifier was purchased (Fideris TesSol, Battle Ground, WA) to humidify aerosols analysed using the VITROCELL® system. Cell viability following clean air and NO_2 exposures was examined at humidity set points between 0 and 100% RH (data not shown). However, it was eventually determined that the system is not appropriate for VITROCELL® applications since it could not provide sufficient simultaneous humidification of two aerosol streams; moreover, maintenance of humidity between the humidifier and the exposure modules proved to be extremely difficult. Heated transfer lines were not in use and consequently it was not possible to deliver an aerosol with humidity above 100% RH at room temperature, which is substantially lower than 100% RH at 37°C.

3.5 Modification of Cell Culture Protocols to Improve Cell Viability

Culture protocols were also modified in an attempt to decrease cell fragility and concomitant susceptibility to low humidity and mechanical (i.e., air flow) stress. Specifically, the cell culture and exposure media were changed from F-12K to RPMI 1640, based on a review of media used in previous VITROCELL® studies. As shown in **Figure 3.7** and **Figure 3.8**, cell viability was improved for VITROCELL® exposures that employed RPMI 1640 media. However, viability was still significantly reduced compared to Incubator Control for both the Clean Air treatment and the 10ppm NO_2 treatment. In addition, 10ppm NO_2 exposure did not significantly reduce viability compared to clean air. RPMI 1640 also improved the performance of the Neutral Red assay since dye precipitation that had been observed with F-12K media was not observed with RPMI 1640 medium (data not shown).

Variations in exposure conditions for the VITROCELL®, i.e. basal media level, FBS supplementation, and aerosol flow rate were also modified in an attempt to improve system performance; however, a reproducible improvement of cellular responses was not observed (data not shown).

The height of the aerosol inlet trumpet above the insert membrane can be adjusted by placing 1 mm thick washers on an insert placed in the VITROCELL® well and lowering the trumpet height to meet the washer(s). Lower trumpet heights were assumed to increase the contact of the aerosol with the insert membrane. However, build-up of condensation on

the insert membrane could potentially block the aerosol flow from the inlet trumpet. This work investigated trumpet height levels between 1 - 3 mm above the insert, but no significant effect on cell viability was observed; a height of 1 mm was used for most experiments (data not shown).

In attempt to produce an ALI-phenotype that would be more amenable to aerosol exposure conditions, cells were cultured for 7 days, with medium changes every 2-3 days, before exposure in the VITROCELL® device. Significant work was required to maintain the cells and the extended incubation produced somewhat over-confluent cultures. In addition, the physical effects of the VITROCELL® exposure were especially apparent in these cultures. **Figure 3.9** is a photograph of VITROCELL®-exposed inserts following NR-stain uptake showing a large non-viable central region. These regions spatially correspond to the trumpet-shaped VITROCELL® inlets, and likely indicate regions of mechanical aerosol impact. **Figure 3.10** is a micrograph of VITROCELL®-exposed cells (100x magnification) taken at the outer circumference of the non-viable (no NR-stain uptake) region. Both the viable and non-viable sections of cells are observable. Notable cell detachment is also observed in this region, but the central region consists mainly of attached non-viable cells.

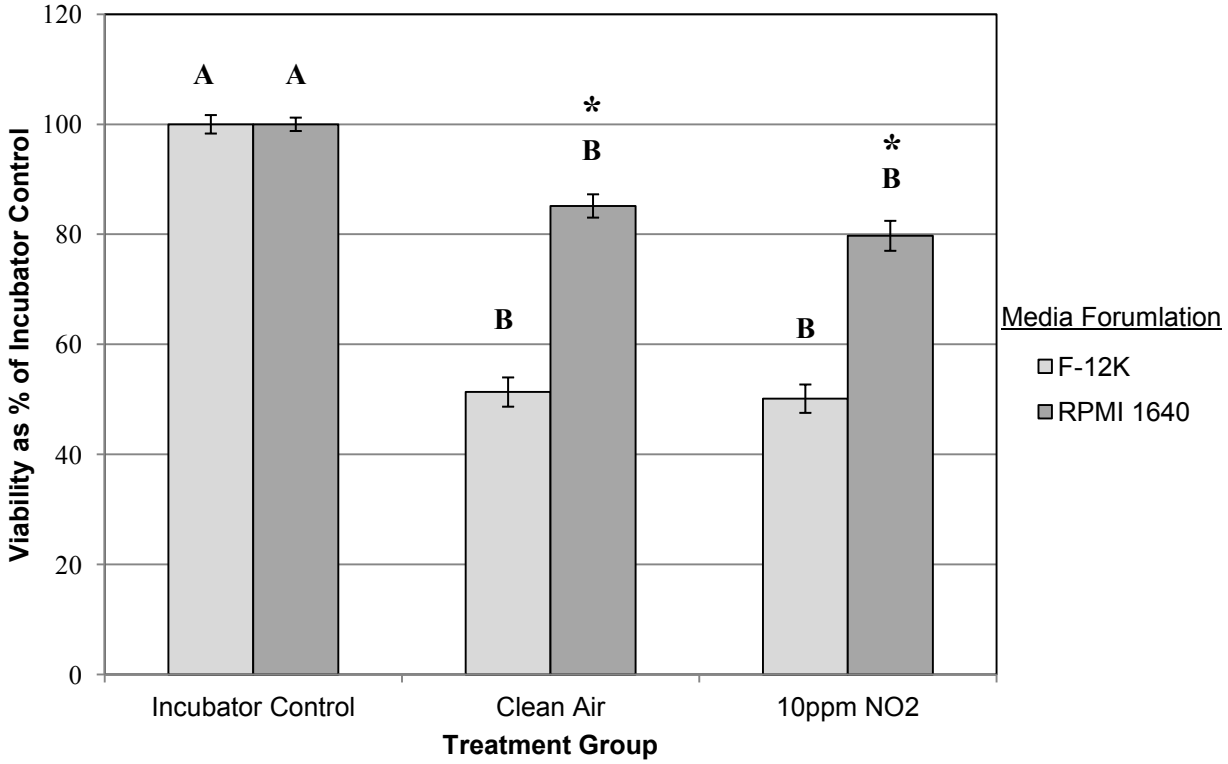

Figure 3.7: The effect of media formulation for cell culture and VITROCELL® exposure cell viability determined using the WST-1 assay. All values are expressed relative to the incubator control. Error bars show the standard error of the mean. Bars accompanied by different letters indicate that for each media formulation, both Clean Air and 10ppm NO_2 exposure are significantly different from their matched Incubator Control but 10ppm NO_2 is not significantly different from Clean Air (at $p<0.05$ as determined by ANOVA with Duncan post-hoc analysis). * indicates that media formulation is significantly different for the same treatment group ($p<0.05$ as determined by unpaired two-tailed t-test.) (n = F-12K media: 18 Incubator Control, 18 Clean Air, 16 10ppm NO_2; RPMI 1640 media: 11 Incubator Control, 11 Clean Air, 11 10ppm NO_2).

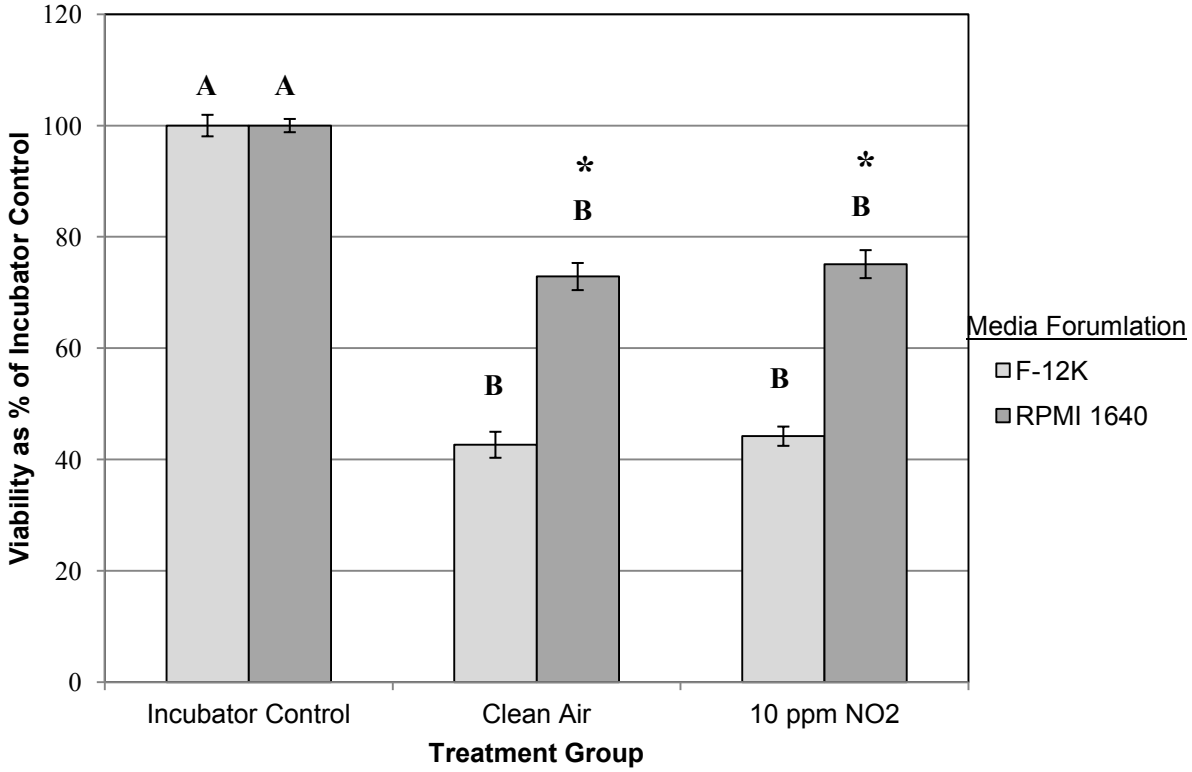

Figure 3.8: The effect of media formulation for cell culture and VITROCELL® exposure cell viability determined using the Neutral Red assay. All values are expressed relative to the incubator control. Error bars show the standard error of the mean. Bars accompanied by different letters indicate that for each media formulation, both Clean Air and 10ppm NO_2 exposure are significantly different from their matched Incubator Control but 10ppm NO_2 is not significantly different from Clean Air (at $p<0.05$ as determined by ANOVA with Duncan post-hoc analysis). * indicates that media formulation is significantly different for the same treatment group ($p <0.05$ as determined by unpaired two-tailed t-test.) (n = F-12K media: 18 Incubator Control, 18 Clean Air, 16 10ppm NO_2; RPMI 1640 media: 11 Incubator Control, 11 Clean Air, 11 10ppm NO_2).

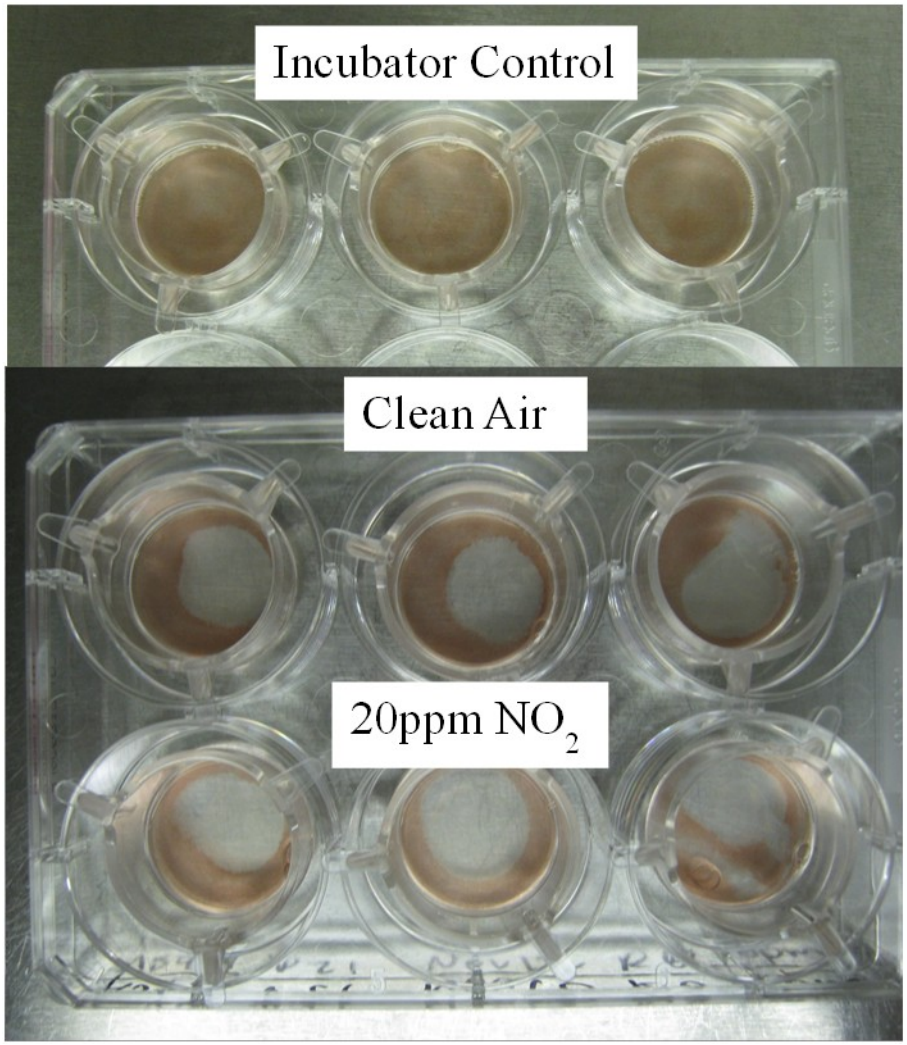

Figure 3.9: Photograph of Neutral Red-stained cells following VITROCELL® air-liquid interface exposure.

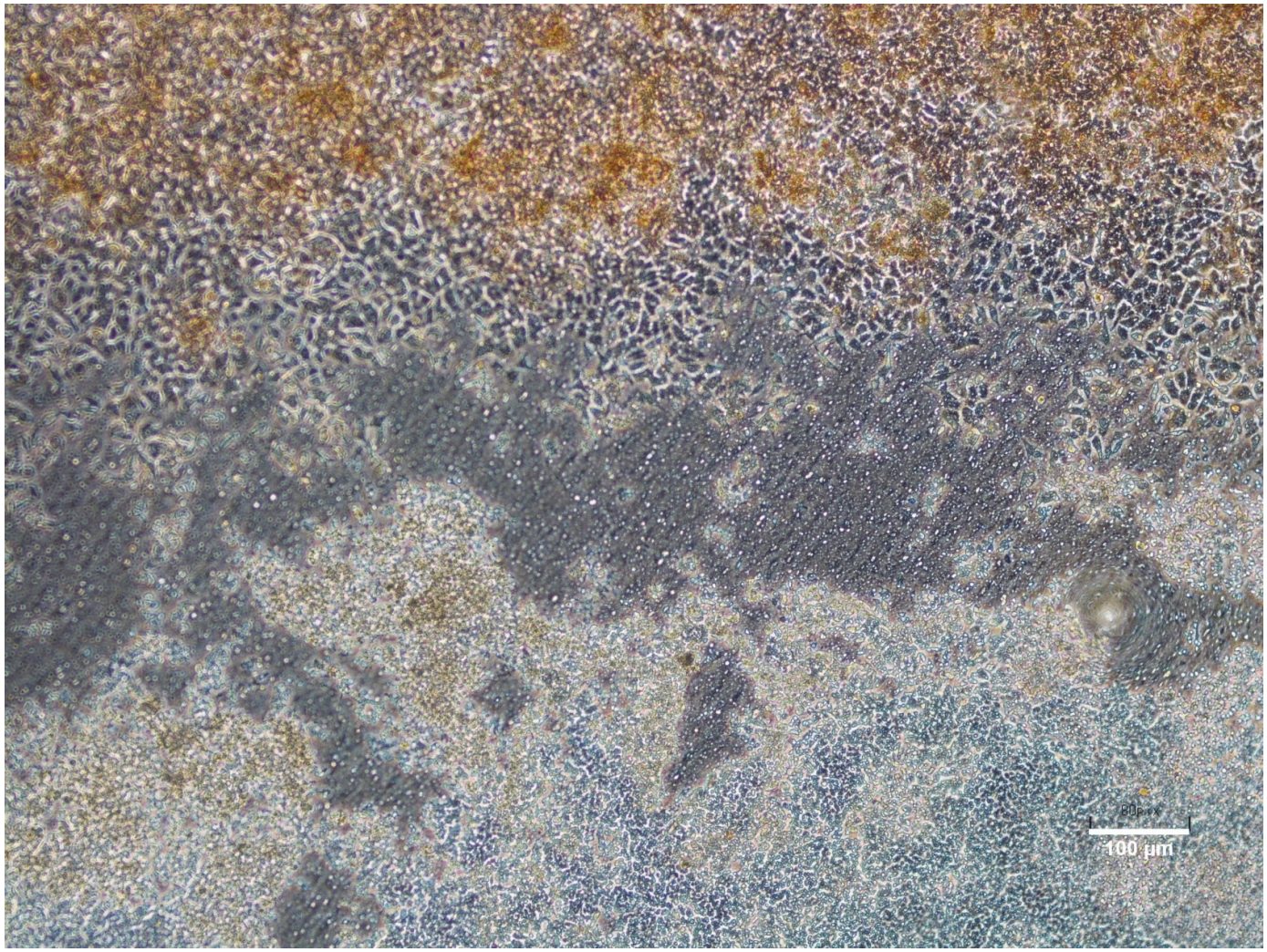

Figure 3.10: Photomicrograph of Neutral Red-stained cells (100x magnification) following VITROCELL® air-liquid interface exposure.

3.6 Optimization of Post-Exposure Incubation Periods for the Caspase III/VII assay

The Caspase III/VII and TBARS assays were modified from the protocol used for initial experiments. For the Caspase assay, there was some concern that assaying the cells immediately after exposure did not allow sufficient time for Caspase activation. A time course analysis was conducted using a positive control (1μM and 4 μM staurosporine) in F-12K culture media (**Figure 3.11**). Three to four replicate experiments were conducted for each time point, with two biological replicates for each exposure condition and time point. Following 1hr exposure with staurosporine, cultures were washed with PBS and allowed to incubate in fresh media until analysis. It was determined that Caspase III/VII activity was significantly increased ($p < 0.05$) when assayed immediately following exposure, i.e., at 0hrs post-exposure incubation. Activity continued to increase when examined at 1hr, 2hr, 3hr, 4hr, and 5hrs post-exposure ($p < 0.05$). Activity was still elevated above the negative control when assayed at 24hrs post-exposure ($p < 0.05$), although it had decreased to levels observed at 5hrs post-exposure. When assayed at 48hrs post-exposure, Caspase III/VII activity was significantly reduced in staurosporine-exposed cultures ($p < 0.05$) compared to unexposed negative controls. Significance was determined by ANOVA with Dunnett post-hoc comparisons to the negative control.

Two replicate VITROCELL® 20ppm NO_2 exposures were assayed for Caspase III/VII activity following 4 hours post-exposure incubation (**Figure 3.12**). Statistical analysis (i.e., ANOVA with Duncan post-hoc analysis, showed that Caspase III/VII activity was significantly reduced in each treatment group ($p < 0.05$). Again, this suggested that aerosol-induced toxicity observed with the VITROCELL® system resulted from mechanisms other than apoptosis, e.g., cell detachment, force-induced rupture, and necrosis.

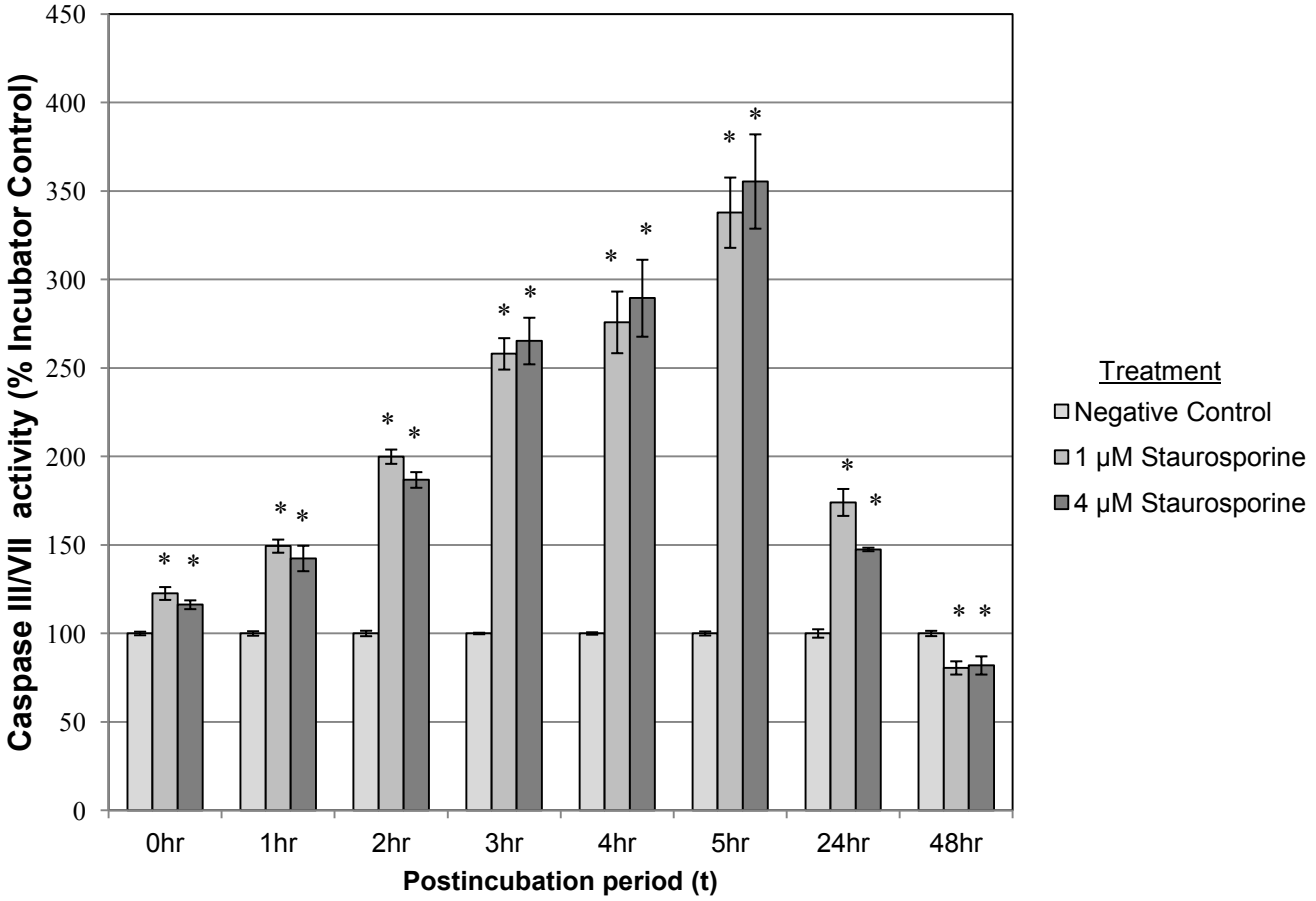

Figure 3.11: Post-exposure incubation time course of Caspase III/VII activity following 1hr exposure to a positive control. All values are expressed relative to negative control. Error bars represent the standard error of the mean. * indicates significantly different from negative control at $p<0.05$ as determined by ANOVA with Dunnett post-hoc analysis. (n = 5 - 8 for each group).

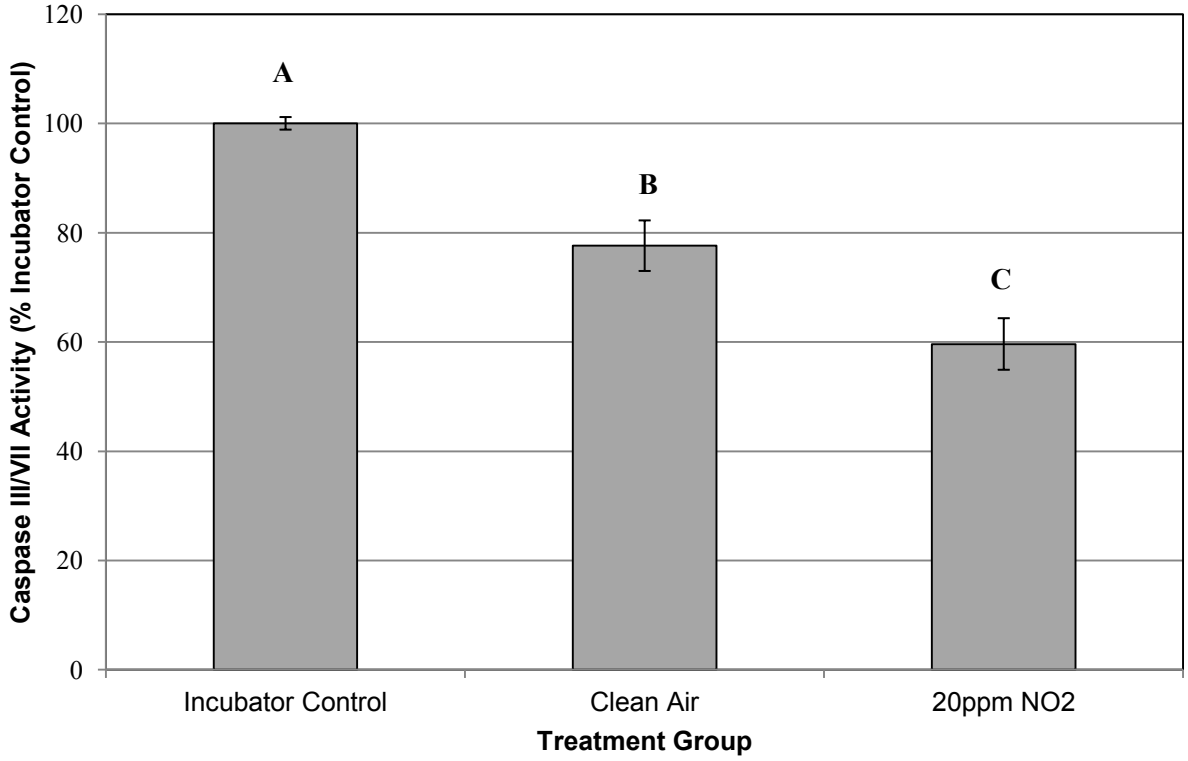

Figure 3.12: Caspase III/VII activity following VITROCELL® exposure to 20ppm NO_2 with 4 hour post-exposure incubation. All values are expressed relative to incubator control. Error bars represent the standard error of the mean. Bars accompanied by different letters indicate that all means are significantly different at $p<0.05$ as determined by ANOVA with Duncan post-hoc analysis.

3.7 Optimization of the TBARS Assay Protocol

The TBARS assay protocol adapted for use with the VITROCELL® system had not previously been used with VITROCELL® exposures. Additionally, due to the logistics of the exposures, the protocol needed to be adapted such that it could be carried out with frozen samples. There was some concern that due to the small number of cells collected from insert membranes, the assay would not be sensitive enough to detect increases in lipid peroxidation in exposed cells. 5mM BHT was added to minimise lipid peroxidation during post-exposure sample handling. **Figure 3.13** shows the mean response for four independent experiments utilizing the finalized protocol with a positive control (1 mM H_2O_2 with 250 μM $FeSO_4$). Three replicate samples were exposed per treatment group for each experiment. Statistical analysis was conducted by unpaired student's t-test, and the treatment response was significantly increased above the unexposed negative control ($p < 0.05$).

Utilizing the same protocol for TBARS analysis, response was measured following two replicate VITROCELL® exposures to 20ppm NO_2. Statistical analysis was conducted by ANOVA with Duncan post-hoc comparisons, and the results are shown in **Figure 3.14.** Only the NO_2 exposure response showed a significant increase above the Incubator Control ($p < 0.05$), and the NO_2 response was not significantly different from the clean air control exposure.

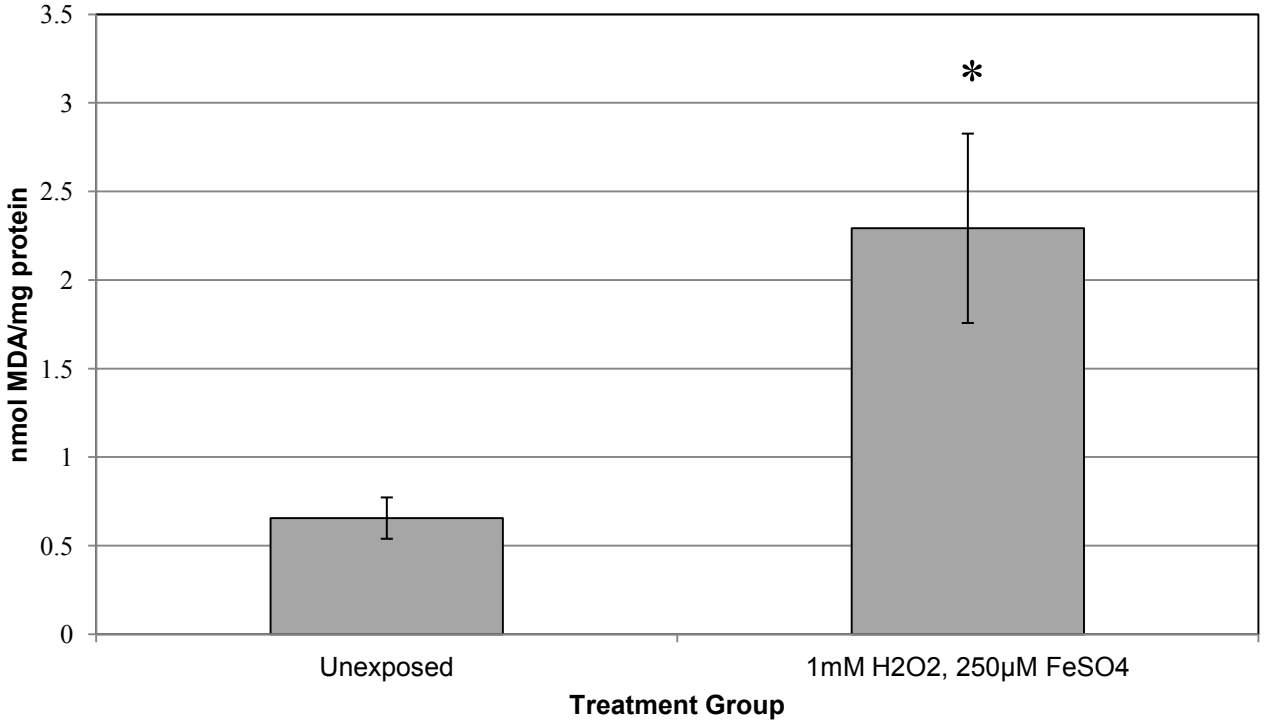

Figure 3.13: Lipid peroxidation quantified using the modified TBARS assay following exposure to a positive control. Error bars represent the standard error of the mean. * indicates significantly different from Unexposed control as determined by unpaired two-tail t-test (n = 12 for each treatment group).

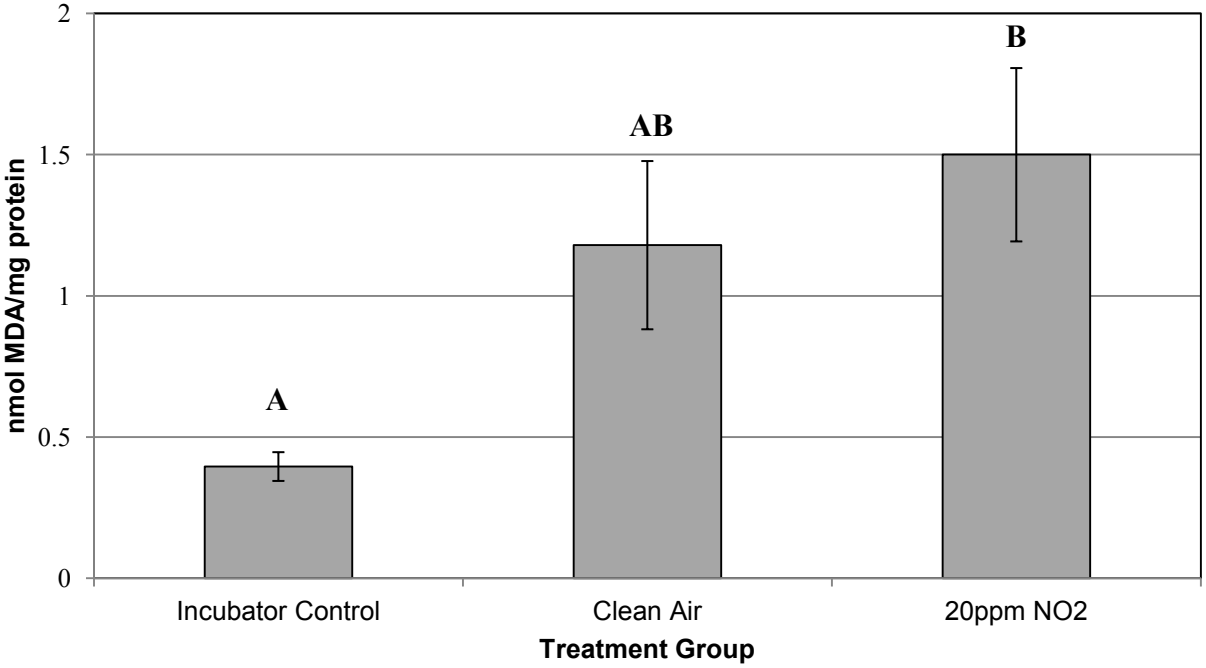

Figure 3.14: Lipid peroxidation quantified by the TBARS assay following VITROCELL® exposure. Error bars represent the standard error of the mean. Bars accompanied by different letters indicate that 20ppm NO_2 is significantly different from Incubator Control but not significantly different from Clean Air control (at $p<0.05$ as determined by ANOVA with Duncan post-hoc analysis). (n = 6 for each treatment group).

3.8: Comparisons Between Greiner Bio-One Thincerts and Corning Transwells

The cell culture and exposure protocols were modified prior to collaboration with the US EPA group in Research Triangle Park, NC (see methods section). Notably, comparisons between two commercially available insert brands (i.e., Greiner Bio-One Thincerts and Corning Transwells) were conducted since US EPA collaborators routinely used the Transwell brand. It was determined that the cells did not grow as well on the Thincerts relative to the Transwells. 400,000 and 500,000 cells were seeded on inserts with and without collagen coating for each insert brand and allowed to grow for 24hrs, then stained with Neutral Red. As shown in **Figure 3.15**, growth on Thincerts showed distinct patches showing variable morphology and limited Neutral Red uptake. However, when viewed by microscopy, the cells present in these areas appeared to be normal. Thus, growth on Transwell inserts appeared to be better (i.e., more uniform) or similar to that observed on Thincerts. These results suggested that a switch to Corning Transwell inserts would not present a problem.

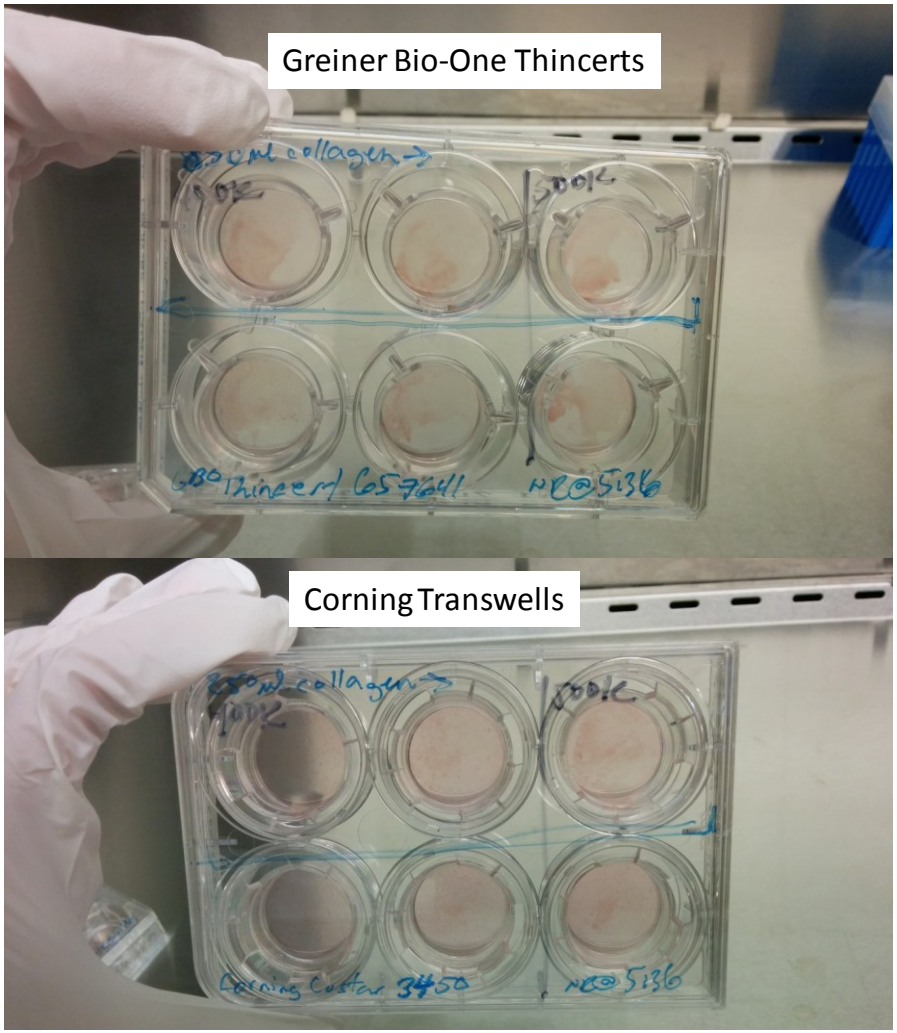

Figure 3.15: Viability of unexposed cells (via Neutral Red uptake) grown on Greiner Bio-One Thincerts and Corning Transwell inserts.

3.9: Additional Modifications of the VITROCELL® Exposure System

Deployment of the VITROCELL® exposure system at the US EPA Highbay facility involved additional system modifications outlined in the Methods section. The possibility of particle losses to the in-line humidifiers was investigated by SMPS measurements anterior and posterior to the humidifier; no significant loss was observed (data not shown). Aerosol humidity and temperature were measured for all exposures conducted with the modified system and the results for each exposure are shown in **Table 3.4**. For the April 10-14 exposure measurements were obtained for the control module only because only one data recorder was available. For all other exposures, data recorders were used concurrently for both modules. The revised humidifier design and higher wattage heater, as described earlier, were incorporated into the system after the April 10-14 and used for all subsequent exposures. The mean values recorded for the April 10-14 (pilot clean air) exposure were 30.6ºC (± 0.5) and 85.0 %RH (± 1.2). For the April 16-14 through May 14-14 exposures, the mean temperature values ranged from 33.4 (± 0.4) - 37.7ºC (± 0.6) for the control module and 33.9 (± 0.4) - 38.9ºC (± 0.7) for the exposure module. The range of relative humidity values was 64.6 (± 1.7) - 88.0 %RH (± 2.1) for the control module and 59.0 (± 4.3) - 79.0 %RH (± 2.9) for the exposure module. There was some concern that particle deposition on the data recorder in the exposure module was negatively affecting the accuracy of the results. When the two data recorders were compared following the exposures on April 24-14, the recorder for the exposure module recorded about 10% lower RH values (data not shown). The sensors were cleaned, recalibrated, and wrapped to protect from particle deposition.

Table 3.4: Temperature and Humidity of the Aerosol Stream Delivered to the VITROCELL® Modules.

Exposure	Date	Exposure #	Mean Temperature (°C)		Mean Humidity (%RH)	
			Control Module	Exposure Module	Control Module	Exposure Module
Air	April 10-14	1	30.6 (± 0.5)	.	85.0 (± 1.2)	.
Diesel	April 16-14	1	34.4 (± 1.0)	35.3 (± 1.0)	64.6 (± 1.7)	74.7 (± 0.9)
Diesel	April 22-14	1	33.8 (± 0.3)	34.5 (± 0.2)	73.9 (± 0.4)	63.0 (± 1.1)
Diesel	April 22-14	2	33.4 (± 0.4)	33.9 (± 0.4)	74.0 (± 0.9)	61.7 (± 0.4)
Diesel	April 24-14	1	33.9 (± 0.6)	35.3 (± 0.9)	87.0 (± 0.8)	60.9 (± 1.6)
Diesel	April 24-14	2	34.5 (± 0.4)	35.5 (± 0.7)	88.0 (± 2.1)	62.2 (± 2.1)
Diesel	April 29-14	1	35.8 (± 1.5)	36.3 (± 1.5)	71.2 (± 2.8)	59.0 (± 1.4)
Diesel	April 29-14	2	36.5 (± 0.5)	37.3 (± 0.7)	78.3 (± 3.2)	63.2 (± 6.3)
Diesel	May 1-14	1	37.2 (± 0.6)	38.3 (± 1.0)	71.1 (± 3.4)	60.6 (± 3.7)
Diesel	May 1-14	2	37.7 (± 0.6)	38.4 (± 0.7)	74.0 (± 4.9)	64.9 (± 7.3)
Diesel	May 6-14	1	37.1 (± 0.8)	38.0 (± 0.9)	75.0 (± 1.6)	59.0 (± 4.3)
Diesel	May 6-14	2	37.2 (± 0.5)	38.9 (± 0.7)	72.9 (± 4.3)	65.1 (± 5.6)
Smog	May 8-14	1	36.6 (± 0.6)	38.1 (± 0.8)	79.6 (± 2.4)	69.0 (± 4.8)
Smog	May 13-14	1	35.6 (± 1.2)	36.9 (± 1.3)	79.4 (± 0.7)	74.6 (± 1.5)
Smog	May 14-14	1	35.6 (± 1.5)	36.5 (± 1.6)	78.1 (± 2.6)	79.0 (± 2.9)

(± standard deviation).

3.10: Clean Air Exposures Conducted at the US EPA NHEERL Highbay Facility Using the Modified VITROCELL® Exposure System

The April 10-14 exposure was conducted to determine whether the modifications to the VITROCELL® exposure system contributed to improved cell viability and to ensure that both modules (i.e., that used for test aerosols and that used for clean air control) exhibited the same baseline responses. Humidified, heated clean air was delivered to both the control and exposure modules and WST-1 was measured at 0 and 24hrs post-exposure; LDH release was measured at 24hrs post-exposure. Statistical analysis was conducted by ANOVA with Duncan post-hoc contrast. As shown in **Figure 3.16**, at 0hrs post-exposure, WST-1 reduction was reduced in both modules compared to the Incubator Control ($p < 0.05$). At 24hrs post-exposure, WST-1 reduction remained reduced in the both modules compared to the Incubator Control (**Figure 3.17**; $p < 0.05$). No significant effect was observed for LDH release (data not shown). Although the reduction in viability observed for clean air exposures is potentially a cause for concern, the magnitude of the effect is reduced relative to that observed in earlier experiments (e.g., **Figure 3.4**). In addition, the results showed no difference between the two modules.

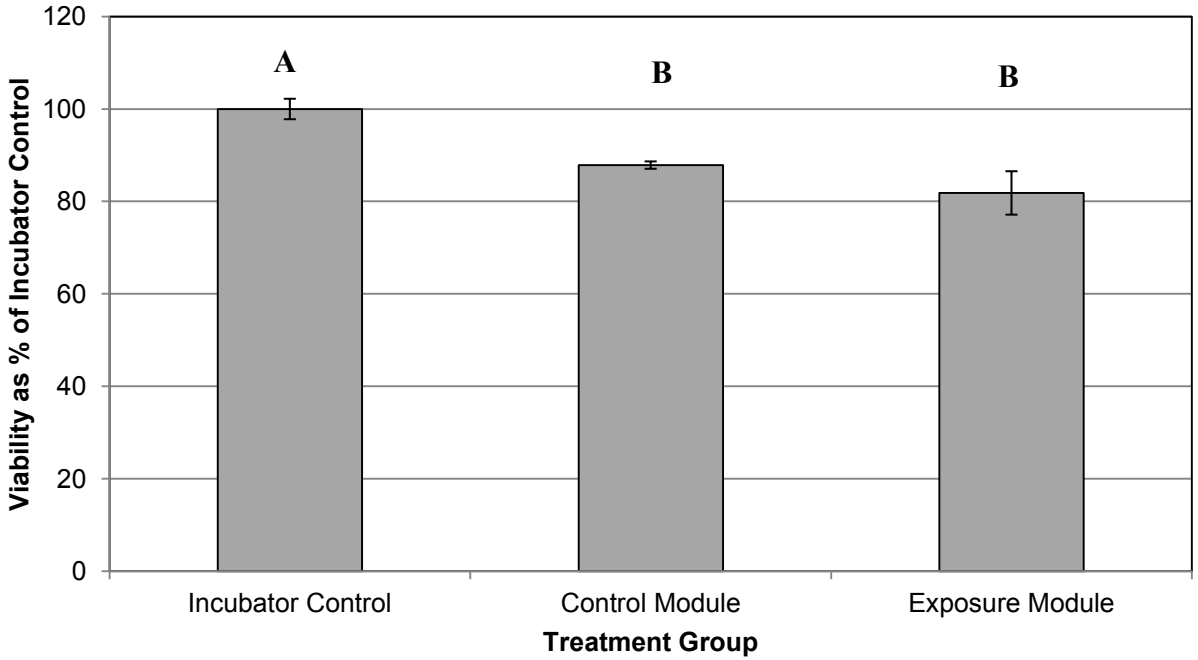

Figure 3.16: Effect of clean air delivered to both VITROCELL® modules (April 10-14). Effect of treatment on viability determined using the WST-1 assay assessed at 0hrs post-exposure. All values are expressed relative to incubator control. Error bars represent the standard error of the mean. Bars accompanied by different letters indicate that all the Control Module and Exposure Module are significantly different from the Incubator Control but not different from each other (at $p<0.05$ as determined by ANOVA with Duncan post-hoc analysis). ($n = 3$ for each treatment group).

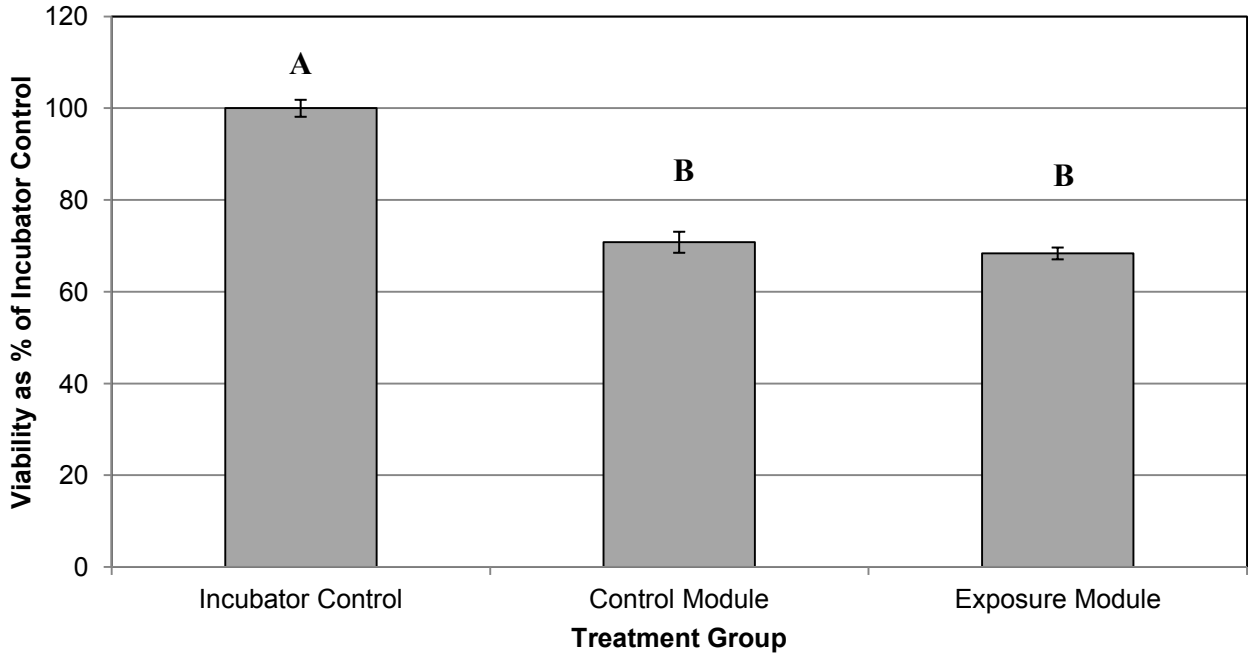

Figure 3.17: Effect of clean air delivered to both VITROCELL® modules (April 10-14). Effect of treatment on viability determined using the WST-1 assay assessed at 24 hrs post-exposure. All values are expressed relative to incubator control. Error bars represent the standard error of the mean. Bars accompanied by different letters indicate that all the Control Module and Exposure Module are significantly different from the Incubator Control but not different from each other (at $p<0.05$ as determined by ANOVA with Duncan post-hoc analysis). ($n = 3$ for each treatment group).

3.11: ULSD Exposures Conducted at the US EPA NHEERL Highbay Facility Using the Modified VITROCELL® Exposure System

Exposures to ULSD exhaust from a diesel generator, as outlined in the Methods section, were conducted between April 16, 2014 and May 6, 2014. A total of 11 ULSD exposures were conducted, with up to two exposures being conducted per exposure day. Statistical analyses for all treatment-related effects were conducted by ANOVA with Duncan post-hoc comparisons.

The emissions characterization results for all ULSD exposures are shown in **Table 3.5.** TEOM measurements reflect the particle mass concentration in the sampling/dilution chamber, and were corrected at a 1:5 (April 16 -24) or 1:2.5 (April 29 - May 6) dilution rate for transfer to the VITROCELL® unit. On days with two exposures, the first exposure was conducted in the morning and the second in the afternoon. Engine set-up and operation was not modified in any given test day, thus permitting replicate exposures in a single day. Target emissions concentrations were generally increased between exposure days in an attempt to elicit a strong diesel exposure response. Whereas the engine load was held constant between exposures, the large variation in CO and NO_x levels between exposures is unexpected. The levels measured on April 22 in particular are unusually low, indicating a potential problem with the engine.

Following initial exposures, it was determined that response was comparable between the Field Control and Incubator Control and the Incubator Control was therefore deemed unnecessary. Specifically, a consistent increase in toxicity or change in gene expression was not found for the Field Control relative to the Incubator Control. When no Incubator Control was used, results were expressed relative to the Field Control.

For the singular April 16, 2014 exposure, samples were assayed for WST-1 and LDH release at 24 hours following exposure. The WST-1 results (**Figure 3.18**) indicated that viability for the Field Control samples (i.e., handling control as described in Methods) is significantly higher compared to the Incubator Control ($p < 0.05$), and viability of the Clean Air and Diesel Exhaust exposures are significantly reduced compared to the Field Control ($p < 0.05$). The Clean Air and Diesel Exhaust exposure samples showed similar viability relative to the Incubator Control (i.e., 99.6% and 94.6%, respectively, relative to

Incubator Control). The LDH results (**Figure 3.19**) indicated that cytotoxicity was significantly increased in the Clean Air samples relative to the Field Control ($p < 0.05$) but not the Incubator Control, and for the Diesel Exhaust samples relative to all other treatment groups ($p < 0.05$).

For the first exposure on April 22, 2014, samples were assayed for WST-1 reduction, LDH release, and gene expression (*HMOX1*, *IL6*, *COX2*, and *TNFA*) at 24 hours post exposure.WST-1 results (**Figure 3.20**) indicate that viability for the Clean Air samples was significantly reduced compared to the Incubator and Field Controls ($p < 0.05$). No other significant effects were observed. The LDH release results (**Figure 3.21**) indicate that cytotoxicity was increased for the Clean Air samples relative to the Field Control ($p < 0.05$), and for the Diesel Exhaust samples relative to both the Incubator and Field Controls ($p < 0.05$). The gene expression results **(Figure 3.22**) indicate that expression of *IL6* was reduced in the Clean Air samples relative to the Incubator and Field Controls, and increased in the Diesel Exhaust samples relative to the Clean Air controls.

For the second exposure on April 22-14, samples were assayed for WST-1 reduction, LDH release, and gene expression (*HMOX1*, *IL6*, *COX2*, *TNFA*) at 24 hours post exposure. The WST-1 and LDH results did not show any significant difference between the treatment groups (data not shown). The gene expression results (**Figure 3.23**) showed upregulation of *TNFA* expression for the Diesel Exhaust samples relative to the Field Control and Clean Air samples ($p < 0.05$). No Incubator Control was conducted for this exposure.

For the two replicate exposures on April 24, 2014, samples were assayed for WST-1, LDH, and gene expression (*HMOX1*, *IL6*, *IL8*, *COX2*, and *TNFA*) at 24 hours post exposure. For exposure 2, LDH release was significantly increased for the Diesel Exhaust samples compared to all other treatment groups (**Figure 3.24**; $p < 0.05$). No other significant treatment effects were observed for any of the endpoints examined (data not shown).

For the first exposure on April 29, 2014, samples were assayed for WST-1, LDH, and gene expression (*HMOX1*, *IL6*, *COX2*, and *TNFA*) at 24 hours following exposure. No significant effect was found for the WST-1 and LDH data (not shown); the gene expression data indicated increased expression of *HMOX1* for the Clean Air and Diesel Exhaust

samples compared to the Incubator Control (**Figure 3.25**; $p < 0.05$). Expression of *TNFA* was also increased for the Diesel Exhaust samples compared to all other groups ($p < 0.05$).

For the second exposure on April 29, 2014, samples were assayed for WST-1, LDH, and gene expression (*HMOX1*, *IL6*, *COX2*. and *TNFA*) at 24 hours following exposure. No significant WST-1 or LDH effects were observed for any treatment group relative controls (not shown). The gene expression data indicated that expression of *TNFA* was significantly decreased in the Diesel Exhaust samples compared to the Field Control (**Figure 3.26**; $p < 0.05$).

For the first exposure on May 1, 2014, samples were assayed for WST-1, LDH, and gene expression (*HMOX1*, *IL6*, *IL8*, *COX2*, and *TNFA*) at 24 hours following exposure. No significant WST-1 or LDH effects were observed for any treatment group relative controls (not shown). *HMOX1* expression was significantly increased in the Diesel Exhaust samples compared to Clean Air and Field Control samples (**Figure 3.27**; $p < 0.05$).

For the second exposure on May 1, 2014, samples were assayed for WST-1, LDH, and gene expression (*HMOX1*, *IL6*, *IL8*, *COX2*, and *TNFA*) at 24 hours following exposure. No significant effect was observed in any of the treatment groups, relative to control, for any of the endpoints examined (data not shown).

For the first exposure on May 6, 2014, samples were assayed at 5 hours post-exposure for WST-1 and LDH, and 6 hours post-exposure for gene expression (*HMOX1*, *IL6*, *IL8*, *COX2*, and *TNFA*). No significant effect was observed for WST-1 and LDH (not shown). For the gene expression results, expression of *HMOX1* was strongly increased in the Diesel Exhaust samples relative to the Field Control and Clean Air samples (**Figure 3.28**; $p < 0.05$).

For the second exposure on May 6, 2014, samples were assayed at 5 hours post-exposure for WST-1 and LDH, and 6 hours post-exposure for gene expression (*HMOX1*, *IL6*, *IL8*, *COX2*, and *TNFA*). No significant effect was observed for WST-1 and LDH (not shown). Again, expression of *HMOX1* was strongly increased for the Diesel Exhaust samples relative to the Field Control and Clean Air samples (**Figure 3.29**; $p < 0.05$). Expression of

IL8 was slightly increased for the Diesel Exhaust samples relative to the Field Control samples ($p < 0.05$).

In light of the limited responses observed following exposure, scanning electron microscopy was employed to examine the deposition of particulate material on the insert membrane. Although this analysis was not repeated, no particle deposition was observed on the membrane following a 1 hour ULSD exposure (data not shown).

Table 3.5 Emissions Characteristics for Diesel Exhaust Exposures Conducted at the US EPA NHEERL Highbay Facility in Research Triangle Park, NC. "Corrected to VITROCELL®" reflects the concentration delivered to the VITROCELL® Unit.

Exposure	Date	Exposure #	Dilution (Engine to VITROCELL®)	Mean Concentration Particle Mass Conc. (µg/m^3) Measured (TEOM)	Mean Concentration Particle Mass Conc. (µg/m^3) Corrected to VITROCELL®	CO (ppm)	NO_x (ppm)
Diesel	April 16-14	1	25.0	2924 (± 61)	585 (± 12)	50.8 (± 0.0)	20.3 (± 0.2)
Diesel	April 22-14	1	21.4	3376 (± 199)	675 (± 40)	2.1 (± 0.2)	1.4 (± 0.3)
Diesel	April 22-14	2	23.0	3243 (± 131)	649 (± 26)	2.6 (± 0.9)	2.1 (± 1.5)
Diesel	April 24-14	1	23.0	3325 (± 346)	665 (± 69)	9.9 (± 0.2)	13.0 (± 0.3)
Diesel	April 24-14	2	23.0	3226 (± 99)	645 (± 20)	7.8 (± 0.2)	11.1 (± 0.3)
Diesel	April 29-14	1	13.6	2772 (± 152)	1109 (± 60.8)	34.6 (± 1.4)	28.1 (± 1.7)
Diesel	April 29-14	2	12.5	3056 (± 365)	1222 (± 146)	38.0 (± 21.6)	44.4 (± 26.0)
Diesel	May 1-14	1	8.3	4513 (± 64)	1805 (± 26)	28.9 (± 1.1)	32.0 (± 0.7)
Diesel	May 1-14	2	8.3	4702 (± 176)	1881 (± 70)	31.7 (± 0.4)	35.2 (± 0.4)
Diesel	May 6-14	1	8.8	4138 (± 295)	1655 (± 118)	35.7 (± 0.5)	34.3 (± 0.4)
Diesel	May 6-14	2	7.1	5281 (± 172)	2112 (± 69)	31.7 (± 0.5)	32.1 (± 0.4)

(± standard deviation).

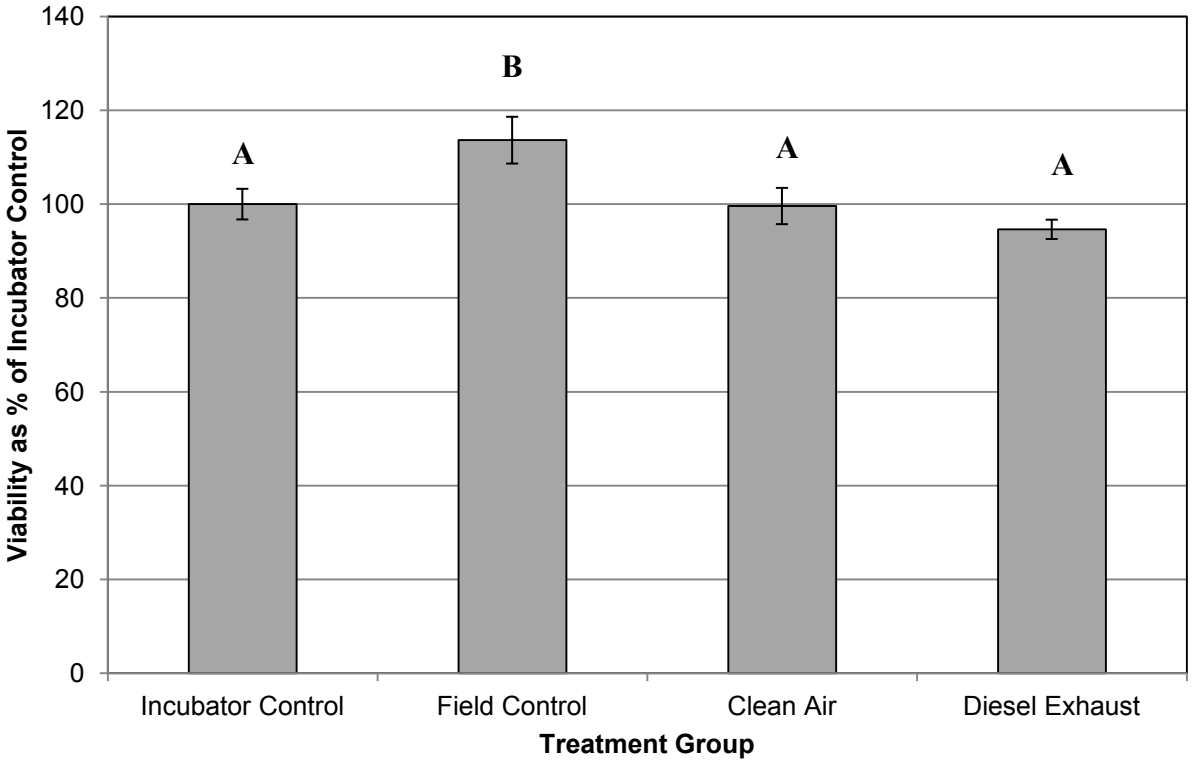

Figure 3.18: Effect of air-liquid interface exposures (i.e., diesel and clean air control) assessed using the modified VITROCELL® system (April 16-14). Cell viability/cytotoxicity was determined using the WST-1 assay conducted 24hrs post-exposure. All values are expressed relative to the incubator control. Error bars show the standard error of the mean. Bars accompanied by different letters indicate significance at $p<0.05$ as determined by ANOVA with Duncan post-hoc analysis. The Field Control had significantly increased viability relative to all other means. ($n = 3$ for each treatment group).

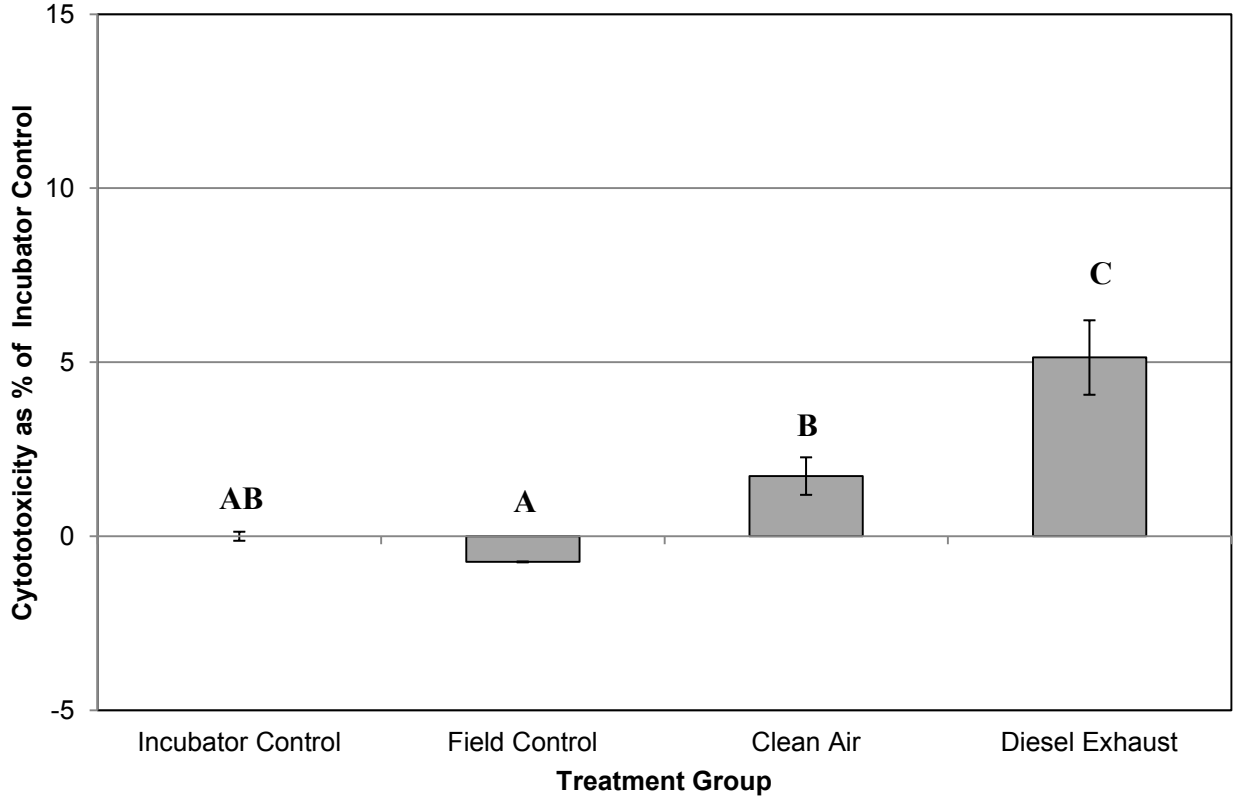

Figure 3.19: Effect of air-liquid interface exposures (i.e., diesel and clean air control) assessed using the modified VITROCELL® system (April 16-14). Cytotoxicity was determined using the LDH Release assay conducted 24hrs post-exposure. All values are expressed relative to the incubator control. 100% cytotoxicity is set equal to the LDH content of the lysed sample. Error bars show the standard error of the mean. Bars accompanied by different letters indicate significance at $p<0.05$ as determined by ANOVA with Duncan post-hoc analysis. The Clean Air control had significantly increased cytotoxicity relative to the Field Control. Diesel Exhaust had significantly increased cytotoxicity relative to all other means. ($n = 3$ for each treatment group).

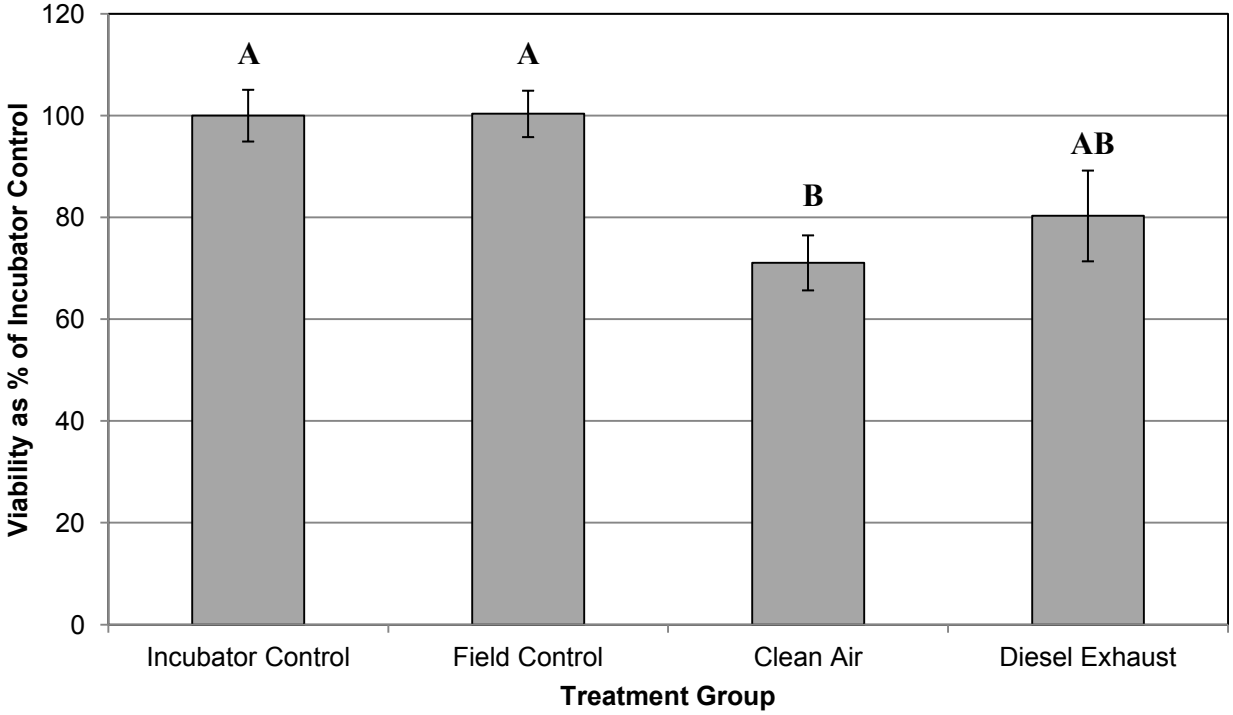

Figure 3.20: Effect of air-liquid interface exposures (i.e., diesel and clean air control) assessed using the modified VITROCELL® system (April 22-14, exposure 1). Cell viability/cytotoxicity was determined using the WST-1 assay conducted 24hrs post-exposure. Values are expressed relative to the Incubator Control. Error bars show standard error of the mean. Bars accompanied by different letters indicate significance at $p<0.05$ as determined by ANOVA with Duncan post-hoc analysis. The Clean Air control had significantly decreased viability relative to the Incubator and Field Controls. (n = 3 for each treatment group).

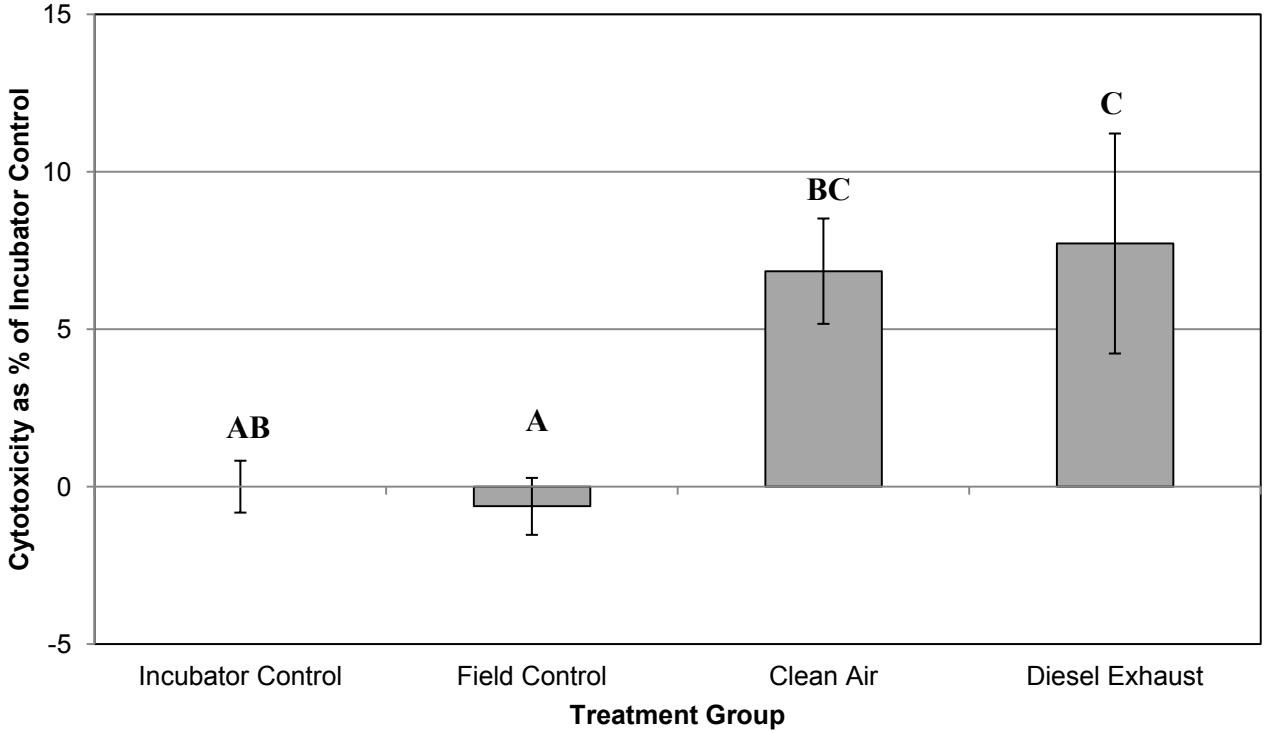

Figure 3.21: Effect of air-liquid interface exposures (i.e., diesel and clean air control) assessed using the modified VITROCELL® system (April 22-14, exposure 1). Cytotoxicity was determined using the LDH Release assay conducted 24hrs post-exposure. All values are expressed relative to the incubator control. 100% cytotoxicity is set equal to the LDH content of the lysed sample. Error bars show the standard error of the mean. Bars accompanied by different letters indicate significance at $p<0.05$ as determined by ANOVA with Duncan post-hoc analysis. The Clean Air control had significantly increased cytotoxicity relative to the Field Control. Diesel Exhaust had significantly increased cytotoxicity relative to the Incubator and Field Controls. (n = 3 for each treatment group).

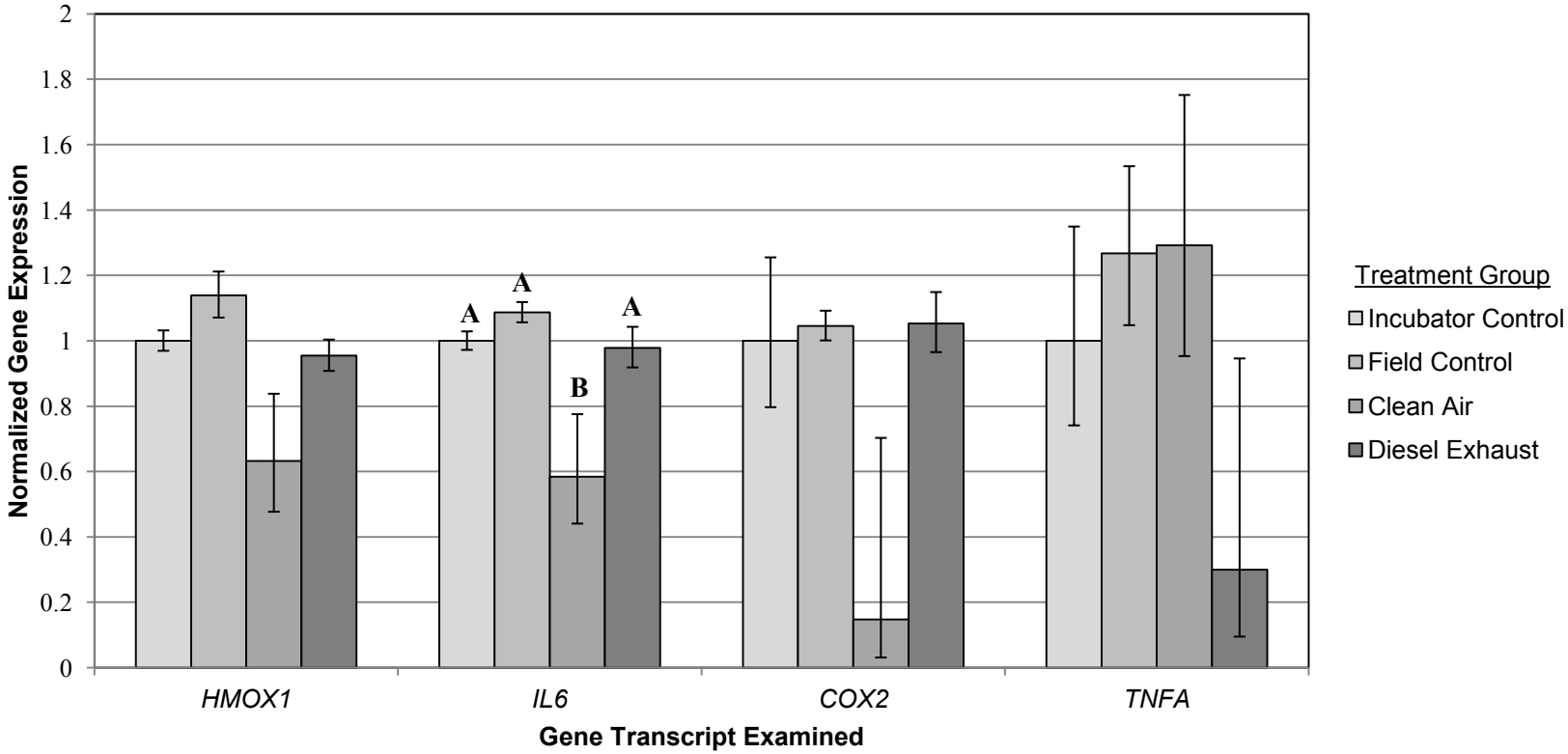

Figure 3.22: Effect of air-liquid interface exposures (i.e., diesel and clean air control) assessed using the modified VITROCELL® system (April 22-14, exposure 1). Response assessed as changes in gene expression 24hrs post-exposure. Values are expressed relative ACTB expression. Error bars show standard error of the mean. Bars accompanied by different letters indicate significance at $p<0.05$ as determined by ANOVA with Duncan post-hoc analysis. The Clean Air control had significantly decreased *IL6* expression relative to all other means (n = 3 for each treatment group).

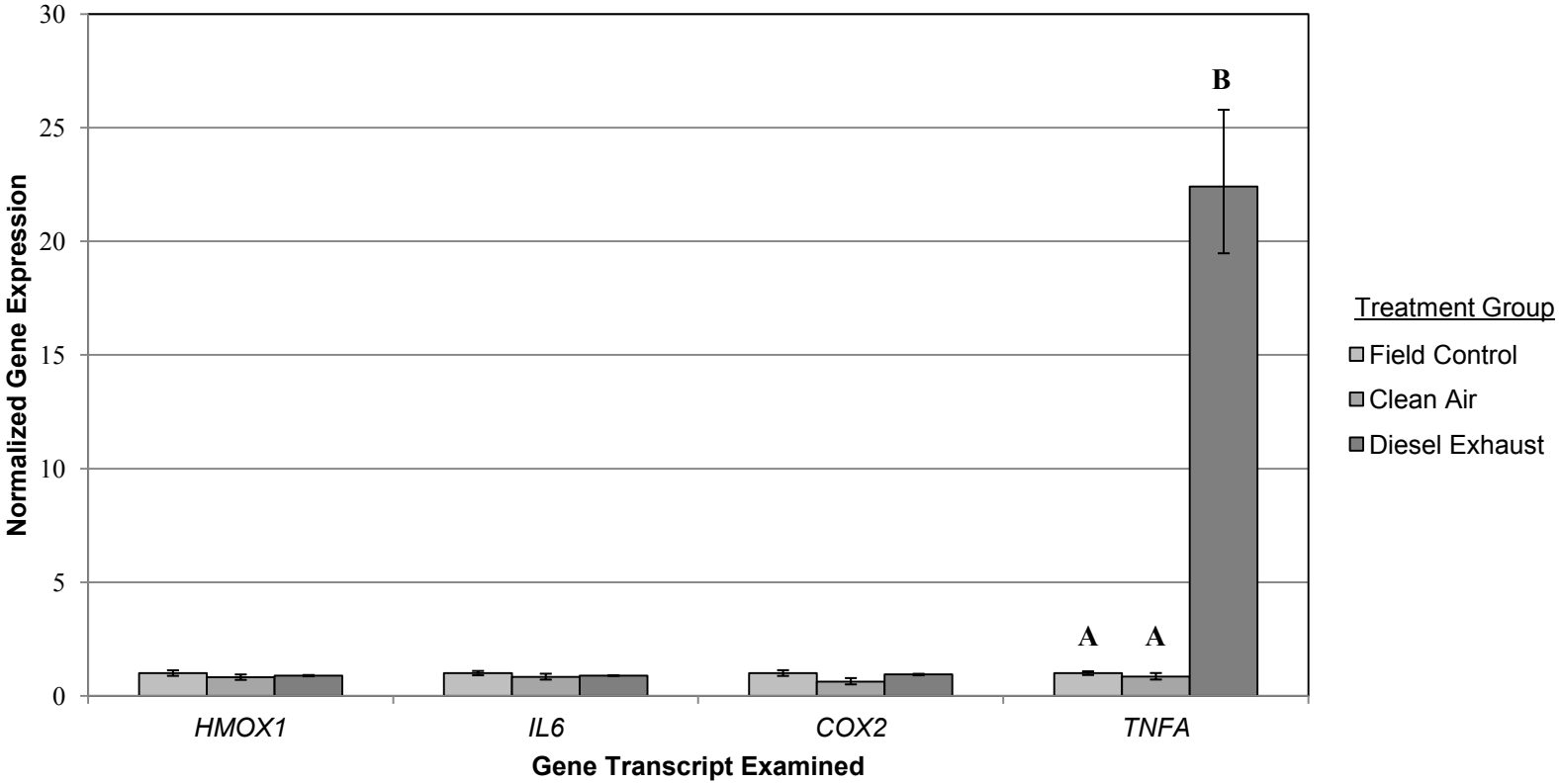

Figure 3.23: Effect of air-liquid interface exposures (i.e., diesel and clean air control) assessed using the modified VITROCELL® system (April 22-14, exposure 2). Response assessed as changes in gene expression 24hrs post-exposure. Values are expressed relative ACTB expression. Error bars show standard error of the mean. Bars accompanied by different letters indicate significance at $p<0.05$ as determined by ANOVA with Duncan post-hoc analysis. Diesel Exhaust-exposed samples had significantly increased *TNFA* expression relative to all other means (n = 3 for each treatment group).

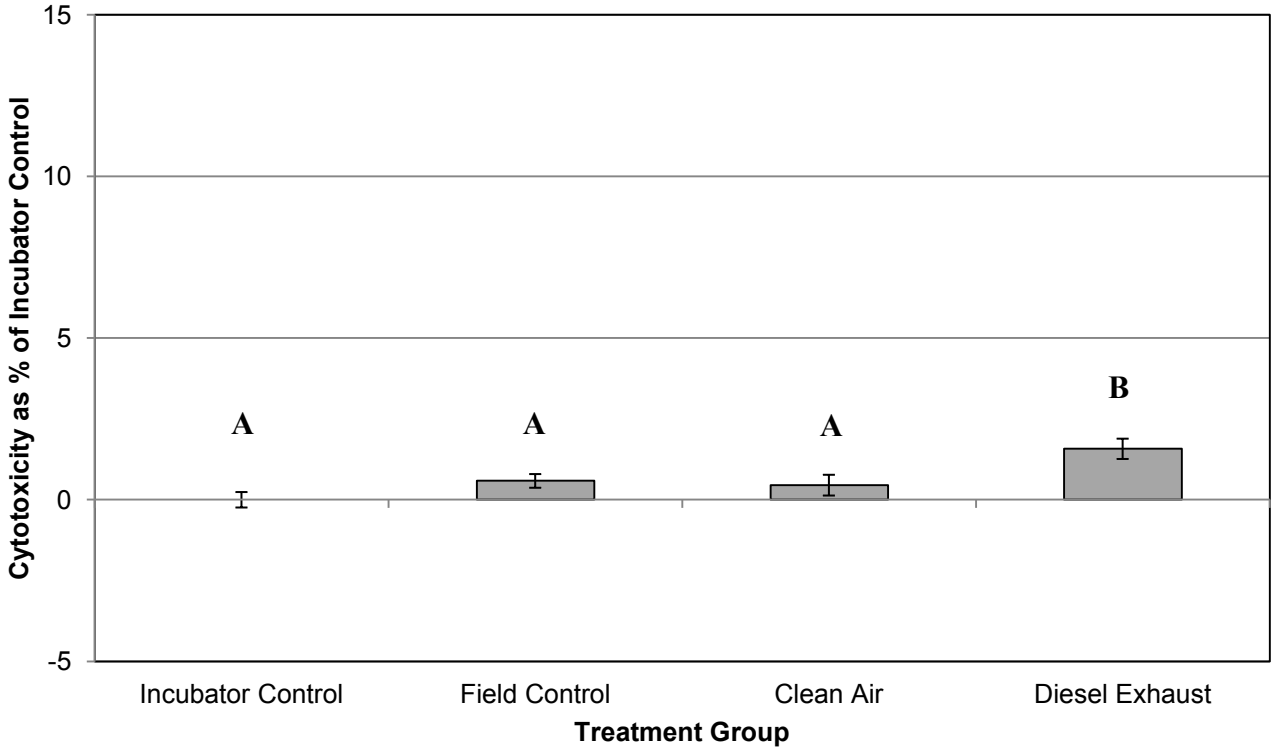

Figure 3.24: Effect of air-liquid interface exposures (i.e., diesel and clean air control) assessed using the modified VITROCELL® system (April 24-14, exposure 2). Cytotoxicity was determined using the LDH Release assay conducted 24hrs post-exposure. All values are expressed relative to the incubator control. 100% cytotoxicity is set equal to the LDH content of the lysed sample. Error bars show the standard error of the mean. Bars accompanied by different letters indicate significance at $p<0.05$ as determined by ANOVA with Duncan post-hoc analysis. The Diesel Exhaust-exposed samples had significantly increased cytotoxicity relative to all other means. ($n = 3$ for each treatment group).

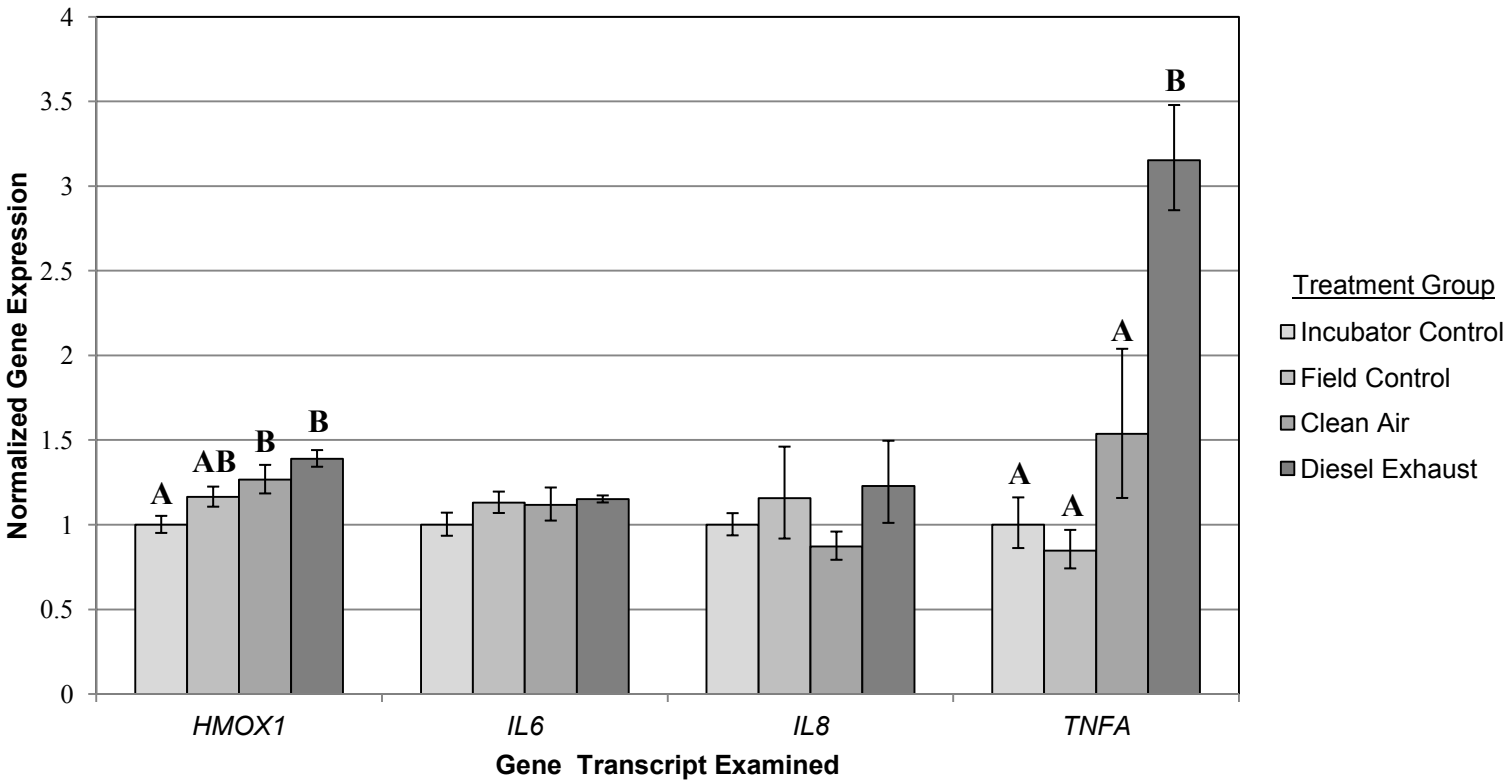

Figure 3.25: Effect of air-liquid interface exposures (i.e., diesel and clean air control) assessed using the modified VITROCELL® system (April 29-14, exposure 1). Response assessed as changes in gene expression 24hrs post-exposure. Values are expressed relative ACTB expression. Error bars show standard error of the mean. Bars accompanied by different letters indicate significance at $p<0.05$ as determined by ANOVA with Duncan post-hoc analysis. Diesel Exhaust-exposed samples had significantly increased *HMOX1* expression relative to Incubator Controls and significantly increased *TNFA* expression relative to all other means. Clean Air controls had significantly increased *HMOX1* expression relative to Incubator Controls (n = 3 for each treatment group).

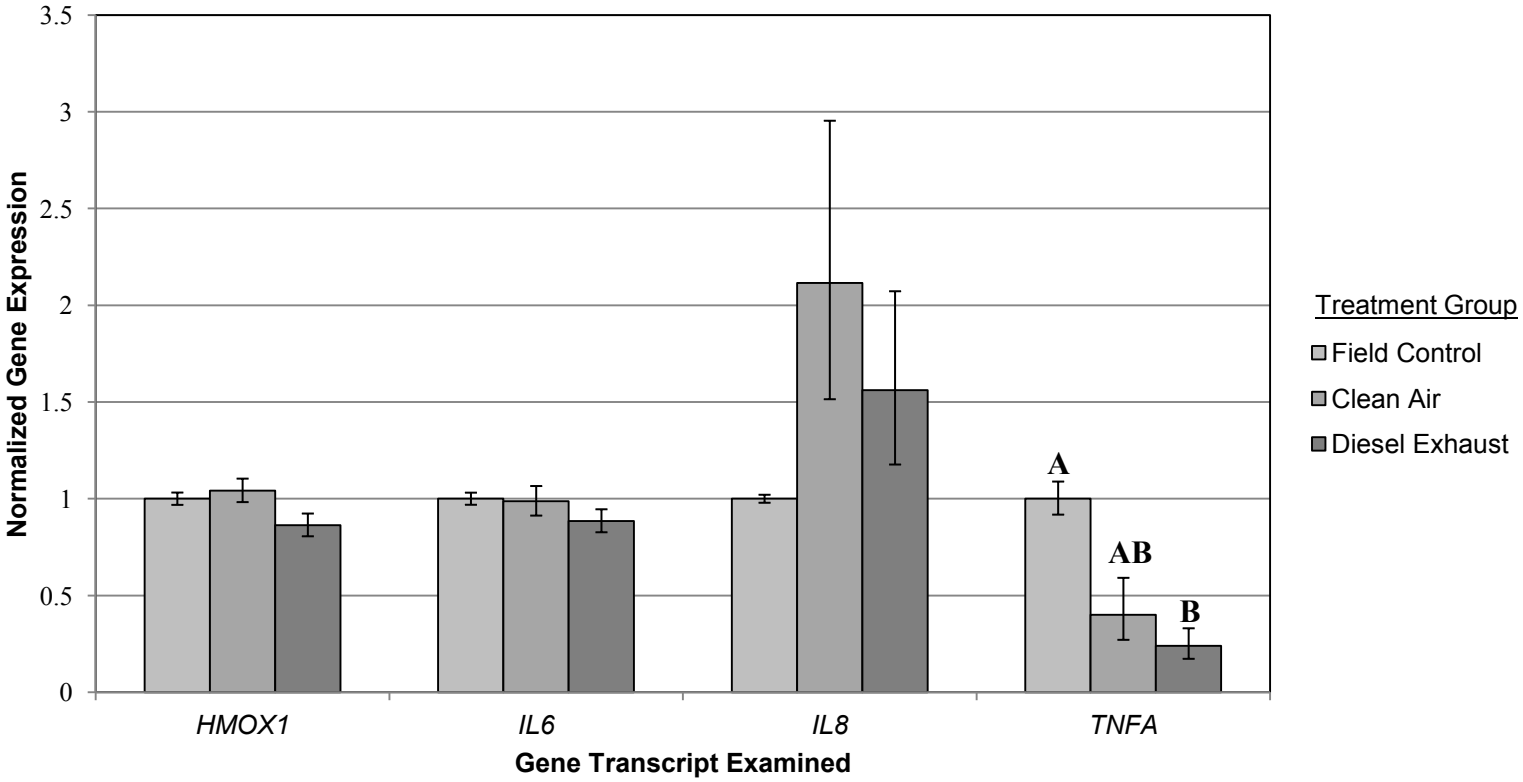

Figure 3.26: Effect of air-liquid interface exposures (i.e., diesel and clean air control) assessed using the modified VITROCELL® system (April 29-14, exposure 2). Response assessed as changes in gene expression 24hrs post-exposure. Values are expressed relative ACTB expression. Error bars show standard error of the mean. Bars accompanied by different letters indicate significance at $p<0.05$ as determined by ANOVA with Duncan post-hoc analysis. Diesel Exhaust-exposed samples had significantly decreased *TNFA* expression relative to Field Controls. (n = 3 for each treatment group).

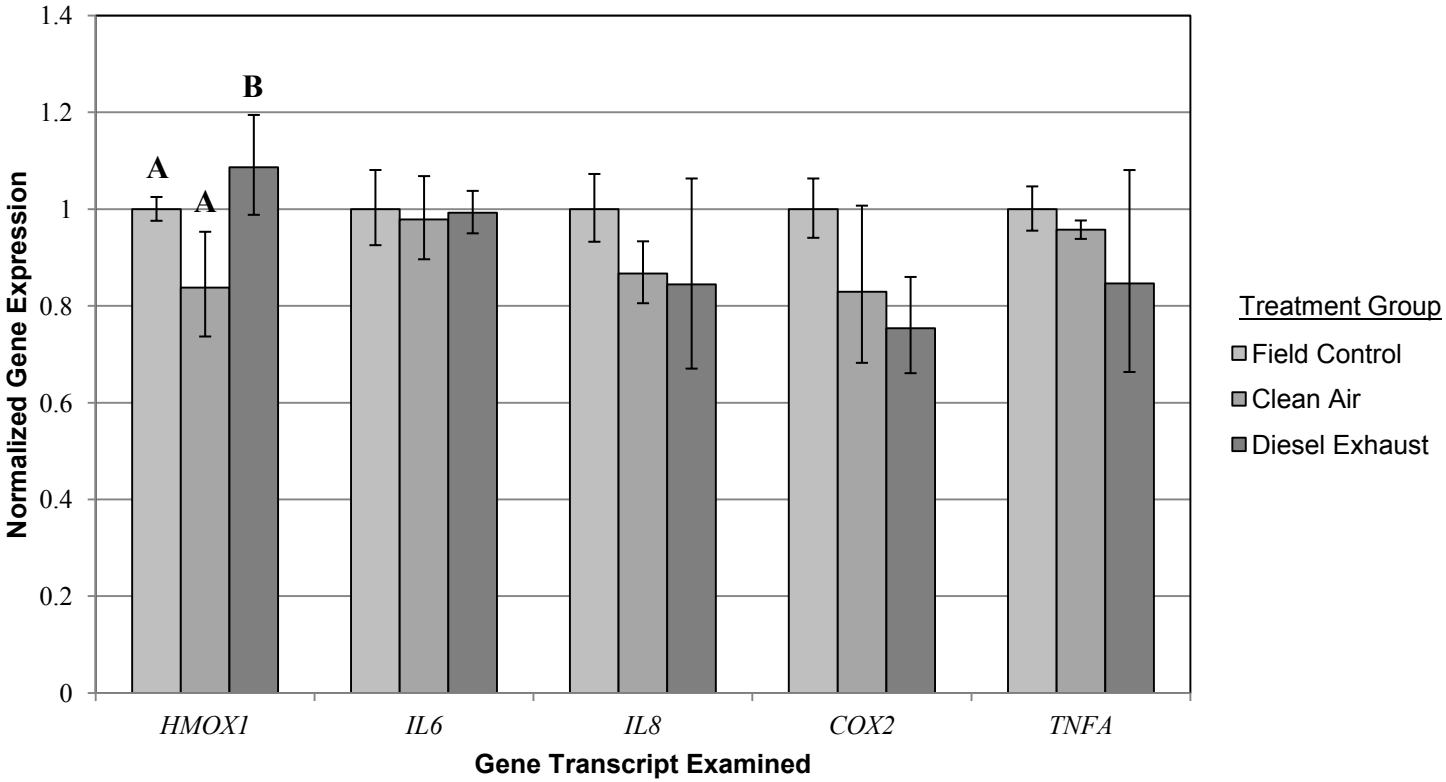

Figure 3.27: Effect of air-liquid interface exposures (i.e., diesel and clean air control) assessed using the modified VITROCELL® system (May 1-14, exposure 1). Response assessed as changes in gene expression 24hrs post-exposure. Values are expressed relative ACTB expression. Error bars show standard error of the mean. Bars accompanied by different letters indicate significance at $p<0.05$ as determined by ANOVA with Duncan post-hoc analysis. Diesel Exhaust-exposed samples had significantly increased *HMOX1* expression relative to all other means. (n = 3 for each treatment group).

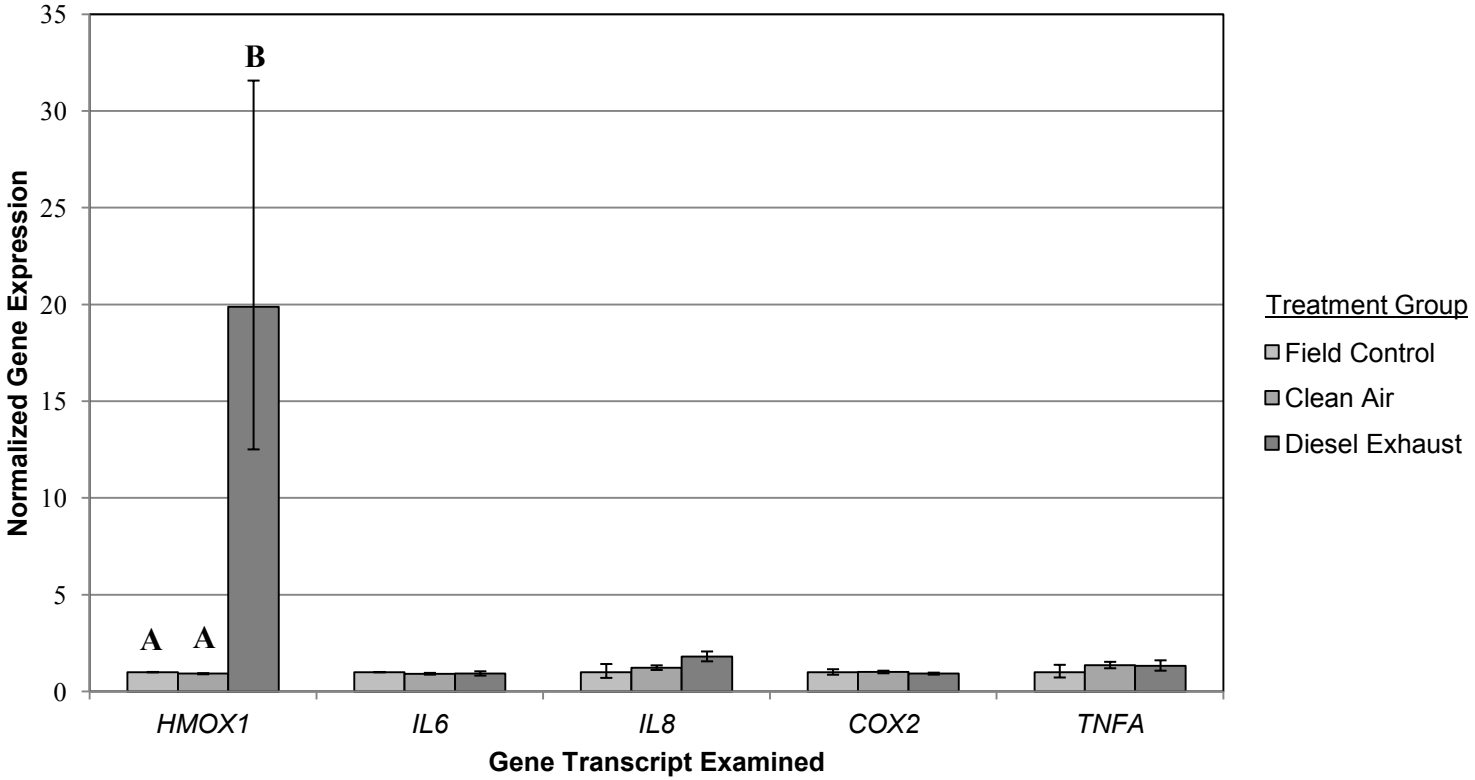

Figure 3.28: Effect of air-liquid interface exposures (i.e., diesel and clean air control) assessed using the modified VITROCELL® system (May 6-14, exposure 1). Response assessed as changes in gene expression 24hrs post-exposure. Values are expressed relative ACTB expression. Error bars show standard error of the mean. Bars accompanied by different letters indicate significance at $p<0.05$ as determined by ANOVA with Duncan post-hoc analysis. Diesel Exhaust-exposed samples had significantly increased *HMOX1* expression relative to all other means. (n = 3 for each treatment group).

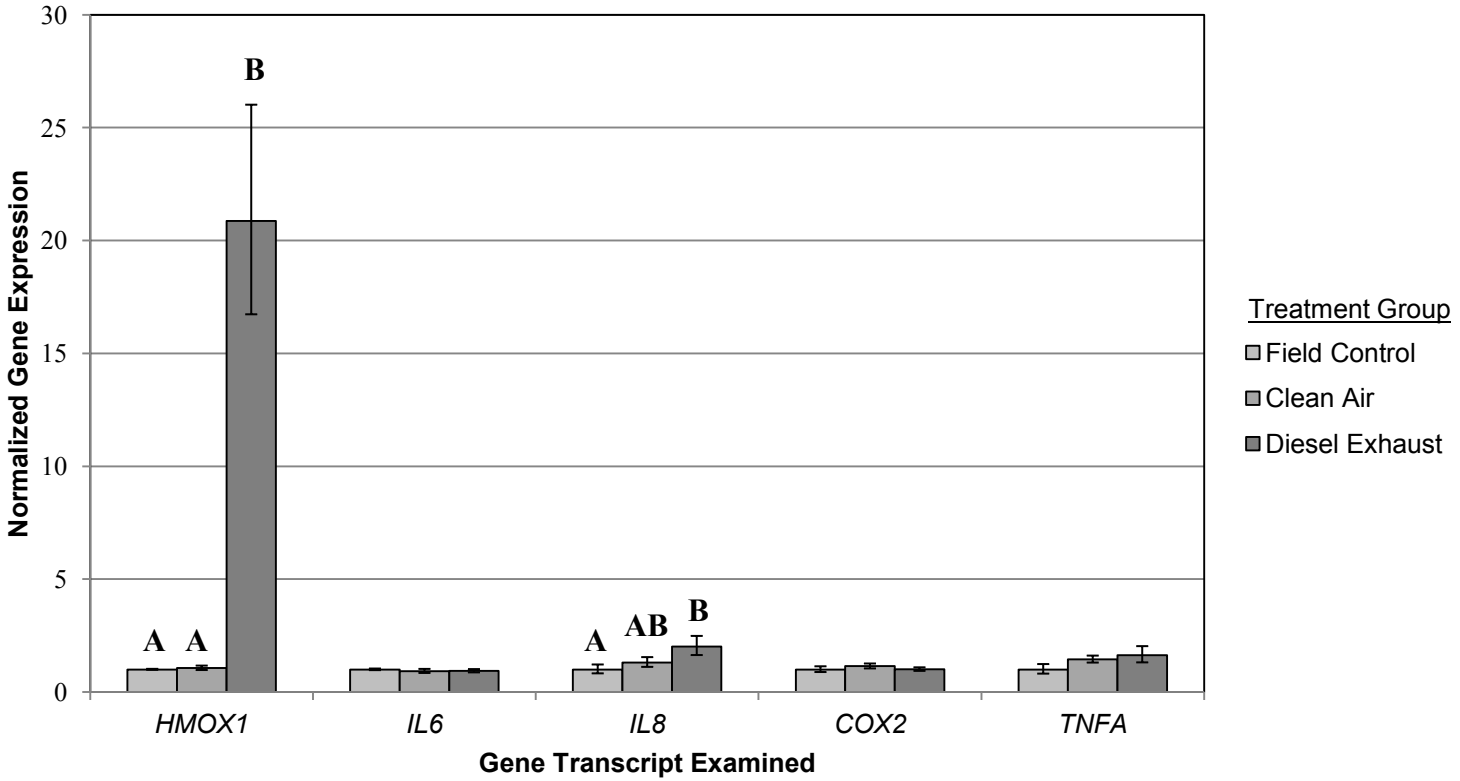

Figure 3.29: Effect of air-liquid interface exposures (i.e., diesel and clean air control) assessed using the modified VITROCELL® system (May 6-14, exposure 2). Response assessed as changes in gene expression 24hrs post-exposure. Values are expressed relative ACTB expression. Error bars show standard error of the mean. Bars accompanied by different letters indicate significance at $p<0.05$ as determined by ANOVA with Duncan post-hoc analysis. Diesel Exhaust-exposed samples had significantly increased *HMOX1* expression relative to all other means and significantly increased *IL8* expression relative to Field Controls. (n = 3 for each treatment group).

3.12: Simulated Urban Atmosphere (Smog) Exposures Conducted at the US EPA NHEERL Highbay Facility Using the Modified VITROCELL® Exposure System and the EPA Mobile Reaction Chamber

Three VITROCELL® exposures to simulated urban atmospheres (smog) were conducted on several afternoons following murine exposures. Toxicological analyses were conducted 24 hours post-exposure for the first exposure, and 5 (WST-1 and LDH) and 6 (gene expression) hours post-exposure for the second and third exposures, respectively. Emissions characterization data are shown in **Table 3.6**.

For the exposure conducted on May 8, 2014, samples were assayed for WST-1, LDH, and gene expression (*HMOX1*, *IL6*, *IL8*, *COX2*, and *TNFA*) at 24 hours post exposure. No significant effects were observed for the WST-1 and LDH endpoints (data not shown). Expression of *HMOX1* was significantly decreased in the Clean Air and Diesel Exhaust samples relative to Field Control (**Figure 3.30**; $p < 0.05$).

For the exposure conducted on May 13, 2014, samples were assayed for WST-1 and LDH at 5 hours post-exposure, and gene expression (*HMOX1*, *IL6*, *IL8*, *COX2*, and *TNFA*) at 6 hours post-exposure. No significant effects were observed for the WST-1 or LDH endpoints (not shown). Expression of *IL8* was significantly increased in the Diesel Exhaust samples compared to the Field Control (**Figure 3.31**; $p < 0.05$). Expression of *TNFA* was significantly increased in the Diesel Exhaust samples compared to the Clean Air and Field Controls, and significantly increased in the Clean Air samples compared to the Field Control (**Figure 3.31**; $p < 0.05$).

For the exposure conducted on May 14, 2014, samples were assayed for WST-1 and LDH at 5 hours post-exposure, and for gene expression (*HMOX1*, *IL6*, *IL8*, *COX2*, and *TNFA*) at 6 hours post-exposure. No significant effects were observed in any treatment groups for any of the endpoints examined (data not shown).

Table 3.6 Characteristics of Simulated Smog Used for VITROCELL® Exposures Conducted at the US EPA NHEERL Highbay Facility in Research Triangle Park, NC.

Exposure	Date	Exposure #	Mean Concentration		
			Particle Mass (μg/m^3)	NO_x (ppm)	O_3 (ppm)
Smog	May 8-14	1	258 (±47)	0.18 (±0.0)	0.09 (±0.0)
Smog	May 13-14	1	266 (±43)	0.18 (±0.0)	0.10 (±0.0)
Smog	May 14-14	1	355 (±106)	0.18 (±0.0)	0.10 (±0.0)

(± standard deviation).

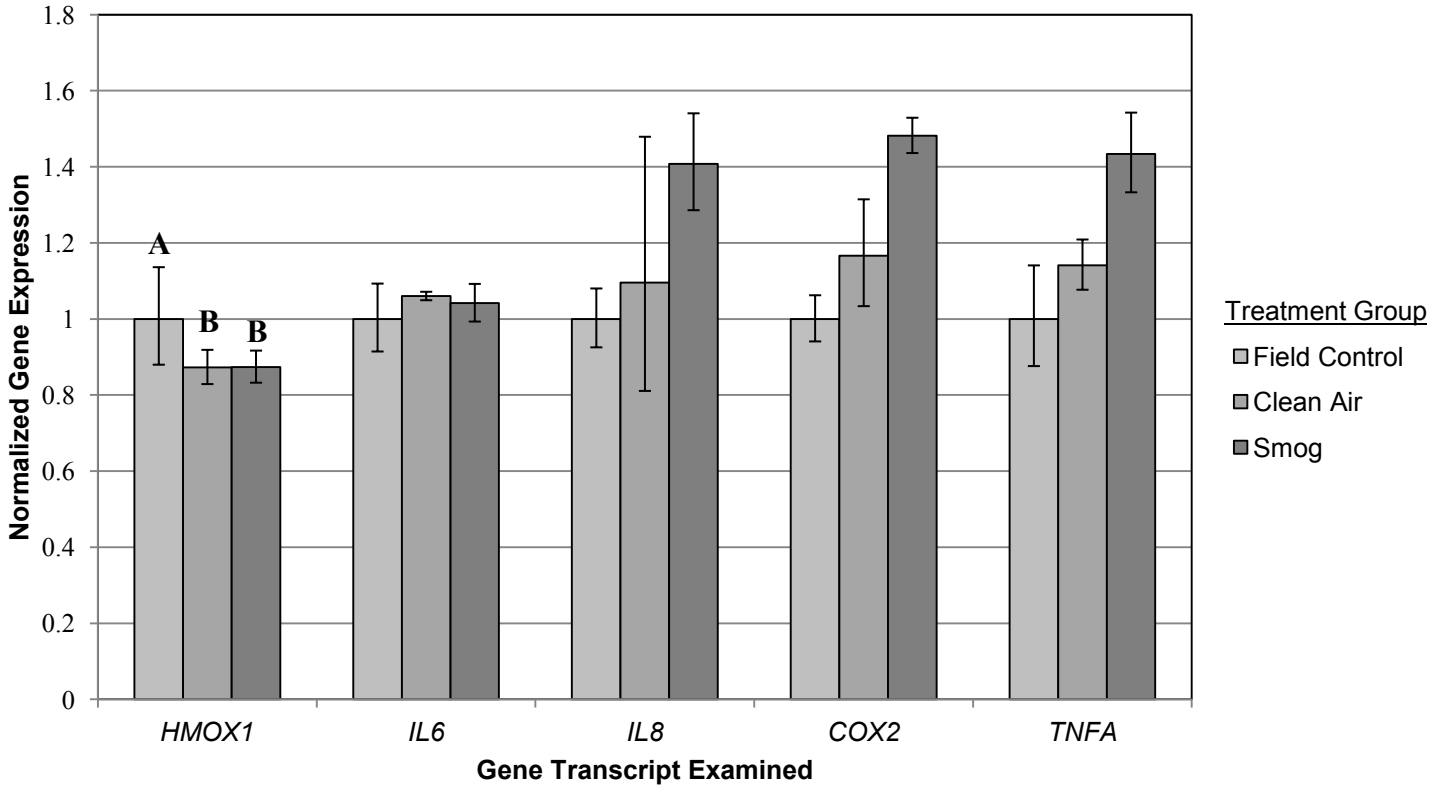

Figure 3.30: Effect of air-liquid interface simulated smog exposures assessed using the modified VITROCELL® system (May 8-14). Response assessed as changes in gene expression 24hrs post-exposure. Values are expressed relative ACTB expression. Error bars show standard error of the mean. Bars accompanied by different letters indicate significance at $p<0.05$ as determined by ANOVA with Duncan post-hoc analysis. Smog-exposed samples and Clean Air controls had significantly decreased *HMOX1* expression relative to Field Controls. (n = 3 for each treatment group).

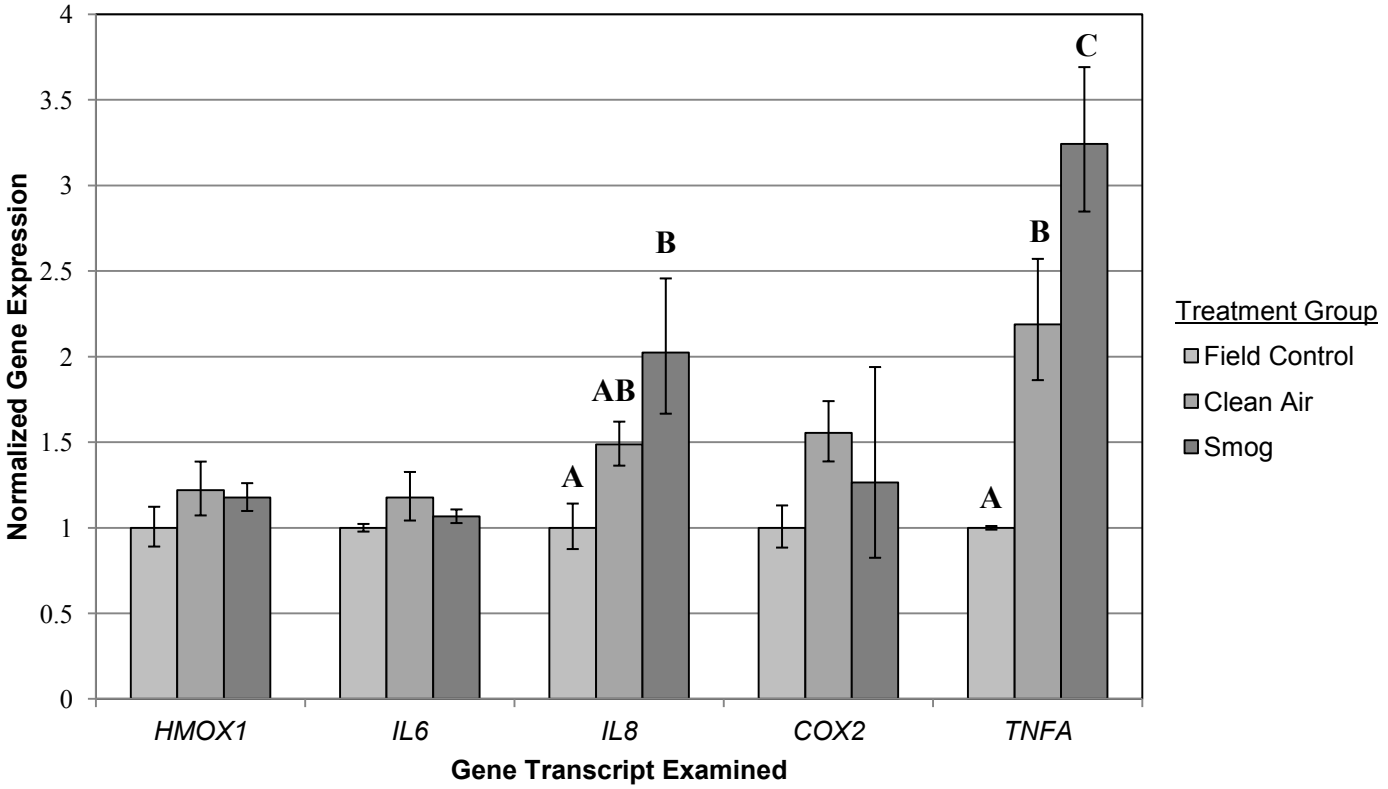

Figure 3.31: Effect of air-liquid interface simulated smog exposures assessed using the modified VITROCELL® system (May 13-14). Response assessed as changes in gene expression 24hrs post-exposure. Values are expressed relative ACTB expression. Error bars show standard error of the mean. Bars accompanied by different letters indicate significance at $p<0.05$ as determined by ANOVA with Duncan post-hoc analysis. Smog-exposed samples had significantly increased *IL8* expression relative to Field Controls and significantly increased *TNFA* expression relative to all other means. Clean Air controls had significantly increased *TNFA* expression relative to Field Controls. (n = 3 for each treatment group).

4.0 DISCUSSION

4.1 Characterization of the Exposure System

The VITROCELL® air-liquid interface exposure system was designed and marketed to permit *in vitro* toxicological characterization of gases and complex aerosols (e.g., vehicular exhaust, cigarette smoke, etc.). The ALI exposure design, which allows direct contact between the cells and the aerosol, constitutes a comparatively better model of the pulmonary exposure in comparison with traditional *in vitro* methods conducted with cells submerged in culture medium. Exposure of whole aerosols is possible, which is of particular interest for studies of complex mixtures. Use of an ALI system permits reduction or elimination of problems related to sample preparation and handling commonly encountered with *in vitro* systems used for examination of aerosols (e.g., collection of particulates and suspension of particulates in liquid medium); however, the results of this study indicate that the VITROCELL® air-liquid interface exposure system is also problematic.

The earliest publications employing the VITROCELL® air-liquid interface exposure system suggest that it can be used without any modifications of the aerosol handling of cell exposure setup, i.e., can be used without modifications to control and maintain system temperature and aerosol humidity (Aufderheide et al. 2001, Knebel et al. 2002, Ritter et al. 2001). However, in this study, preliminary deployment of the system for toxicological characterization of diesel exhaust found that control cells exposed to clean air exhibited a consistent, significant reduction in cell viability relative to unexposed controls maintained in a tissue culture incubator. The observation that the clean air control affects cell viability limits the utility of the system for analyses of diluted diesel exhaust; and moreover, diminishes confidence in the results obtained during early experiments conducted at Environment Canada (see Results Section 3.2). Although the results did show a significant reduction in cell viability for the diesel exhaust exposed cells, relative to the synthetic air control, it is clear that exposure to the clean air alone contributes to a significant reduction in viability (i.e., ~45% relative to incubator control, Figure 3.2). The diesel exhaust induced a statistically significant reduction in viability in comparison with the clean air (i.e., an additional ~20% relative to incubator control). However, the effect of the clean air and the limited dynamic range to detect a toxicologically meaningful response of a test aerosol (i.e., below 45% viability for clean air) clearly indicated that it would be necessary

to scrutinise the VITROCELL® setup used here, relative to that employed in the studies summarised in Table 1.5. In order to maximise the ability to detect toxicologically meaningful responses it was necessary to determine the cause of the clean air effect and introduce system modifications to minimise effects that are not induced by the test aerosol (e.g., vehicle exhaust).

Detailed scrutiny of the VITROCELL® setup used in this study indicates that it differs from the system employed in some of the aforementioned, early studies summarised in **Table 1.5**. For example, although the system that was purchased from VITROCELL® GmbH for this study, which was not modified for the early diesel exhaust exposures, is based on the CULTEX design published by Aufderheide et al (2001), it differs substantially in physical layout i.e., the modules support 24 mm diameter inserts versus the original 12 mm inserts, the aerosol inlet was changed to the aforementioned trumpet structure, and the shape of the basal media wells was modified. Thus, it is not unreasonable to assert that the exposure parameters used in the original studies (e.g., prior to 2006) are not necessarily ideal for use with commercially distributed version purchased for this work.

The original ALI conceptual design put forward by Michaela Aufderheide, then at the Hannover Medical School in Hannover, (Aufderheide and Mohr 1999, Aufderheide and Mohr 2000, Aufderheide et al. 2001, Knebel et al. 2002, Ritter et al. 2001) asserted that exposure of cells to unmodified aerosols at an ALI (i.e., no humidity and/or temperature adjustment) is possible due to the establishment of a microclimate over the cells via the evaporation of liquid from the basal side of the membrane. This microclimate is reliant on equilibrium between the gas-flow rate and basal media pressure, with the latter being proportional to the media level surrounding the insert. Thus, aerosol flow rate and basal media level will likely influence cell viability; however, early investigations in this study, which examined flow rates between 0.5 and 8.3 ml/min and basal media levels of 10 - 11.5 ml, did not show any significant effect on viability (results not shown). The flow rate of 8.3 ml/min initially adopted for this work is based on the publication of Ritter et al (2001) who noted that cell viability could be maintained at this flow rate. Later analyses employed a flow rate of 5 ml/min to coincide with other publications using the commercially available

VITROCELL® system (Gminski et al. 2010, Kim et al. 2013, Persoz et al. 2010, Persoz et al. 2011).

The VITROCELL® module, as per the website, is compatible with semi-permeable membrane inserts from Greiner Bio-One, Corning, and BD Labware. Apart from well size, no distinction is made regarding the suitability or physical properties of the inserts. Translucent Greiner Bio-One Thincert membranes were used for the pilot diesel exposures; however, as noted these were replaced with comparable transparent membranes for later experiments since the latter are easier to examine microscopically to determine confluency and cell morphology. When transitioning between the two insert types, it was observed that basal media more readily crossed the translucent membranes, likely due to the increased pore density, i.e., 1×10^8 pores/cm^2 compared to 2×10^6 pores/cm^2 for the transparent membranes. The pore size of both membranes was 0.4 μm. Thus membrane choice will almost certainly influence basal media pressure and the establishment of the aforementioned microclimate in the cell exposure area; moreover, the original CULTEX system (i.e., predecessor of the VITROCELL®) used 12 mm 12-well plate inserts instead of the 24 mm 6-well plate inserts used here. The Corning Transwell inserts used for later experiments conducted at the US EPA facility have a 0.4 μm pore size and a pore density of 4×10^6 pores/cm^2. This is comparable to the transparent Greiner Bio-One Thincerts; however, the results showed improved viability of cells cultured on the Corning Transwell inserts.

Exposure medium choice was also shown to significantly influence cell viability. Compared to F-12K media, RPMI 1640 significantly improved post-exposure cell viability. Although F-12K is the medium recommended by the ATCC for cultivation of A549 cells, RPMI 1640 is commonly used for air-liquid interface exposures (Pariselli et al. 2006, Olivera et al. 2007, Mulhopt et al. 2007). In particular, Pariselli et al. noted improved cell viability following substitution of RPMI 1640 for F12-K. This was attributed to pH instability associated with the use of F12-K for ALI exposures, which increased up to 7.8 without CO_2 supplementation (Pariselli et al. 2006). In this work, both F-12K and RPMI 1640 were supplemented with 20 mM HEPES to minimise pH fluctuations. Exposures utilizing BEAS-2B cells used the ATCC-recommended media supplemented with 20 mM

HEPES and observed no comparable decreases in cell viability. However, it would be useful for future work to examine A549 responses following exposure in the modified exposure system and BEAS-2B responses following exposure in the unmodified exposure system.

With respect to the use of FBS in the exposure medium, the literature is inconsistent, i.e., some publications replace the culture media with FBS-free media 4 - 24 hours before exposure to allow adaptation of the cells, whereas others use reduced or FBS-free media only during exposure, and still others include FBS during exposure. FBS encourages cell growth, can improve cell attachment, and may protect cells from effects related to handling/exposure stress. Although components of a test aerosol could potentially interact/react with FBS proteins, such as serum protein oxidation by diesel exhaust particles, this was generally not a concern for VITROCELL® exposures since the test aerosol is not in intimate contact with the media during the exposure (Chiang et al. 2013). Although prolonged incubation without FBS will undoubtedly have an adverse effect on the cells, removal of FBS before the exposure encourages cell cycle synchronization in G1, and this may reduce variability in the recorded responses (Banfalvi 2011). Examinations of cells exposed under conditions both with and without FBS did not show any significant difference in viability (results not shown).

Although, as noted earlier, publications describing the original VITROCELL® concept and design suggested that aerosol modifications are not required, the majority of recent publications that employed the commercially distributed versions of the VITROCELL® indicate that aerosol humidification is advisable (Pariselli et al. 2006, Olivera et al. 2007, Mulhopt et al. 2007, Anderson et al. 2010, Gminski et al. 2010, Tang et al. 2012, Xie et al. 2012, Weber et al. 2013, Panas et al. 2014). Maintenance of high humidity, i.e., above 100% RH at ambient temperature, requires a heated environment. At standard atmospheric pressures, assuming that ambient temperature is about 22°C, 100% RH is equal to only 19 g/m^3 compared to 44 g/m^3 at 37°C. Therefore, supplemental heating of the VITROCELL® setup is required to maintain a stable temperature that permits maintenance of physiologic humidity. As an additional benefit, supplemental heating prevents condensation at the VITROCELL® exhaust port.

In summary, experimental manipulation of the VITROCELL® setup, as well as the protocols for maintenance and preparation of cultures for ALI exposures showed that a wide array of variables can influence system performance, and by extension, its utility for reliable toxicological characterisation of test aerosols. Variables examined and found to influence the viability of VITROCELL®-exposed cells include media formulation, insert type, and aerosol properties (e.g., humidity). The need to modify the aerosol (e.g., humidify) will likely alter the physical properties of the delivered aerosol and its components (e.g., particulate matter); however, this is not necessarily a drawback since the aerosol properties will be similarly modified during inhalation. Nevertheless, the need to modify the commercially-available version of the VITROCELL® system calls into question its suitability for routine, reliable examination of complex aerosols. For example, system features such as the circulating water bath are ineffective for maintaining the aerosol temperature, and essential modifications to maintain temperature of the VITROCELL® and its surrounding environment, which are discussed below, eliminate the need for the supplied water bath.

4.2 Responses to Diesel Exhaust

The light-duty Volkswagen diesel engine study, i.e., the Environment Canada study conducted prior to substantial modification of the VITROCELL® setup, found a consistent, significant reduction in cell viability following diesel exhaust exposure, relative to the clean-air and unexposed (incubator) controls. Moreover, comparisons between fuel formulations indicated limited differences in WST-1 reduction across blends, with only B20 canola being significantly different (i.e., increased viability) relative to ULSD. Apoptosis, as measured by Caspase 3/7 activation, was significantly reduced following ULSD exposure, relative to the clean air and unexposed controls. It is important to emphasise here that each of the diesel exhaust samples were only examined at a single concentration (i.e., 40-fold dilution), and the observed variations in response across fuel formulation will reflect changes in the composition of the exhaust. The results obtained indicate that the B100 tallow and B100 canola emissions contain reduced particle concentrations and increased NO_x concentrations, relative to ULSD or B20 blends. However, statistical analyses failed to show a significant difference between the effects of B100 emissions and ULSD emissions.

The aforementioned results also showed that exposure to clean air elicited significant reductions in cell viability and apoptosis relative to the unexposed controls, and it was hypothesised that the effect of the control air was significantly influenced by humidity. The *synthetic* air used for the clean air control was identical to that used for the earlier experiments conducted at Health Canada (i.e., purchased cylinder of compressed air). In contrast, HEPA-filtered ambient (room) air was used to dilute the light-duty diesel exhaust. Initially, it was thought that a compressed cylinder of high-purity air would be an ideal control for the diesel exposure. Since it is standardised by the manufacturer, the potential for confounding effects related to variability in the composition of ambient air could be minimised. In addition, distribution of compressed high-purity air to the VITROCELL® apparatus is readily implemented in comparison with the setup required to distribute conditioned ambient air. It is particularly important to emphasise that while physiologically desirable absolute humidity equates to 44 g/m^3 at standard atmospheric pressures, the cylinder of compressed synthetic air had an absolute humidity below only 0.5 g/m^3, and the ambient room air used to dilute the light-duty diesel exhaust had an absolute humidity of approximately 5 g/m^3. Thus, interpretation of the results for the light-duty diesel exhausts, relative to clean air control, is somewhat limited since the humidity was not matched across the treatments (i.e., diesel versus clean air control), and the markedly lower humidity of the synthetic air used as a control for experiments conducted at Environment Canada likely contributed to reductions in viability of cells exposed to control air. Moreover, one might contend that the actual difference between the diesel exhaust effect and the effect of an appropriately matched control would be greater than that observed in this study. If a similar setup is used in future, it would be advisable to compare the effect of synthetic air to HEPA-filtered ambient air.

In contrast to the aforementioned aerosol conditions, the optimized exposure aerosols studied at the U.S. EPA facility had an absolute humidity of 25 - 34 g/m^3. However, it should be noted that these values are indicative of the aerosol delivered to the VITROCELL® module, and specific characterization of the aerosol in contact with the cells, i.e., that presumably modified by the microclimate around the cells, is not possible due to the enclosed construction of the module. Based on statements in early

VITROCELL® publications, it seems reasonable to assert that the microclimate in the module may increase aerosol humidity around the cells.

Following optimization of the exposure system (i.e., temperature and humidity establishment and control), exposures conducted at the US EPA NHEERL's Highbay facility noted markedly improved variability of the clean air controls compared to earlier experiments. More specifically, of the 11 ULSD exhaust exposures, only 3 exposures provided results indicating that the clean air-exposed response is significantly different from the unexposed controls. Nevertheless, the variability in the clean air results across multiple experiments (e.g., Figures 3.18, 3.19, 3.20, 3.21) is cause for concern. Additional scrutiny of the 3 aforementioned exposures indicated unusually high viability of the field control on April 16th, 2014, unusually low viability of the air-exposed control on April 22nd (i.e., viability lower than diesel exposure), and a significant increase in *HMOX1* expression relative to the incubator control on April 29th. Of the 11 ULSD exhaust exposures, the diesel-exposed group exhibited statistically significantly differences for 9 exposures. The diesel response was significantly different, on at least one endpoint, from all other treatment groups (i.e., clean air, field control, incubator control) for 7 of the exposures. Of these, the diesel exhaust-exposed samples showed significantly increased cytotoxicity, as measured by the LDH assay, for 2 exposures (April 16 exposure 1, April 24 exposure 2). Expression of *TNFA* was significantly increased relative to all control groups for 2 of the exposures (April 22 exposure 2, April 29 exposure 1). Expression of *HMOX1* was significantly increased for 3 exposures (May 1 exposure 1, May 6 exposure 1, May 6 exposure 2). Notably, the May 6th exposures were the only ULSD exposures analyzed at 6 hours following the exposure; all others were assayed at 24 hours post-exposure. The increase in the *HMOX1* response was much stronger for the May 6th exposures relative to the May 1st exposure.

Although the results obtained in this phase of the study did, in some instances, show a toxicological response, the magnitude and direction of the responses across the various endpoints was highly variable. The endpoints examined in this study were selected for their ability to monitor cell viability, pro-inflammatory signalling and oxidative stress. All of these endpoints have been shown to be significantly altered in cells exposed to

combustion-derived aerosols such as diesel exhaust (Ristovski et al. 2012). For example, several authors have documented significant decreases in viability (Gualtieri et al. 2014), significant increases in the expression of pro-inflammatory cytokine genes such as IL6, IL8 and TNF (Totlandsdal et al. 2012), and oxidative stress response genes such as *HMOX1* following exposure to diesel exhaust (Omura et al. 2009), as well as complex aerosols containing vehicular exhaust (e.g., urban air, (Vaccari et al. 2014)). Moreover, several studies successfully used the VITROCELL® system to document these types of responses to combustion-derived aerosols such as diesel exhaust. It is unfortunately difficult to objectively evaluate the biological responses, or in some instances, lack thereof, obtained for the aerosol doses investigated in this study (i.e., 1.1-2 mg/m^3 diesel particulates for 1hr at VITROCELL® flow rates of 5-8.3 ml/min). Although numerous studies have employed a wide range of *in vivo* or *in vitro* assessment methods to examine the toxicological properties of combustion-derived aerosols, or materials derived from combustion-derived aerosols (e.g., particulate matter), very few studies have employed ALI devices such as the VITROCELL®. Comparisons of the responses obtained in this study with those published in the peer-reviewed literature are discussed below in Section 4.4.

It should also be noted that exposures at the Environment Canada facility utilized A549 (adenocarcinomic alveolar epithelial) cells whereas exposures at the U.S. EPA facility utilized BEAS-2B (virally transformed normal human bronchial) cells, somewhat limiting the direct comparability of the response. However, both A549 and BEAS-2B cells have both been used previously in VITROCELL®-related publications (Persoz et al. 2012, Weber et al. 2013). Both cell lines have been shown previously to have limited CYP activity (Garcia-Canton et al. 2013) indicating that metabolically-activated compounds are likely not a major contributor to response with either cell line as used.

4.3 Responses to Simulated Urban Atmosphere (Smog)

The U.S. EPA Mobile Reaction Chamber was used to generate simulated urban aerosols and three pilot experiments investigated the effect of the aerosols. The results obtained, which are based on analyses 6- or 24 hours post-exposure failed to show any significant decreases in cell viability. However, the control air results showed a significant effect relative to unexposed field controls (e.g., increased *TNFA* expression May 13th). For the

smog-exposed group, only *TNFA* expression for the May 13th exposure showed a significant increase relative to all other treatment groups. For the May 13th exposure, *IL8* expression was significantly increased relative to the field control, but not the clean air control. No significant effect of exposure was observed for the May 14 exposure.

Relative to the aforementioned responses for ULSD, cytotoxicity was generally lower for the smog exposures (e.g., significant increases in LDH leakage for some ULSD exposures). Significant increases in expression of *TNFA* relative to the control air was observed for both exposure aerosols; however the effect was not consistent for either treatment. Increased *HMOX1* expression, relative to clean air controls, was observed for some of the ULSD exposures, but was not observed for the smog exposures. A slight increase in *IL8* expression was observed for one of the smog exposures (i.e., significantly different from the field control but not the clean air control), whereas this effect was not observed in any of the diesel exposures. Interestingly, the murine exposure studies conducted in parallel with the VITROCELL® indicated that female C57BL/6 mice exposed for 4 hours to the same atmosphere used in this study experienced acute cardiac and ventilatory effects, i.e., increased breathing frequency, decreased inspiratory time, decreased heart rate, cardiac dysrhythmia and non-conducted p-waves, which were reversed within 24hrs following exposure (Hazari et al. 2015).

Although the results obtained failed to show a robust toxicological response to the simulated urban atmosphere examined, many studies have clearly shown that exposures to urban air can adversely affect cellular function (Doyle et al. 2007, Koehler et al. 2013); effects that are commonly investigated and recorded include proinflammatory signalling and oxidative stress responses (Sexton et al. 2004). Ideally, the MRC employed in this study can ultimately be used in conjunction with an ALI exposure system such as the VITROCELL® to determine the identity of the putative toxicants in urban air; and moreover, identify the factors that contribute to temporal modifications in the chemical and toxicological properties of complex atmospheric aerosols containing a multitude of criteria contaminants (e.g., ozone, NO_x, particulates, hydrocarbons, etc.).

4.4 Comparison to Responses Observed in the Literature

As noted in the Introduction, numerous studies have examined the effects of combustion-derived aerosols such as diesel exhaust on experimental animals *in vivo* as well as cultured mammalian cells *in vitro*. For example, with respect to genetic and related effects pertaining to carcinogenesis, IARC Monograph 105 contains detailed summaries of published *in vivo* and *in vitro* studies (i.e., Tables 4.4, 4.5 and 4.6, IARC, 2013). Unfortunately, differences in the *in vivo* or *in vitro* exposure regimes, relative to that employed here; prohibit direct comparisons with this study. For example, several *in vivo* inhalation studies summarised in IARC Monograph 105 (IARC Monograph, Table 4.4) employed whole body exposures to diluted diesel emissions (i.e., up to 7mg/m^3) for extended periods of time (e.g., up to 24 months). A wide range of additional studies employed exposure regimes such as intratracheal instillation to expose experimental animals to isolated diesel particulates (IARC Monograph, Tables 4.4 and 4.5). The *in vitro* studies summarised by IARC (i.e., Table 4.6) predominantly examined diesel particulate matter suspended in liquid culture medium (i.e., 0.1 – 1.0 mg/mL). Very few studies have employed an ALI exposure device such as the VITROCELL® to examine the toxicological effects of combustion-derived aerosols such as diesel exhaust. Knebel et al. (2002) and Seagrave et al. (2007) used the VITROCELL® to examine cellular responses to diluted diesel exhaust. More specifically, the Knebel et al. study, which used a VITROCELL® setup that predated commercial distribution, exposed HFBE21 cells to emissions from a 75 horsepower, six cylinder, Volkswagen diesel engine with no aftertreatment. Particle number concentrations were between 1 x 10^4 and >1 x10^9 (above detection limit), depending on the operating conditions and dilution used. The results obtained did not show an effect of clean air on cell survival and viability; in contrast, undiluted exhaust induced a 50% reduction in cell survival and a 70% reduction in cell viability measured using the WST-1 assay. Exposure to 1:100 diluted exhaust induced only a 3% reduction in cell survival, and only a 17% reduction in viability as WST-1 reduction. Exposure to a 1:100 dilution of exhaust generated under “higher load", which had increased CO and NO_x and a 3-fold increase in particle concentration, elicited approximately 15% reduction in cell survival and a 40% reduction in viability measured as WST-1 reduction. Seagrave et al. (2007) exposed differentiated primary human airway epithelial cells (EpiAirway, MatTek,

Ashland, MA) to emissions from a single-cylinder 5.5kW Yanmar diesel generator using a steady-state 5kW load. Emissions were diluted to 1:50 total dilution (i.e., 3 mg/m^3 TPM) and supplemented with 5% CO_2. Following a 1 hour exhaust exposure, the authors noted significantly increased cytotoxicity (LDH leakage), reduced viability (WST-1), reduced alkaline phosphatase activity, reduced glutathione activity, increased levels of HO-1 protein, and decreased levels of IL-4 and IL-6 protein expression. Thus, these authors, as well as Knebel et al. (2002), readily detected significant toxicological responses to dilute diesel exhaust, despite the fact that similar exposures conducted for this study did not show consistent impacts on cell viability, proinflammatory signalling and oxidative stress. Interestingly, the Seagrave et al. study examined an aerosol with 3mg/m^3 TPM, whereas the maximum mass concentration for the studies herein was only slightly greater than 2mg/m^3 (see Table 1.1). In addition, it should be noted that although the Seagrave et al. study examined human primary cells from three separate donors, the VITROCELL® results are based on only a single exposure for each culture (i.e., no replicates). A comparable VITROCELL® study of a conditioned aerosol (i.e., temperature and humidity) containing fly ash from a municipal waste incinerator, which employed exposures as long as 6 hrs at flow rates up to 300 ml/min (0.62 mg/m^3), failed to show a significant reduction in viability of BEAS-2B cells co-cultured with THP-1 myeloid leukemia cells (via Alamar Blue reduction), relative to the filtered air control (Diabate et al. 2008, Mulhopt et al. 2007). However, the study did show significant elevation of *IL8* release in fly ash aerosol-exposed cells (i.e., 6 hrs, 0.62 mg/m^3, 100 ml/min). Thus, one might assert that longer VITROCELL® exposures, conducted at higher flow rates, may improve the ability to detect aerosol-induced toxicological responses. However, such tests would require proper aerosol conditioning (i.e., temperature and humidity).

It is also worth noting that the Knebel et al. and Seagrave et al. studies employed different cells than those used for this study, and it is possible that the cells employed in these earlier studies are more sensitive to combustion-derived aerosols. For example, the Seagrave et al study examined effects on differentiated primary human airway epithelial cells, and primary cells are generally regarded as more sensitive to toxicant effects (Ekwall et al. 1990). Nevertheless, it is surprising that these studies were able to readily detect robust toxicological effects in the exposed cells; and moreover, little or no effects of the clean air.

In contrast, the exposures conducted for this study were hampered by response variability and substantial reductions in cell viability for the control air alone. Concomitantly, a great deal of effort was expended to improve the VITROCELL® system and the reliability of VITROCELL® ALI results.

4.5 Exposure Characterization

The limited effect of exposures to even high concentrations of diesel exhaust (i.e., >2mg/m^3) observed using the optimized exposure system may be due to poor deposition of particles on the surfaces of the cells exposed in the VITROCELL®. Particle loss in the VITROCELL® was characterized by SMPS prior to the initial ULSD pilot study and the results showed a 62% reduction in total particle number concentration. However, the flow rate used for that characterization method was 300 ml/min due to the requirements of the SMPS instrument. This flow rate is much higher than the 15 - 25 ml/min/module (5 - 8.3 ml/min/well) used for the reported diesel experiments, and likely reflect high particle losses due to impaction. Impaction is known to contribute to deposition losses when the particle momentum prohibits change in direction in an area where there is a rapid change in the direction of the bulk flow. Impaction losses are especially great at high velocity, aerodynamic diameter greater than 1μm, and high particle density (Tsuda et al. 2013). Additionally, the aforementioned pilot analysis of particle losses investigated the difference in particle number anterior and posterior to the VITROCELL®, and did not distinguish between deposition on the insert membrane versus losses to the module walls and tubing, e.g., particles are attracted to plastic such as the polystyrene plastic walls of the transwells. In contrast to the aforementioned SMPS results, Mulhopt et al. (2007) and Diabaté et al (2008) characterized inhalable fly ash and, using SMPS measurement anterior and posterior to the VITROCELL®, found 2.3% deposition efficiency in the VITROCELL® system at flow rates of 300 ml/min. Similarly, the Seagrave et al. (2007) study examined deposition of fluorescent microspheres in size ranges relevant to diesel particle emissions (0.14 μm and 0.5 μm). Using SMPS with a flow rate of 300 ml/min they noted a deposition of about 10%. These latter values are more consistent with the theoretical expectations for deposition of combustion-derived particulate material in the VITROCELL® exposure module. As noted in the Introduction, particulate material in combustion emissions such as diesel exhaust are multi-modal with the bulk of the particles

belonging to the nuclei (i.e., 3-30nm) and accumulation modes (30 to 500nm). In general, deposition of particulate material is controlled by four physical forces: sedimentation, diffusion, electrostatic, and impaction. The latter two do not apply to the VITROCELL® system; electrostatic since the particles are not charged, and impaction because the flow rates are far too low. However, sedimentation and diffusion will apply to low flow circumstances such as those associated with VITROCELL® operation, with diffusion playing an increasingly important role as particle size decreases. The theoretical maximum deposition by diffusion for particles in the 10nm range is about 18%; decreasing rapidly with increasing size to approximately 3% at 100nm and <2% at 200nm (Tsuda et al. 2013). Thus, the aforementioned published values of approximately 2-10% could reasonably be expected to be applicable to combustion-derived particulates in vehicular exhaust.

Following system set up at the U.S. EPA's Highbay facility and optimisation for diesel exposures scanning electron microscopy was employed to examine the deposition of particulate material on the insert membrane. Although this analysis was not repeated, no particle deposition was observed on the membrane following a 1 hour ULSD exposure (results not shown). The possibility of particle losses to the in-line humidifiers was investigated by SMPS measurements anterior and posterior to the humidifier; no significant loss was observed (results not shown). Therefore, despite the initial SMPS analysis conducted at Environment Canada, subsequent analyses, as well as work published by others and theoretical expectations, suggests that particle deposition in the VITROCELL® exposure area will be very limited. This is unfortunate since it can reasonably be expected to hamper the detection of toxicological responses for combustion-derived aerosols that contain particulate material that is known to contribute to overall toxicological activity (Totlandsdal et al. 2012). Indeed, it may not be possible to employ an instrument such as the VITROCELL® to reliably assess the toxicological activity of complex aerosols with fine combustion-derived particulates unless deposition is electrostatically augmented.

4.6 Alternative ALI Exposure Systems

Alternative ALI exposure systems are available, and the design of some systems may permit improved particle deposition relative to that observed for the VITROCELL®. For

example, some systems employ high voltage charging and electrostatic precipitation to increase particle deposition. Electrostatic precipitators have been routinely employed for the collection of airborne dust (Jaworek et al. 2006), and the newer VITROCELL® Automated Exposure Station incorporates electrostatic deposition. The CULTEX® Radial Flow System (RFS) is a commercial system developed and marketed by the group who designed the ALI system that ultimately became known as the VITROCELL®. This product, which is manufactured and sold by a separate company (i.e., Cultex Laboratories GmbH) is based on the original design published by Aufderheide et al., includes an optional component for electrostatic deposition (i.e., the CULTEX® EDD) (Aufderheide et al. 2013, Steinritz et al. 2013). The CULTEX® system still uses the internal circulating water bath for temperature maintenance; therefore, conditioning of the aerosol must be conducted separately. The Quantaire™ is a commercialization of a novel ALI exposure system developed at the University of North Carolina at Chapel Hill (de Bruijne et al. 2009, Zavala 2014). This system incorporates aerosol humidification, temperature control, and electrostatic precipitation of particles into the system design. In addition, the system contains separate modules for assessment of gases or complex particulate-containing aerosols.

4.7 Summary & Conclusions

As stated in the introduction, the goals of this project were to develop optimized toxicity assessment protocols for use with the VITROCELL® Exposure System and subsequently verify the utility of the system for toxicological assessment of diluted diesel emissions. Thorough evaluation of the reliability of a biological test method requires investigations of accuracy, precision, sensitivity, and response range. Effective determination of accuracy is hampered by a lack of suitable reference materials and established points of reference (e.g., responses for existing test methods). Investigations of sensitivity and response ranges require prior identification of suitable standards and reference materials to evaluate test performance. Although agents such as ozone and NO_2 can be employed as toxicological standards for evaluation of test performance, development of suitable standards for combustion-derived aerosols is hampered by variations across test runs due to variations in fuel formulation and the combustion process. Although determinations of accuracy, sensitivity and response ranges for VITROCELL® toxicological assessments are

ultimately necessary, the task was beyond the scope of this thesis. In contrast, it was possible to investigate analytical precision; and moreover, employ precision to evaluate the utility of the VITROCELL® systems for toxicological assessments of complex aerosols such as diesel exhaust. Early experiments (i.e., those conducted at Environment Canada) indicated that the coefficients of variation for the WST-1 endpoint are in the range of 15.5% for the clean air control and 23.4% for diesel exhaust. Although this is suitable with respect to analytical precision, comparisons of the clean air responses to the incubator control indicated unacceptable declines in cell viability (e.g., approximately 40% below incubator control). Subsequent modifications of the VITROCELL® installation essentially eliminated toxicological response to the clean air control, relative to the field control (i.e., incubator samples transported to the aerosol exposure laboratory). Analysis of analytical precision for the modified VITROCELL® system indicates that CV values vary from 1.6% to 487.8% depending on endpoint. CV values were substantially elevated for the LDH leakage assay relative to other assays. Without considering the LDH assay, the highest CV is 99.5%. A summary of CV values for the various endpoints employed to assess diesel emissions and simulated smog are summarised in **Appendix A**. With respect to the hypothesis outlined on p. 27, these values are deemed to be suitable to permit deployment of the VITROCELL® system for toxicological characterisation of complex aerosols, provided response is analyzed at multiple endpoints. These analyses are based on within-run variability on responses, and subsequent research should investigate between-run variations. In addition, follow-up research should investigate sensitivity and detection limits for selected reference agents, response linearity across a range of exposure levels, and, if possible, response accuracy and specificity. The latter would likely require "spiking experiments" whereby components of combustion emissions that are known to be toxic are added to a test aerosol to augment toxicological responses. Although desirable to validate a toxicological assessment methodology, determining the accuracy and specificity of an ALI assessment system could constitute a substantial analytical challenge.

The stated hypothesis is that the commercially-available VITROCELL® system for *in vitro* air-liquid interface exposure of cultured animal cells can be deployed for reliable toxicological characterization of complex aerosols such as diluted diesel exhaust. Unfortunately, the results obtained and presented in this thesis indicate that the

VITROCELL® system required extensive modifications to maintain temperature and aerosol humidity such that background responses attributable to clean air can be minimised. Moreover, even after extensive modification and numerous attempts to examine a wide range of toxicological responses (e.g., viability and survival, oxidative stress, pro-inflammatory signalling) in two cell lines (i.e., A549 and BEAS-2B), across a wide range of aerosols including light-duty diesel exhaust, diesel generator exhaust, simulated urban smog, and various concentrations of NO_2, the magnitude of the responses relative to the appropriate controls were weak and highly variable. Moreover, for some endpoints (e.g., LDH release, *HMOX1* and *IL6* gene expression) the within-run precision of the measured responses, as indicated by the CV values in Appendix A, exceed the value specified in the hypothesis (i.e., 25%). Given the extensive literature on the toxicological activity of combustion-derived aerosols such as diesel exhaust, the failure to document a consistent and robust response is troubling. With respect to the stated hypothesis, it seems unlikely that the commercially-available version of the VITROCELL® used for this study can be deployed for reliable toxicity assessment of aerosols such as diesel exhaust and simulated smog. Alternative systems that incorporate aerosol conditioning (i.e., humidification) and high voltage charging for electrostatic deposition of particles on the apical surface of the cells may prove to be superior, and indeed, may permit reliable *in vitro* toxicity assessment of combustion-derived aerosols at the air-liquid interface. A reliable *in vitro* system could be employed for comparative analyses of diesel and gasoline engine emissions across a range of engine deigns, fuel formulations an exhaust aftertreatment. Moreover, such a system could be used to examine toxicological responses in human primary pulmonary cells obtained from normal and diseased individuals.

5.0 REFERENCES

Ames, B.N., Durston, W.E., Yamasaki, E. and Lee, F.D. 1973. Carcinogens are mutagens: A simple test system combining liver homogenates for activation and bacteria for detection. Proc. Natl. Acad. Sci. U. S. A. **70**(8): 2281-2285.

Anderson, S.E., Jackson, L.G., Franko, J. and Wells, J.R. 2010. Evaluation of dicarbonyls generated in a simulated indoor air environment using an in vitro exposure system. Toxicol. Sci. **115**(2): 453-461.

Anderson, S.E., Khurshid, S.S., Meade, B.J., Lukomska, E. and Wells, J.R. 2013. Toxicological analysis of limonene reaction products using an in vitro exposure system. Toxicol. in. Vitro. **27**(2): 721-730.

Arey, J. 2004. A tale of two diesels. Environ. Health Perspect. **112**(8): 812-813.

Aufderheide, M., and Gressmann, H. 2007. A modified ames assay reveals the mutagenicity of native cigarette mainstream smoke and its gas vapour phase. Exp. Toxicol. Pathol. **58**(6): 383-392.

Aufderheide, M., and Mohr, U. 2004. A modified CULTEX system for the direct exposure of bacteria to inhalable substances. Exp. Toxicol. Pathol. **55**(6): 451-454.

Aufderheide, M., and Mohr, U. 2000. CULTEX--an alternative technique for cultivation and exposure of cells of the respiratory tract to airborne pollutants at the air/liquid interface. Exp. Toxicol. Pathol. **52**(3): 265-270.

Aufderheide, M., and Mohr, U. 1999. CULTEX--a new system and technique for the cultivation and exposure of cells at the air/liquid interface. Exp. Toxicol. Pathol. **51**(6): 489-490.

Aufderheide, M., Knebel, J.W. and Ritter, D. 2003a. Novel approaches for studying pulmonary toxicity in vitro. Toxicol. Lett. **140-141**: 205-211.

Aufderheide, M., Knebel, J.W. and Ritter, D. 2003b. An improved in vitro model for testing the pulmonary toxicity of complex mixtures such as cigarette smoke. Exp. Toxicol. Pathol. **55**(1): 51-57.

Aufderheide, M., Halter, B., Mohle, N. and Hochrainer, D. 2013. The CULTEX RFS: A comprehensive technical approach for the in vitro exposure of airway epithelial cells to the particulate matter at the air-liquid interface. Biomed. Res. Int. **2013**: 734137.

Aufderheide, M., Ritter, D., Knebel, J.W. and Scherer, G. 2001. A method for in vitro analysis of the biological activity of complex mixtures such as sidestream cigarette smoke. Exp. Toxicol. Pathol. **53**(2-3): 141-152.

Bakand, S., and Hayes, A. 2010. Troubleshooting methods for toxicity testing of airborne chemicals in vitro. J. Pharmacol. Toxicol. Methods. **61**(2): 76-85.

Banfalvi, G. 2011. Overview of cell synchronization. Methods Mol. Biol. **761**: 1-23.

Bardet, G., Achard, S., Loret, T., Desauziers, V., Momas, I. and Seta, N. 2014. A model of human nasal epithelial cells adapted for direct and repeated exposure to airborne pollutants. Toxicol. Lett. **229**(1): 144-149.

Bayram , H., Fakili, F., Gögebakan, B., Bayraktar, R., Öztuzcu, S., Dikensoy, Ö. and Chung, K.F. 2013. Effect of serum on diesel exhaust particulates (DEP)-induced apoptosis of airway epithelial cells in vitro. Toxicol. Lett. **218**(3): 215-223.

Bennett, S. 2014. Chapter 3: Engine basics. *In* Modern Diesel Technology: Diesel engines. Cengage Learning, Stamford, CT. pp. 45-58.

Berridge, M.V., and Tan, A.S. 1998. Trans-plasma membrane electron transport: A cellular assay for NADH- and NADPH-oxidase based on extracellular, superoxide-mediated reduction of the sulfonated tetrazolium salt WST-1. Protoplasma. **205**(1-4): 74-82.

Berridge, M.V., Herst, P.M. and Tan, A.S. 2005. Tetrazolium dyes as tools in cell biology: New insights into their cellular reduction. Biotech. Ann. Rev. **11**(SUPPL.): 127-152.

Boatright, K.M., and Salvesen, G.S. 2003. Mechanisms of caspase activation. **15**: 725-731.

Borenfreund, E., and Puerner, J.A. 1985. A simple quantitative procedure using monolayer cultures for cytotoxicity assays (HTD/NR-90). J. Tissue Cult. Methods. **9**(1): 7-9.

Bradford, M.M. 1976. A rapid and sensitive method for the quantitation of microgram quantities of protein utilizing the principle of protein-dye binding. Anal. Biochem. **72**: 248-254.

Brahmajothi, M.V., Mason, S.N., Whorton, A.R., McMahon, T.J. and Auten, R.L. 2010. Transport rather than diffusion-dependent route for nitric oxide gas activity in alveolar epithelium. Free Radical Biology and Medicine. **49**(2): 294-300.

Breheny, D., Cunningham, F., Kilford, J., Payne, R., Dillon, D. and Meredith, C. 2014. Application of a modified gaseous exposure system to the in vitro toxicological assessment of tobacco smoke toxicants. Environ. Mol. Mutagen. **55**(8): 662-672.

Carey, P.M. 1987. Air Toxics Emissions from Motor Vehicles (Technical Report). EPA-AA-TSSPA-86–5. US Environmental Protection Agency, Washington, DC.

Chan, T. 2010a. Brief summary for vitrocell photometer testing. Internal Report, Emissions Research Measurement Section, Air Quality Research Division, Environment Canada, Ottawa.

Chan, T. 2010b. Brief summary of PM losses in vitrocell. Internal Report, Emissions Research Measurement Section, Air Quality Research Division, Environment Canada, Ottawa.

Chiang, L.L., Chen, H.C., Lee, C.N., Chuang, K.J., Chen, T.T., Yeh, C.T., Wang, L.S., Lee, W.H., Lin, L.Y., Tseng, H.E. and Chuang, H.C. 2013. Serum protein oxidation by diesel exhaust particles: effects on oxidative stress and inflammatory response in vitro. Chem. Biol. Interact. **206**(2): 385-393.

Chuang, H.C., Cheng, Y.L., Lei, Y.C., Chang, H.H. and Cheng, T.J. 2013. Protective effects of pulmonary epithelial lining fluid on oxidative stress and DNA single-strand breaks caused by ultrafine carbon black, ferrous sulphate and organic extract of diesel exhaust particles. Toxicol. Appl. Pharmacol. **266**(3): 329-334.

Claxton, L.D., Creason, J., Leroux, B., Agurell, E., Bagley, S., Bryant, D.W., Courtois, Y.A., Douglas, G., Clare, C.B. and Goto, S. 1992. Results of the IPCS collaborative study on complex mixtures. Mutat. Res. **276**(1-2): 23-32.

Claxton, L.D. 2015. The history, genotoxicity, and carcinogenicity of carbon-based fuels and their emissions. Part 3: Diesel and gasoline. Mutat Res Rev Mutat Res. **763**: 30-85

Cooney, D.J., and Hickey, A.J. 2011. Cellular response to the deposition of diesel exhaust particle aerosols onto human lung cells grown at the air-liquid interface by inertial impaction. Toxicol. in. Vitro. **25**(8): 1953-1965.

Cooney, D.J., and Hickey, A.J. 2008. The generation of diesel exhaust particle aerosols from a bulk source in an aerodynamic size range similar to atmospheric particles. Int. J. Nanomedicine. **3**(4): 435-449.

Cyrys, J., Peters, A., Soentgen, J. and Wichmann, H.E. 2014. Low emission zones reduce PM10 mass concentrations and diesel soot in german cities. J. Air Waste Manag. Assoc. **64**(4): 481-487.

Darquenne, C. 2012. Aerosol deposition in health and disease. J. Aerosol Med. Pulm. Drug Deliv. **25**(3): 140-147.

de Bruijne, K., Ebersviller, S., Sexton, K.G., Lake, S., Leith, D., Goodman, R., Jetters, J., Walters, G.W., Doyle-Eisele, M., Woodside, R., Jeffries, H.E. and Jaspers, I. 2009. Design and testing of electrostatic aerosol in vitro exposure system (EAVES): An alternative exposure system for particles. Inhal. Toxicol. **21**(2): 91-101.

Diabate, S., Mulhopt, S., Paur, H.R. and Krug, H.F. 2008. The response of a co-culture lung model to fine and ultrafine particles of incinerator fly ash at the air-liquid interface. Altern. Lab. Anim. **36**(3): 285-298.

Diaz-Sanchez, D., Garcia, M.P., Wang, M., Jyrala, M. and Saxon, A. 1999. Nasal challenge with diesel exhaust particles can induce sensitization to a neoallergen in the human mucosa. J. Allergy Clin. Immunol. **104**(6): 1183-1188.

Dockery, D.W., Pope, C.A.,3rd, Xu, X., Spengler, J.D., Ware, J.H., Fay, M.E., Ferris, B.G.,Jr and Speizer, F.E. 1993. An association between air pollution and mortality in six U.S. cities. N. Engl. J. Med. **329**(24): 1753-1759.

Doyle, M., Sexton, K.G., Jeffries, H. and Jaspers, I. 2007. Atmospheric photochemical transformations enhance 1,3-butadiene-induced inflammatory responses in human epithelial cells: The role of ozone and other photochemical degradation products. Chem. Biol. Interact. **166**(1-3): 163-169.

Ekwall, B., Silano, V., Paganuzzi-Stammati, A. and Zucco, F. 1990. Chapter 7. toxicity tests with mammalian cell cultures. *In* Short-term Toxicity Tests for Non-genotoxic Effects. *Edited by* P. Bourdeau, E. Somers, G.M. Richardson and J.R. Hickman. Scientific Committee on Problems of the Environment 41, IPCS Joint Symposia 8, John Wiley and Sons, New York, NY. pp. 75-97.

Elihn, K., Cronholm, P., Karlsson, H.L., Midander, K., Odnevall Wallinder, I. and Moller, L. 2013. Cellular dose of partly soluble cu particle aerosols at the air-liquid interface using an in vitro lung cell exposure system. J. Aerosol Med. Pulmon. Drug Deliv. **26**: 84-93.

Elliott, M.A. 1958. Diesel fuel combustion. *In* Literature of the combustion of petroleum. *Advances in chemistry series*, vol. 20. American Chemical Society, Washington, DC. pp. 280-293.

Fosten, J. 2012. Rising household diesel consumption in the united states: A cause for concern? evidence on asymmetric pricing. Energy Econ. **34**(5): 1514-1522.

Fraga, C.G., Leibovitz, B.E. and Tappel, A.L. 1988. Lipid peroxidation measured as thiobarbituric acid-reactive substances in tissue slices: Characterization and comparison with homogenates and microsomes. Free Radic. Biol. Med. **4**(3): 155-161.

Frohlich, E., Bonstingl, G., Hofler, A., Meindl, C., Leitinger, G., Pieber, T.R. and Roblegg, E. 2013. Comparison of two in vitro systems to assess cellular effects of nanoparticles-containing aerosols. Toxicol. in. Vitro. **27**(1): 409-417.

Garcia-Canton, C., Minet, E., Anadon, A. and Meredith C. 2013. Metabolic characterization of cell systems used in in vitro toxicology testing: Lung cell system BEAS-2B as a working example. Toxicol. In Vitro. **27**(6): 1719-1727.

Ghio, A.J., Sobus, J.R., Pleil, J.D. and Madden, M.C. 2012. Controlled human exposures to diesel exhaust. Swiss Med. Wkly. **142**: w13597.

Giard, D.J., Aaronson, S.A., Todaro, G.J., Arnstein, P., Kersey, J.H., Dosik, H. and Parks, W.P. 1973. In vitro cultivation of human tumors: Establishment of cell lines derived from a series of solid tumors. J. Natl. Cancer Inst. **51**(5): 1417-1423.

Gminski, R., Tang, T. and Mersch-Sundermann, V. 2010. Cytotoxicity and genotoxicity in human lung epithelial A549 cells caused by airborne volatile organic compounds emitted from pine wood and oriented strand boards. Toxicol. Lett. **196**(1): 33-41.

Gordon, C.J., Schladweiler, M.C., Krantz, T., King, C. and Kodavanti, U.P. 2012. Cardiovascular and thermoregulatory responses of unrestrained rats exposed to filtered or unfiltered diesel exhaust. Inhal. Toxicol. **24**(5): 296-309.

Government of Canada. 2002. Sulphur in diesel fuel regulations (SOR/2002-254). Canada Gazette, Part II. **136**(16).

Government of Canada. 2003. On-road vehicle and engine emissions regulations (SOR/2003-2). Canada Gazette, Part II. **137**(1).

Government of Canada. 2005. Off-road compression-ignition engine emission regulations (SOR/2005-32). Canada Gazette, Part II. **139**(4).

Government of Canada. 2010a. Passenger automobile and light truck greenhouse gas emission regulations (SOR/2010-201). Canada Gazette, Part II. **144**(21).

Government of Canada. 2010b. Renewable fuels regulations (SOR/2010-189). Canada Gazette, Part II. **144**(18).

Government of Canada. 2011. Regulations amending the off-road compression-ignition engine emission regulations (SOR/2011-261). Canada Gazette, Part II. **145**(25).

Government of Canada. 2013. Heavy-duty vehicle and engine greenhouse gas emission regulations (SOR/2013-24). Canada Gazette, Part II. **146**(15).

Gualtieri, M., Capasso, L., D'Anna, A. and Camatini, M. 2014. Organic nanoparticles from different fuel blends: In vitro toxicity and inflammatory potential. J. Appl. Toxicol. **34**(11): 1247-1255.

Harkema, J.R., Wagner, J.G., Kaminski, N.E., Morishita, M., Keeler, G.J., McDonald, J.D., Barrett, E.G. and HEI Health Review Committee. 2009. Effects of concentrated ambient particles and diesel engine exhaust on allergic airway disease in brown norway rats. Res. Rep. Health Eff. Inst. **(145)**(145): 5-55.

Hasheminassab, S., Daher, N., Ostro, B.D. and Sioutas, C. 2014. Long-term source apportionment of ambient fine particulate matter (PM2.5) in the los angeles basin: A focus on emissions reduction from vehicular sources. Environ. Pollut. **193**: 54-64.

Hashimoto, S., Gon, Y., Takeshita, I., Matsumoto, K., Jibiki, I., Takizawa, H., Kudoh, S. and Horie, T. 2000. Diesel exhaust particles activate p38 MAP kinase to produce interleukin 8 and RANTES by human bronchial epithelial cells and N-acetylcysteine attenuates p38 MAP kinase activation. Am. J. Respir. Crit. Care Med. **161**(1): 280-285.

Hawley, B., and Volckens, J. 2013. Proinflammatory effects of cookstove emissions on human bronchial epithelial cells. Indoor Air. **23**(1): 4-13.

Hazari, M.S., Chesnutt, K., Stratford, K., Haykal-Coates, N., Krantz, Q.T., King, C., Farraj, A.K. and Gilmour, I. 2015. A single exposure to photochemical smog causes airway irritation and cardiac dysrhythmia in mice. Abstract submitted for poster presentation at the 2015 annual meeting of the Society of Toxicology, San Diego, CA.

Health Effects Institute. 2012. Advanced collaborative emissions study (ACES) subchronic exposure results: Biologic responses in rats and mice and assessment of genotoxicity. Boston, MA. Health Effects Institute Research Report 166, Health Effects Institute, Boston, MA.

Herzog, F., Clift, M.J., Piccapietra, F., Behra, R., Schmid, O., Petri-Fink, A. and Rothen-Rutishauser, B. 2013. Exposure of silver-nanoparticles and silver-ions to lung cells in vitro at the air-liquid interface. Part. Fibre Toxicol. **10**: 11.

Hesterberg, T.W., Long, C.M., Bunn, W.B., Sax, S.N., Lapin, C.A. and Valberg, P.A. 2009. Non-cancer health effects of diesel exhaust: A critical assessment of recent human and animal toxicological literature. Crit. Rev. Toxicol. **39**(3): 195-227.

Hesterberg, T.W., Long, C.M., Sax, S.N., Lapin, C.A., McClellan, R.O., Bunn, W.B. and Valberg, P.A. 2011. Particulate matter in new technology diesel exhaust (NTDE) is quantitatively and qualitatively very different from that found in traditional diesel exhaust (TDE). J. Air Waste Manag. Assoc. **61**(9): 894-913.

Hiura, T.S., Kaszubowski, M.P., Li, N. and Nel, A.E. 1999. Chemicals in diesel exhaust particles generate reactive oxygen radicals and induce apoptosis in macrophages. J. Immunol. **163**(10): 5582-5591.

IARC. 2013. IARC **M**onographs on the Evaluation of Carcinogenic Risks to Human. Volume 105, Diesel and Gasoline Engine Exhausts and Some Nitroarenes**.** International Agency for Research on Cancer, Lyon, France, 703pp.

Ishiyama, M., Suiga, M., Sasamoto, K., Mizoguchi, M. and He, P.-. 1993. A new sulfonated tetrazolium salt that produces a highly water-soluble formazan dye. Chemical and Pharmaceutical Bulletin. **41**(6): 1118-1122.

Jaworek, A., Balachandran, W., Krupa, A., Kulon, J. and Lackowski, M. 2006. Wet electroscrubbers for state of the art gas cleaning. Environ. Sci. Technol. **40**(20): 6197-6207.

Johnson, J. 1988. Automotive emissions. *In* Air Pollution, the Automobile, and Public Health. *Edited by* A.Y. Watson, R.R. Bates and D. Kennedy. National Academy Press, Washington, DC.

Jorres, R., and Magnussen, H. 1990. Airways response of asthmatics after a 30 min exposure, at resting ventilation, to 0.25 ppm NO2 or 0.5 ppm SO2. Eur. Respir. J. **3**(2): 132-137.

Kilford, J., Thorne, D., Payne, R., Dalrymple, A., Clements, J., Meredith, C. and Dillon, D. 2014. A method for assessment of the genotoxicity of mainstream cigarette-smoke by use of the bacterial reverse-mutation assay and an aerosol-based exposure system. Mutat. Res. **769**: 20-28.

Kim, J.S., Peters, T.M., O'Shaughnessy, P.T., Adamcakova-Dodd, A. and Thorne, P.S. 2013. Validation of an in vitro exposure system for toxicity assessment of air-delivered nanomaterials. Toxicol. in. Vitro. **27**(1): 164-173.

Kittelson, D.B. 1998. Engines and nanoparticles: A review. J. Aerosol Sci. **29**(5-6): 575-588.

Kittelson, D., Watts, W. and Johnson, J. 2002. Diesel aerosol sampling methodology - CRC E-43: Final report. Dept. of Mechanical Engineering, University of Minnesota, Minneapolis, MN.

Klein, S.G., Serchi, T., Hoffmann, L., Blomeke, B. and Gutleb, A.C. 2013. An improved 3D tetraculture system mimicking the cellular organisation at the alveolar barrier to study the potential toxic effects of particles on the lung. Part. Fibre Toxicol. **10**: 31-8977-10-31.

Knebel, J.W., Ritter, D. and Aufderheide, M. 2002. Exposure of human lung cells to native diesel motor exhaust--development of an optimized in vitro test strategy. Toxicol. in. Vitro. **16**(2): 185-192.

Kodavanti, U.P., Thomas, R.F., Ledbetter, A.D., Schladweiler, M.C., Bass, V., Krantz, Q.T., King, C., Nyska, A., Richards, J.E., Andrews, D. and Gilmour, M.I. 2013. Diesel exhaust induced pulmonary and cardiovascular impairment: The role of hypertension intervention. Toxicol. Appl. Pharmacol. **268**(2): 232-240.

Koehler, C., Thielen, S., Ginzkey, C., Hackenberg, S., Scherzed, A., Burghartz, M., Paulus, M., Hagen, R. and Kleinsasser, N.H. 2013. Nitrogen dioxide is genotoxic in urban concentrations. Inhal. Toxicol. **25**:341-347.

Koehler, C., Ginzkey, C., Friehs, G., Hackenberg, S., Froelich, K., Scherzed, A., Burghartz, M., Kessler, M. and Kleinsasser, N. 2011. Ex vivo toxicity of nitrogen dioxide in human nasal epithelium at the WHO defined 1-h limit value. Toxicol. Lett. **207**(1): 89-95.

Koehler, C., Ginzkey, C., Friehs, G., Hackenberg, S., Froelich, K., Scherzed, A., Burghartz, M., Kessler, M. and Kleinsasser, N. 2010. Aspects of nitrogen dioxide toxicity in environmental urban concentrations in human nasal epithelium. Toxicol. Appl. Pharmacol. **245**(2): 219-225.

Konczol, M. 2012. Optimization of an air-liquid interface exposure system (vitrocell(R)) to study the effects of diesel exhaust on human A549 lung cells. Final report for Health Canada contract 4500272125, Environmental Health Science and Research Bureau, Health Canada, Ottawa.

Korzeniewski, C., and Callewaert, D.M. 1983. An enzyme-release assay for natural cytotoxicity. J. Immunol. Methods. **64**(3): 313-320.

Krewski, D., Acosta, D.,Jr, Andersen, M., Anderson, H., Bailar, J.C.,3rd, Boekelheide, K., Brent, R., Charnley, G., Cheung, V.G., Green, S.,Jr, Kelsey, K.T., Kerkvliet, N.I., Li, A.A., McCray, L., Meyer, O., Patterson, R.D., Pennie, W., Scala, R.A., Solomon, G.M., Stephens, M., Yager, J. and Zeise, L. 2010. Toxicity testing in the 21st century: A vision and a strategy. J. Toxicol. Environ. Health B Crit. Rev. **13**(2-4): 51-138.

Krysko, D.V., Vanden Berghe, T., D'Herde, K. and Vandenabeele, P. 2008. Apoptosis and necrosis: Detection, discrimination and phagocytosis. Methods **44**: 205-221.

Kumagai, Y., Taira, J. and Sagai, M. 1995. Apparent inhibition of superoxide dismutase activity in vitro by diesel exhaust particles. Free Radic. Biol. Med. **18**(2): 365-371.

Lamkanfi, M., and Kanneganti, T.D. 2010. Caspase-7: A protease involved in apoptosis and inflammation. Int. J. Biochem. Cell Biol. **42**: 21-24.

Lechner, J.F., and LaVeck, M.A. 1985. A serum-free method for culturing normal human bronchial epithelial cells at clonal density. J. Tissue Cult. Meth. **9**(2): 43-48.

Lenz, A.G., Karg, E., Lentner, B., Dittrich, V., Brandenberger, C., Rothen-Rutishauser, B., Schulz, H., Ferron, G.A. and Schmid, O. 2009. A dose-controlled system for air-liquid interface cell exposure and application to zinc oxide nanoparticles. Part. Fibre Toxicol. **6**: 32.

Lenz, A.G., Stoeger, T., Cei, D., Schmidmeir, M., Semren, N., Burgstaller, G., Lentner, B., Eickelberg, O., Meiners, S. and Schmid, O. 2014. Efficient bioactive delivery of aerosolized drugs to human pulmonary epithelial cells cultured in air-liquid interface conditions. Am. J. Respir. Cell Mol. Biol. **51**(4): 526-535.

Lewtas, J. 2007. Air pollution combustion emissions: Characterization of causative agents and mechanisms associated with cancer, reproductive, and cardiovascular effects. Mutat. Res. **636**(1-3): 95-133.

Li, X., Shang, P., Peng, B., Nie, C., Zhao, L., Liu, H. and Xie, J. 2012. Effects of smoking regimens and test material format on the cytotoxicity of mainstream cigarette smoke. Food Chem. Toxicol. **50**(3-4): 545-551.

Lies, K.H., Hartung, A., Postulka, A., Gring, H. and Schulze, J. 1986. Composition of diesel exhaust with particular reference to particle bound organics including formation of artifacts. *In* Carcinogenic and Mutagenic Effects of Diesel Engine Exhaust. *Edited by* N. Ishinishi, A. Koizumi, R.O. McClellan and W. Stöber. Elsevier, Amsterdam, pp. 65–82.

Livak, K.J., and Schmittgen, T.D. 2001. Analysis of relative gene expression data using real-time quantitative PCR and the 2-ΔΔCT method. Methods. **25**(4): 402-408.

Ma, J.Y., Young, S.H., Mercer, R.R., Barger, M., Schwegler-Berry, D., Ma, J.K. and Castranova, V. 2014. Interactive effects of cerium oxide and diesel exhaust nanoparticles on inducing pulmonary fibrosis. Toxicol. Appl. Pharmacol. **278**(2): 135-147.

Mathis, C., Poussin, C., Weisensee, D., Gebel, S., Hengstermann, A., Sewer, A., Belcastro, V., Xiang, Y., Ansari, S., Wagner, S., Hoeng, J. and Peitsch, M.C. 2013. Human bronchial epithelial cells exposed in vitro to cigarette smoke at the air-liquid interface resemble bronchial epithelium from human smokers. Am. J. Physiol. Lung Cell. Mol. Physiol. **304**(7): L489-503.

McDonald, J.D., Harrod, K.S., Seagrave, J., Seilkop, S.K. and Mauderly, J.L. 2004. Effects of low sulfur fuel and a catalyzed particle trap on the composition and toxicity of diesel emissions. Environ. Health Perspect. **112**(13): 1307-1312.

MECA (Manufacturers of Emission Controls Association). 2010. Emission control technologies for diesel-powered vehicles. Washington, DC. Manufacturers of Emission Controls Association, Washington, DC.

Mori, Y., Murakami, S., Sagae, T., Hayashi, H., Sakata, M., Sagai, M. and Kumagai, Y. 1996. Inhibition of catalase activity in vitro by diesel exhaust particles. J. Toxicol. Environ. Health. **47**(2): 125-134.

Morrow, P.E. 1988. Possible mechanisms to explain dust overloading of the lungs. Fundam. Appl. Toxicol. **10**(3): 369-384.

Mulhopt, S., Paur, H.R., Diabate, S. and Krug, H.F. 2007. Chapter 31. in vitro testing of inhalable fly ash at the air liquid interface. *In* Advanced Environmental Monitoring. *Edited by* Y.J. Kim and U. Platt. Springer Netherlands, pp. 402-414.

Mutlu, E., Warren, S.H., Matthews, P.P., King, C., Linak, W.P., Kooter, I.M., Schmid, J.E., Ross, J.A., Gilmour, M.I. and Demarini, D.M. 2013. Bioassay-directed fractionation and sub-fractionation for mutagenicity and chemical analysis of diesel exhaust particles. Environ. Mol. Mutagen. **54**(9): 719-736.

National Research Council. 1983. Feasibility of Assessment of Health Risks from Vapor-phase Organic Chemicals in Gasoline and Diesel Exhaust. National Academy of Sciences, Washington, DC.

Oberdorster, G., Elder, A. and Rinderknecht, A. 2009. Nanoparticles and the brain: Cause for concern? J. Nanosci Nanotechnol. **9**(8): 4996-5007.

Office of Energy Efficiency. 2009. 2009 Canadian Vehicle Summary Report. Chapter 1: Canada's on-road vehicle fleet [online]. Natural Resources Canada. Available from http://oee.nrcan.gc.ca/publications/statistics/cvs09/chapter1.cfm?attr=0 [cited October 12 2014].

Olivera, D.S., Boggs, S.E., Beenhouwer, C., Aden, J. and Knall, C. 2007. Cellular mechanisms of mainstream cigarette smoke-induced lung epithelial tight junction permeability changes in vitro. Inhal. Toxicol. **19**(1): 13-22.

Omura, S., Koike, E. and Kobayashi, T. 2009. Microarray analysis of gene expression in rat alveolar epithelial cells exposed to fractionated organic extracts of diesel exhaust particles. Toxicology. **262**(1): 65-72.

Panas, A., Comouth, A., Saathoff, H., Leisner, T., Al-Rawi, M., Simon, M., Seemann, G., Dossel, O., Mulhopt, S., Paur, H.R., Fritsch-Decker, S., Weiss, C. and Diabate, S. 2014. Silica nanoparticles are less toxic to human lung cells when deposited at the air-liquid interface compared to conventional submerged exposure. Beilstein J. Nanotechnol. **5**: 1590-1602.

Pandya, R.J., Solomon, G., Kinner, A. and Balmes, J.R. 2002. Diesel exhaust and asthma: Hypotheses and molecular mechanisms of action. Environ. Health Perspect. **110 Suppl 1**: 103-112.

Pariselli, F., Sacco, M.G. and Rembges, D. 2006. Dynamic in-vitro exposure of human derived cells to indoor priority pollutants. Report EUR 22285 EN. European Commission, Directorate-General, Joint Research Centre, Ispra, Italy.

Persoz, C., Achard, S., Momas, I. and Seta, N. 2012. Inflammatory response modulation of airway epithelial cells exposed to formaldehyde. Toxicol. Lett. **211**(2): 159-163.

Persoz, C., Achard, S., Leleu, C., Momas, I. and Seta, N. 2010. An in vitro model to evaluate the inflammatory response after gaseous formaldehyde exposure of lung epithelial cells. Toxicol. Lett. **195**(2-3): 99-105.

Persoz, C., Leleu, C., Achard, S., Fasseu, M., Menotti, J., Meneceur, P., Momas, I., Derouin, F. and Seta, N. 2011. Sequential air-liquid exposure of human respiratory cells to chemical and biological pollutants. Toxicol. Lett. **207**(1): 53-59.

Phalen, R.F., Oldham, M.J. and Wolff, R.K. 2008. The relevance of animal models for aerosol studies. J. Aerosol Med. Pulm. Drug Deliv. **21**(1): 113-124.

Pope, C.A.,3rd, Burnett, R.T., Thun, M.J., Calle, E.E., Krewski, D., Ito, K. and Thurston, G.D. 2002. Lung cancer, cardiopulmonary mortality, and long-term exposure to fine particulate air pollution. JAMA. **287**(9): 1132-1141.

Ramachandran, G., Paulsen, D., Watts, W. and Kittelson, D. 2005. Mass, surface area and number metrics in diesel occupational exposure assessment. J. Environ. Monit. **7**(7): 728-735.

Reddel, R.R., Ke, Y., Gerwin, B.I., McMenamin, M.G., Lechner, J.F., Su, R.T., Brash, D.E., Park, J.B., Rhim, J.S. and Harris, C.C. 1988. Transformation of human bronchial epithelial cells by infection with SV40 or adenovirus-12 SV40 hybrid virus, or transfection via strontium phosphate coprecipitation with a plasmid containing SV40 early region genes. Cancer Res. **48**(7): 1904-1909.

Repetto, G., del Peso, A. and Zurita, J.L. 2008. Neutral red uptake assay for the estimation of cell viability/ cytotoxicity. Nature Protocols. **3**(7): 1125-1131.

Ristovski, Z.D., Miljevic, B., Surawski, N.C., Morawska, L., Fong, K.M., Goh, F. and Yang, I.A. 2012. Respiratory health effects of diesel particulate matter. Respirology. **17**(2): 201-212.

Ritter, D., Knebel, J. and Aufderheide, M. 2004. Comparative assessment of toxicities of mainstream smoke from commercial cigarettes. Inhal. Toxicol. **16**(10): 691-700.

Ritter, D., Knebel, J.W. and Aufderheide, M. 2003. Exposure of human lung cells to inhalable substances: A novel test strategy involving clean air exposure periods using whole diluted cigarette mainstream smoke. Inhal. Toxicol. **15**(1): 67-84.

Ritter, D., Knebel, J.W. and Aufderheide, M. 2001. In vitro exposure of isolated cells to native gaseous compounds--development and validation of an optimized system for human lung cells. Exp. Toxicol. Pathol. **53**(5): 373-386.

Rosenblatt, D., Meloche, E., Rideout, G. and Hendron, J. 2008. Evaluation of a prototype selective catalytic reduction system on a heavy-duty diesel engine using biodiesel and ULSD fuels. ERMD Report #06-29. Emissions Research and Measurement Division Environment Canada, Environmental Technology Centre, Ottawa, ON.

Russell, A. 2013. Chapter 4. combustion emissions. *In* Air Pollution and Cancer. *Edited by* K. Straif, A. Cohen and J. Samet. IARC Scientific Publications, pp. 49-64.

Sagai, M., Saito, H., Ichinose, T., Kodama, M. and Mori, Y. 1993. Biological effects of diesel exhaust particles. I. in vitro production of superoxide and in vivo toxicity in mouse. Free Radic. Biol. Med. **14**(1): 37-47.

Schlage, W.K., Iskandar, A.R., Kostadinova, R., Xiang, Y., Sewer, A., Majeed, S., Kuehn, D., Frentzel, S., Talikka, M., Geertz, M., Mathis, C., Ivanov, N., Hoeng, J. and Peitsch, M.C. 2014. In vitro systems toxicology approach to investigate the effects of repeated cigarette smoke exposure on human buccal and gingival organotypic epithelial tissue cultures. Toxicol. Mech. Methods. **24**(7): 470-487.

Schuetzle, D., and Frazier, J.A. 1986. Factors influencing the emission of vapor and particulate phase components from diesel engines. Dev Toxicol Environ Sci. **13**:41–63.

Seagrave, J., Dunaway, S., McDonald, J.D., Mauderly, J.L., Hayden, P. and Stidley, C. 2007. Responses of differentiated primary human lung epithelial cells to exposure to diesel exhaust at an air-liquid interface. Exp. Lung Res. **33**(1): 27-51.

Sen, B., Mahadevan, B. and DeMarini, D.M. 2007. Transcriptional responses to complex mixtures: A review. Mutat. Res. **636**(1-3): 144-177.

Sexton, K.G., Jeffries, H.E., Jang, M., Kamens, R.M., Doyle, M., Voicu, I. and Jaspers, I. 2004. Photochemical products in urban mixtures enhance inflammatory responses in lung cells. Inhal. Toxicol. **16 Suppl 1**: 107-114.

Singh, P., DeMarini, D.M., Dick, C.A., Tabor, D.G., Ryan, J.V., Linak, W.P., Kobayashi, T. and Gilmour, M.I. 2004. Sample characterization of automobile and forklift diesel exhaust particles and comparative pulmonary toxicity in mice. Environ. Health Perspect. **112**(8): 820-825.

Snow, S.J., McGee, J., Miller, D.B., Bass, V., Schladweiler, M.C., Thomas, R.F., Krantz, T., King, C., Ledbetter, A.D., Richards, J., Weinstein, J.P., Conner, T., Willis, R., Linak, W.P., Nash, D., Wood, C.E., Elmore, S.A., Morrison, J.P., Johnson, C.L., Gilmour, M.I. and Kodavanti, U.P. 2014. Inhaled diesel emissions generated with cerium oxide nanoparticle fuel additive induce adverse pulmonary and systemic effects. Toxicol. Sci. **142**:403-417 .

Steinritz, D., Mohle, N., Pohl, C., Papritz, M., Stenger, B., Schmidt, A., Kirkpatrick, C.J., Thiermann, H., Vogel, R., Hoffmann, S. and Aufderheide, M. 2013. Use of the cultex(R) radial flow system as an in vitro exposure method to assess acute pulmonary toxicity of fine dusts and nanoparticles with special focus on the intra- and inter-laboratory reproducibility. Chem. Biol. Interact. **206**(3): 479-490.

Switalla, S., Knebel, J., Ritter, D., Krug, N., Braun, A. and Sewald, K. 2010. Effects of acute in vitro exposure of murine precision-cut lung slices to gaseous nitrogen dioxide and ozone in an air-liquid interface (ALI) culture. Toxicol. Lett. **196**(2): 117-124.

Takenaka, H., Zhang, K., Diaz-Sanchez, D., Tsien, A. and Saxon, A. 1995. Enhanced human IgE production results from exposure to the aromatic hydrocarbons from diesel

exhaust: Direct effects on B-cell IgE production. J. Allergy Clin. Immunol. **95**(1 Pt 1): 103-115.

Talikka, M., Kostadinova, R., Xiang, Y., Mathis, C., Sewer, A., Majeed, S., Kuehn, D., Frentzel, S., Merg, C., Geertz, M., Martin, F., Ivanov, N.V., Peitsch, M.C. and Hoeng, J. 2014. The response of human nasal and bronchial organotypic tissue cultures to repeated whole cigarette smoke exposure. Int. J. Toxicol., in press. DOI: 10.1177/1091581814551647.

Tang, T., Gminski, R., Konczol, M., Modest, C., Armbruster, B. and Mersch-Sundermann, V. 2012. Investigations on cytotoxic and genotoxic effects of laser printer emissions in human epithelial A549 lung cells using an air/liquid exposure system. Environ. Mol. Mutagen. **53**(2): 125-135.

Thorley, A.J., Ruenraroengsak, P., Potter, T.E. and Tetley, T.D. 2014. Critical determinants of uptake and translocation of nanoparticles by the human pulmonary alveolar epithelium. ACS Nano. **8**(11): 11778-11789.

Thorne, D., Kilford, J., Payne, R., Haswell, L., Dalrymple, A., Meredith, C. and Dillon, D. 2014. Development of a BALB/c 3T3 neutral red uptake cytotoxicity test using a mainstream cigarette smoke exposure system. BMC Res. Notes. **7**: 367-0500-7-367.

Thorne, D., Kilford, J., Payne, R., Adamson, J., Scott, K., Dalrymple, A., Meredith, C. and Dillon, D. 2013. Characterisation of a vitrocell(R) VC 10 in vitro smoke exposure system using dose tools and biological analysis. Chem. Cent. J. **7**(1): 146-153X-7-146.

Totlandsdal, A.I., Herseth, J.I., Bolling, A.K., Kubatova, A., Braun, A., Cochran, R.E., Refsnes, M., Ovrevik, J. and Lag, M. 2012. Differential effects of the particle core and organic extract of diesel exhaust particles. Toxicol. Lett. **208**(3): 262-268.

Totlandsdal, A.I., Orevik, J., Cochran, R.E., Herseth, J. I., Bolling, A.K., Lag, M., Schwarze, P., Lilleaas, E., Holme, J.A. and Kubatova A. 2014. The occurrence of polycyclic aromatic hydrocarbons and their derivatives and the proinflammatory potential of fractionated extracts of diesel exhaust and wood smoke particles. J Environ Sci Health A Tox Hazard Subst Environ Eng. **49**(4): 383-396.

Tsuda, A., Henry, F.S. and Butler, J.P. 2013. Particle transport and deposition: Basic physics of particle kinetics. Compr. Physiol. **3**(4): 1437-1471.

USDOE. 2010. Diesel Power: Clean Vehicles for Tomorrow [online]. Vehicle Technologies Program, U.S. Department of Energy. Available from https://www1.eere.energy.gov/vehiclesandfuels/pdfs/diesel_technical_primer.pdf [cited Sept. 26 2014].

USEPA. 2002a. Health assessment document for diesel engine exhaust. EPA/600/8-90/057F. United States Environmental Protection Agency, Office of Research and Development, National Center for Environmental Assessment, Washington, DC.

USEPA. 2002b. A comprehensive analysis of biodiesel impacts on exhaust emissions (draft technical report). EPA420-P-02-001. United States Environmental Protection Agency. Office of Transportation and Air Quality, Assessment and Standards Division, Washington, DC.

USEPA. 2008. Integrated science assessment for oxides of nitrogen – health criteria. EPA/600/R-08/071. United States Environmental Protection Agency, Office of Research and Development, National Center for Environmental Assessment, Research Triangle Park, NC.

Utell, M.J., and Frampton, M.W. 2000. Toxicologic methods: Controlled human exposures. Environ. Health Perspect. **108 Suppl 4**: 605-613.

Vaccari, M., Mascolo, M.G., Rotondo, F., Morandi, E., Quercioli, D., Perdichizzi, S., Zanzi, C., Serra, S., Poluzzi, V., Angelini, P., Grilli, S. and Colacci, A. 2014. Identification of pathway-based toxicity in the BALB/c 3T3 cell model. Toxicol. in. Vitro., in press. DOI:10.1016/j.tiv.2014.10.002.

Valberg, P.A., Long, C.M. and Sax, S.N. 2006. Integrating studies on carcinogenic risk of carbon black: Epidemiology, animal exposures, and mechanism of action. J. Occup. Environ. Med. **48**(12): 1291-1307.

Watson, A.Y., and Green, G.M. 1995. Noncancer effects of diesel emissions: Animal studies. *In* Diesel exhaust: Critical Analysis of Emissions, Exposure, and Health

Effects. A Special Report of the Institute's, Health Effects Institute, Boston, MA. pp. 139-164.

Weber, S., Hebestreit, M., Wilms, T., Conroy, L.L. and Rodrigo, G. 2013. Comet assay and air-liquid interface exposure system: A new combination to evaluate genotoxic effects of cigarette whole smoke in human lung cell lines. Toxicol. in. Vitro. **27**(6): 1987-1991.

Weichenthal, S., Van Ryswyk, K., Kulka, R., Sun, L., Wallace, L. and Joseph, L. 2014. In-vehicle exposures to particulate air pollution in canadian metropolitan areas: The urban transportation exposure study. Environ. Sci. Technol., in pres. DOI: dx.doi.org/10.1021/es504043a.

Williams, R., Rankin, N., Smith, T., Galler, D. and Seakins, P. 1996. Relationship between the humidity and temperature of inspired gas and the function of the airway mucosa. Crit. Care Med. **24**(11): 1920-1929.

Wolff, R.K. 1986. Effects of airborne pollutants on mucociliary clearance. Environ. Health Perspect. **66**: 223-237.

Wolz, L., Krause, G., Scherer, G., Aufderheide, M. and Mohr, U. 2002. In vitro genotoxicity assay of sidestream smoke using a human bronchial epithelial cell line. Food Chem. Toxicol. **40**(6): 845-850.

Wong, B.A. 2007. Inhalation exposure systems: Design, methods and operation. Toxicol. Pathol. **35**(1): 3-14.

Xie, Y., Williams, N.G., Tolic, A., Chrisler, W.B., Teeguarden, J.G., Maddux, B.L., Pounds, J.G., Laskin, A. and Orr, G. 2012. Aerosolized ZnO nanoparticles induce toxicity in alveolar type II epithelial cells at the air-liquid interface. Toxicol. Sci. **125**(2): 450-461.

Yu, C.P., and Yoon, K.J. 1991. Retention modeling of diesel exhaust particles in rats and humans. Res. Rep. Health Eff. Inst. **40**(40): 1-24.

Zaebst, D.D., Blade, L.M., Morris J.A., et al. 1988. Elemental carbon as a surrogate index of diesel exhaust exposure. *ln* Proceedings of the American Industrial Hygiene Conference, 15–20 May 1988, San Francisco, CA. National Institute for Occupational

Safety and Health, Division of Surveilance, Hazard Evaluation and Field Studies, Cincinnati, OH.

Zavala, J. 2014. Development of an electrostatic air sampler as an alternative method for aerosol in vitro exposure studies. PhD Thesis, Department of Environmental Sciences and Engineering, Gillings School of Global Public Health, University of North Carolina, Chapel Hill, NC.

Zhang, H., Hu, J., Kleeman, M. and Ying, Q. 2014. Source apportionment of sulfate and nitrate particulate matter in the eastern United States and effectiveness of emission control programs. Sci. Total Environ. **490**: 171-181.

Zhang, Z.H. and Balasubramanian R. 2014. Physicochemical and toxicological characteristics of particulate matter emitted from a non-road diesel engine: comparative evaluation of biodiesel-diesel and butanol-diesel blends. J. Hazard Mater. **15**(264): 395-402

6.0 APPENDICES

Appendix A: Analytical precision (coefficient of variation) of results obtained from cell viability (WST-1), cytotoxicity (LDH), and gene expression (*HMOX1*, *IL6*, *IL8*, *COX2*, *TNFA*) assays following aerosol exposures utilizing the optimized VITROCELL® exposure system**.**

Exposure	Date	Exposure #	Endpoint Examined	Coefficient of Variation (%) Control Module	Exposure Module
Air	April 10-14	1	WST-1 (0hr)	1.6	10.0
			WST-1 (24hr)	4.0	3.3
			LDH	56.5	67.2
Diesel	April 16-14	1	WST-1	6.7	3.8
			LDH	54.0	36.1
Diesel	April 22-14	1	WST-1	13.2	19.2
			LDH	42.3	78.4
			HMOX1	18.1	3.8
			IL6	20.9	6.0
			COX2	61.9	6.3
			TNFA	16.7	43.1
Diesel	April 22-14	2	WST-1	14.1	14.1
			LDH	150.0	67.8
			HMOX1	9.9	2.2
			IL6	12.3	1.4
			COX2	14.1	2.7
			TNFA	4.9	9.0
Diesel	April 24-14	1	WST-1	1.8	10.6
			LDH	80.0	229.7
			HMOX1	4.3	3.7
			IL6	2.7	4.2
			IL8	5.9	15.1
			COX2	3.2	3.0
			TNFA	1.5	5.2
Diesel	April 24-14	2	WST-1	4.2	3.8
			LDH	123.1	34.5
			HMOX1	2.2	1.8
			IL6	1.4	1.0
			IL8	24.5	11.1
			COX2	6.9	3.9
			TNFA	3.0	2.0
Diesel	April 29-14	1	WST-1	6.2	15.4
			LDH	101.8	133.3
			HMOX1	4.3	2.4
			IL6	6.2	1.3
			IL8	13.2	37.4
			TNFA	11.2	4.7

Diesel	April 29-14	2	WST-1	12.2	7.3
			LDH	424.1	54.7
			HMOX1	4.0	4.3
			IL6	5.5	4.5
			IL8	99.5	55.4
			TNFA	15.8	11.7
Diesel	May 1-14	1	WST-1	18.4	23.2
			LDH	487.8	274.2
			HMOX1	7.0	4.4
			IL6	6.7	3.1
			IL8	12.6	18.5
			COX2	8.4	5.0
			TNFA	4.1	7.2
Diesel	May 1-14	2	WST-1	13.6	8.7
			LDH	188.6	25.2
			HMOX1	4.3	5.8
			IL6	3.7	4.1
			IL8	8.9	20.3
			COX2	5.9	3.3
			TNFA	3.4	7.2
Diesel	May 6-14	1	WST-1	3.3	9.6
			LDH	19.7	145.4
			HMOX1	1.1	25.1
			IL6	1.6	4.0
			IL8	5.6	9.7
			COX2	1.8	2.0
			TNFA	2.7	4.5
Diesel	May 6-14	2	WST-1	14.1	18.2
			LDH	42.5	514.3
			HMOX1	3.1	13.7
			IL6	3.4	2.8
			IL8	9.3	14.0
			COX2	3.0	2.4
			TNFA	2.6	5.0
Smog	May 8-14	1	WST-1	14.2	7.0
			LDH	130.4	366.0
			HMOX1	1.7	1.9
			IL6	0.5	1.9
			IL8	12.7	4.2
			COX2	3.4	1.3
			TNFA	1.2	1.7
Smog	May 13-14	1	WST-1	2.1	3.8
			LDH	43.9	164.4
			HMOX1	5.5	2.4
			IL6	5.2	1.4
			IL8	5.8	9.4
			COX2	3.5	9.8
			TNFA	3.3	2.4

Smog	May 14-14	1	WST-1	9.6	3.7
			LDH	316.6	287.3
			HMOX1	3.3	5.1
			IL6	2.9	4.2
			IL8	10.6	10.8
			COX2	7.5	4.7
			TNFA	4.5	4.0